NASA Technical Memorandum 101640

Global/Local Stress Analysis of Composite Structures

J. B. Ransom

August 1989

National Aeronautics and Space Administration

Langley Research Center
Hampton, Virginia 23665-5225

ABSTRACT

A method for performing a global/local stress analysis is described and its capabilities are demonstrated. The method employs spline interpolation functions which satisfy the linear plate bending equation to determine displacements and rotations from a global model which are used as "boundary conditions" for the local model. Then, the local model is analyzed independent of the global model of the structure. This approach can be used to determine local, detailed stress states for specific structural regions using independent, refined local models which exploit information from less–refined global models. The method presented is not restricted to having a priori knowledge of the location of the regions requiring local detailed stress analysis. This approach also reduces the computational effort necessary to obtain the detailed stress state. Criteria for applying the method are developed. The effectiveness of the method is demonstrated using a classical stress concentration problem and a graphite–epoxy blade–stiffened panel with a discontinuous stiffener.

LIST OF TABLES

LIST OF FIGURES

Table of Contents

LIST OF SYMBOLS

$\mathbf{a}$	Vector of unknown spline coefficients of the interpolation function
a_i	Polynomial coefficients of the interpolation function, $i = 0, 1, \ldots, 9$
A	Cross–sectional area
A_{net}	Net cross–sectional area, $(W - 2r_0)h$
b	Stiffener spacing
D	Flexural rigidity for isotropic plate, $\frac{Eh^3}{12(1-\nu^2)}$
E	Young's modulus of elasticity
$\mathbf{f}$	Spline interpolation function
F_i	Natural logarithm coefficients of the interpolation function, $i = 1, 2, \ldots, n$
h	Panel thickness
h_s	Blade–stiffener height
K_t	Stress concentration factor, $\frac{(\sigma_x)_{max}}{(\sigma_x)_{nom}}$
l	Number of points on the local model boundary
L	Panel length
n	Number of points in the interpolation region
N_x	Longitudinal stress resultant
$(N_x)_{avg}$	Average running load per inch
$(N_x)_{max}$	Maximum longitudinal stress resultant, $(\sigma_x)_{max}h$
$(N_x)_{nom}$	Nominal longitudinal stress resultant, $(\sigma_x)_{nom}h$
N_y	Transverse inplane stress resultant
$(N_y)_{max}$	Maximum transverse inplane stress resultant
p_i	Applied point load on panel, $i = 1, 2, \ldots, n$

P	Applied load
q	Pressure loading on panel
r_0	Radius of the panel cutout
r_i	Radial coordinate of the i-th node in the interpolation region or along the local model boundary
R_I	Radius of the interpolation region
R_L	Radius of the circular local model
$\mathbf{S}$	Spline coefficient matrix
U_e	Element strain energy per unit area
$(U_e)_{max}$	Maximum element strain energy per unit area
w	Out–of–plane deflection
W	Panel width
x_i	x coordinate of the i-th node in the interpolation region or along the local model boundary
y_i	y coordinate of the i-th node in the interpolation region or along the local model boundary
ε	Parameter used to facilitate spline matrix computation
$\Delta\sigma$	Change in stress
ν	Poisson's ratio
σ_x	Longitudinal stress
$(\sigma_x)_{max}$	Maximum longitudinal stress
$(\sigma_x)_{nom}$	Nominal longitudinal stress, $\frac{P}{A_{net}}$
Ω_{ij}	Natural logarithm terms of the spline matrix, $i, j = 1, 2, \ldots, n$
∇^4	Biharmonic operator

Chapter 1

Introduction

1.1 Overview

Discontinuities and eccentricities, which are common in practical structures, increase the difficulty in predicting accurately detailed local stress distributions, especially when the component is built of a composite material, such as a graphite–epoxy material. The use of composite materials in the design of aircraft structures introduces added complexity due to the nature of the material systems and the complexity of the failure modes. The design and certification process for aerospace structures requires an accurate stress analysis capability. Detailed stress analyses of complex aircraft structures and their subcomponents are required and can severely tax even today's computing resources. Embedding detailed "local" finite element models within a single "global" finite element model of an entire airframe structure may be impractical due to the computational cost associated with the large number of degrees of freedom required for such a global detailed model. If the design load envelope of the structural component is extended, new regions with high stress gradients may be discovered. In that case, the entire analysis with embedded local refinements may have to be repeated and thereby further reducing the practicality of this brute force approach for obtaining the detailed stress state. Adaptive mesh refinement methods may be used to embed the local refinement in the global finite element model. The increased number of degrees of freedom again reduces the practicality of this approach in the global/local analysis realm. Also in structural applications, triangular elements introduced through unstructured remeshing methods

may adversely affect the solution because they are inherently stiffer than quadrilateral elements, and hence may require a more complicated structured remeshing method.

The phrase global/local analysis has a myriad of definitions among analysts. The concept of global and local may change with every analysis level, and also from one analyst to another (see Fig. 1.1). An analyst may consider the entire aircraft structure to be the global model, and a fuselage section to be the local model. At another level, the fuselage or wing may be the global model, and a stiffened panel is the local model. Laminate theory is used by some analysts to represent the global model, and micromechanics models are used for the local model. At the materials level, global/local variational models (*e.g.*, refs. [1, 2]) may be used to define detailed response functions in a particular, predetermined local region of interest, while the remainder of the global domain may be represented by effective properties. The global–local model is developed to examine the elastic stress field in laminates containing many layers. In the context of global/local analysis, the laminate is the global model, while each layer is a local model. The upward–intergrated top–down–structured analysis [3] makes use of several hierarchical global/local levels to perform a nonlinear structural analysis of a helicopter composite blade/vane component. In the iterative solution process, the blade/vane component is initially considered as the global model while the laminate is the local model. At a subsequent analysis level, the laminate becomes the global model and a unidirectional ply is the local model. The material properties are updated during each iteration and used in the "upward" analyses of the lamina, laminate, and the global structure.

A detailed, local analysis may be performed completely independent of the global analysis whereby the number of degrees of freedom in the local analysis is limited to only those in the local refined model. The global/local stress analysis

methodology, herein, is defined as a procedure to determine local, detailed stress states for specific structural regions using information obtained from an independent global stress analysis. The global/local analysis methodology in this study employs the finite element method in both global and local analyses.

1.2 Review of Previous Work

Since a single definition of global/local analysis is not practical, a wide range of information is found in the open literature (*e.g.*, refs. [4-20]). Global/local analysis research areas include such methods as substructuring, submodeling (*e.g.*, linear constraint methods, and the specified boundary stiffness/force method) and exact zooming. In addition, hybrid techniques such as reduced basis methods are other examples of global/local analysis methods.

1.2.1 Substructuring

The substructuring technique is perhaps the most common technique for global/local analysis in that it reduces a complex structure to smaller, more manageable components, and simplifies the structural modeling. A specific region of the structure may be modeled by a substructure or multiple levels of substructures to determine the detailed response. Wilkins [6] made use of multi–level substructuring or "telescoping" to study damage tolerance of composite structures. In some nonlinear problems, substructuring may be used if the material or geometric nonlinearity is localized, while the remainder of the structure remains linear [7, 8]. The part of the structure which is assumed to remain linear during loading is defined as one or multiple substructures, while the part of the structure which undergoes nonlinear deformation is defined as a nonlinear substructure. Here, the linear part of the structure may be considered the global model, and the nonlinear region is the local model.

1.2.2 Submodeling

Submodeling refers to any method that uses a node by node correspondence for the displacement field at the global/local interface boundary. The ANSYS finite element analysis program [9] employs such a method. The analyst may define an independent, more refined local model by transitioning from coarsely–spaced boundary nodes of the global model to a more refined internal local model using triangular elements (see Fig. 1.2). Research has also been proposed with variable–order elements for mesh transitioning (*e.g.*, refs. [10, 11]) as shown in Fig. 1.3. Griffin and Vidussoni [12] employ a form of submodeling to perform a two–dimensional to three–dimensional global/local analysis. The specified boundary displacement (SBD) method [13, 14] involves developing a subregion model of the portion of the structure of interest and applying displacement boundary conditions derived from the global structural solution to simulate the effect of the rest of the structure upon the subregion. The SBD method uses the finite element shape functions to produce displacement constraints to be applied to the specified boundary nodes. The rigid (RSPLINE) element in MSC/NASTRAN [15] provides a straightforward method for changing mesh size while providing an approximation to the actual motions at the dependent degrees of freedom. However, since the interpolation is one–dimensional, it does not guarantee the continuity of stresses across the global/local interface boundary.

The linear constraint method [13, 14] uses a global structural model which has been locally refined in the area of interest. Linear constraint equations, based on the element shape functions, are applied to any additional nodes on the global/local interface boundary added for element refinement. One of the drawbacks of this method is that, the entire global model must be reanalyzed every time the local area of interest changes or the mesh refinement of the area of interest changes.

The specified boundary stiffness/force (SBSF) method [16] uses an independent subregion model with stiffnesses and forces as boundary terms. These stiffnesses and forces represent the effect of the rest of the structure upon the subregion. The stiffness terms are incorporated in the stiffness of the subregion model and the forces are applied on the boundary of the local model.

1.2.3 Efficient and Exact Zooming

An efficient zooming technique, as described in reference [17], employs static condensation and exact structural reanalysis methods. Although this efficient zooming technique involves the solution of a system of equations of small order, all the previous refinement processes are needed to proceed to a new refinement level. An "exact" zooming technique [18] employs an expanded stiffness matrix approach rather than the reanalysis method described in reference [17]. The "exact" zooming technique utilizes results of only the previous level of refinement. For both methods, separate locally–refined subregion models are used to determine the detailed stress distribution in a known critical region. The subregion boundary is coincident with nodes in the global model or the previously refined subregion model which is akin to the submodeling technique discussed in the preceding subsection. The "efficient" and "exact" zooming techniques differ in the matrix operations used to condense out the degrees of freedom outside of the subregion area. The stiffness terms for the locally–refined region are added to the stiffness matrix of the global structure. The degrees of freedom corresponding to the nodes in the global model outside the locally–refined region are condensed out from this augmented stiffness matrix. The system is, therefore, reduced to one that involves the degrees of freedom of the global model within the locally–refined region of the structure and the degrees of freedom of any additional nodes introduced by the refinement process. The locally–refining process may be continued with multiple levels of local refinement until satisfactory results are obtained. For multiple levels of local refinement,

displacements contained in the final, most refined portion of the structure are obtained first. In the "exact" zooming method, the displacements in the final, most refined subregion are obtained on the basis of the stiffness or flexibility terms of the previous locally–refined region only. Next, the response in the global region, as well as the response within various other levels of refinement, can be computed. Although these methods are computationally expensive, the results presented for an isotropic plate with a central hole are as accurate as a complete model with embedded local mesh refinement and no constraint equations are introduced.

1.2.4 Hybrid Techniques

In the global variational methods, the domain of the governing equation is treated as a whole, and an approximate solution is constructed from a sequence of linearly independent functions (*i.e.*, Fourier series) that satisfy the geometric boundary conditions. In the finite element method, the domain is subdivided into small regions or elements within which approximating functions (usually low–order polynomials) are used to describe the continuum behavior. Hybrid techniques, such as the global/local finite element method as presented by Dong [19], make use of two or more methods in different domains of the structure.

Global/local finite element analysis may refer to an analysis technique that simultaneously utilizes conventional finite element modeling around a local discontinuity with classical Rayleigh-Ritz approximations for the remainder of the structure. For example, Dong considers the natural frequency of a simply–supported rectangular isotropic plate with and without a hole. By employing the Ritz method to obtain an approximation sequence, the frequency of the plate with no hole may be deduced from Hamilton's principle. However, for the plate with a hole, the selection of an approximation sequence that satisfies both the boundary conditions at the free edge around the hole and the exterior edges is difficult. The finite element method

may be employed, but is impractical due to the computational effort required to obtain the solution. The Global–Local Finite Element Method (GLFEM) [19] is an alternative approach. A local finite element mesh is established to model the physical behavior around the hole. For a small hole, the frequency of the plate does not change from that of the plate with no hole. Therefore, a global approximation sequence may be used for the remainder of the plate. Continuity of the displacements and rotations at the interface between the two regions must be enforced. The computational effort is reduced as a result of the use of the limited number of finite element degrees of freedom. The Global–Local Finite Element Method, however, presupposes that the analyst can identify an approximation sequence for the global behavior. The selection of this approximation sequence may, therefore, restrict GLFEM to regular geometries and specific boundary conditions.

Problems with singularities (*i.e.*, crack tips) limit the accuracy of an analysis performed with conventional finite elements. To overcome the shortcomings of the conventional finite element, the finite element analysis employs special crack tip elements to model the existing singularities. However, experience and judgement are required to select the appropriate element size and the number of terms in the series expansion used to represent the mechanical field. The GLFEM provides an alternative approach. In contrast to the preceding example of the GLFEM, Dong models the local region around the crack tip with approximation functions. Beyond the crack tip, a region may be used which includes the approximation functions and also the finite element representation. Outside the overlap region, conventional finite elements may be used for the remainder of the structure. As in the previous example, the approach is limited to problems for which the analyst can identify the approximation functions.

Another type of hybrid method is the reduced basis method. A reduced basis method uses a set of basis vectors (*e.g.*, Rayleigh-Ritz vectors, vibration mode

shapes) to reduce the size of the problem. Reduced basis methods have been used to identify the local geometrically nonlinear regions of structures. Then, a nonlinear analysis of only these local regions may be performed. A mixed local and global functions approach for the collapse of shell structures is presented in reference [20]. The approach is based on a mixture of global, reduced basis vectors and local, finite element analysis. Conventional finite element modeling of the nonlinear system is performed. The system of equations is reduced by selecting a limited number of Rayleigh-Ritz functions (basis vectors). The complex nonlinear analysis strategy and the difficulty in selecting the approximation functions reduce the viability of this approach.

The aforementioned global/local methods, with the exception of the submodeling technique, require that the analyst know where the critical region is located before performing the global analysis. However, a global/local methodology which does not require a priori knowledge of the location of the local region(s) requiring special modeling could offer advantages in many situations by providing the modeling flexibility required to address detailed local models as their need is identified.

1.3 Objectives and Scope

The overall objective of the present study is to develop such a computational strategy for obtaining the detailed stress state of composite structures. Specific objectives are:

1. To develop a method for performing global/local stress analysis of composite structures
2. To develop criteria for defining the global/local interface region and local modeling requirements
3. To demonstrate the computational strategy on representative structural analysis problems

The scope of the present study includes the global/local linear two–dimensional stress analysis of finite element structural models. The method developed is not restricted to having a priori knowledge of the locations of the regions requiring detailed stress analysis. The guidelines for developing the computational strategy include the requirements that it be compatible with general–purpose finite element computer codes, valid for a wide range of elements, extendible to geometrically nonlinear analysis, and cost–effective. In addition, the computational strategy should include a procedure for automatically identifying the critical region and defining the global/local interface region. Satisfying these guidelines will provide a general–purpose global/local computational strategy for use by the aerospace structural analysis community.

The organization of the remainder of this study is as follows. The global/local methodology, as defined in the overview, is reviewed in Chapter 2. The global/local terminology is discussed, and the approach for the complete global/local analysis is outlined. The global/local method is based on a spline interpolation of a global solution to obtain "boundary conditions" for the local analysis. Global and local modeling issues are discussed as well as the definition of the global/local interface boundary and the global interpolation strategy. The mathematical formulation for the spline interpolation is presented in Chapter 3. The spline interpolation functions satisfy the linear plate bending equation (*i.e.*, $D\nabla^4 w = q$). The implementation of the spline interpolation is discussed. The computational strategy for the global/local analysis is presented in Chapter 4. Numerical results are presented in Chapter 5. Conclusions and recommendations are given in Chapter 6. The derivation of the spline interpolation function is presented in Appendix A. Runstreams for the global and local analyses of an isotopic panel with a circular cutout are given in Appendices B and C.

Chapter 2

Global/Local Methodology

Global/local stress analysis methodology is defined as a procedure to determine local, detailed stress states for specific structural regions using information obtained from an independent global stress analysis. The local model refers to any structural subregion within the defined global model. The global stress analysis is performed independent of the local stress analysis. The interpolation region encompassing the critical region is specified. A surface spline interpolation function is evaluated at every point in the interpolation region yielding a spline matrix, $\mathbf{S}(x,y)$, and unknown coefficients, $\mathbf{a}$. The global field is used to compute the unknown coefficients. An independent, more refined local model is generated within the previously–defined interpolation region. The global displacement field is interpolated producing a local displacement field which is applied as a "boundary condition" on the boundary of the local model. Then, a complete local finite element analysis is performed.

The development of a global/local stress analysis capability for structures has been underway for several years and has taken several different approaches as is evident from the literature review. The methodology for a global/local analysis generally involves four key components. The first component is an "adequate" global analysis. In this context, "adequate" implies that the global structural behavior is accurately determined and that local structural details are at least grossly incorporated. The second component is a strategy for identifying, in the global model, regions requiring further study. The third component is an interpolation procedure that does not require coincident nodes along the global/local interface boundary. Finally, the fourth component is an "adequate" local analysis. In this

context, "adequate" implies that the local detailed stress state is accurately determined and that compatibility requirements along the global/local interface are satisfied. The development of a global/local stress analysis methodology requires an understanding of each key component and insight into their interaction.

The global/local stress analysis methodology presented herein provides an alternative to existing strategies which require a priori knowledge of the location of a critical region and often require embedding detailed finite element models in a global finite element model to obtain an accurate detailed stress state. Unlike most of the global/local methods reviewed, the method described does not require having to know, a priori, the region(s) requiring a detailed stress analysis. In practice, the global analysis model is "adequate" for the specified design load cases. However, these load cases frequently change in order to extend the operating region of the structure or to account for previously unknown effects. In these incidents, the global analysis may identify new "hot spots" that require further study. The proposed methodology provides an analysis tool for these local analyses.

A global/local stress analysis methodology is described in subsequent sections. The terminology used to describe the different components of the solution strategy is discussed. The components of the global/local analysis method, which includes global modeling, interpolation, and local modeling are discussed.

2.1 Terminology

The terminology of the global/local methodology presented herein is depicted in Fig. 2.1 to illustrate the components of the analysis procedure. The global model is a finite element model of a complete structure or a subcomponent of a structure (see Fig. 2.1a). A region requiring a more detailed interrogation is subsequently identified by the structural analyst. This region may be obvious, such as a region around a cutout in a panel, or not so obvious, such as a local buckled region of

a curved panel loaded in compression. Because the location of these regions are usually unknown prior to performing the global analysis, the structural analyst must develop a global model with sufficient detail to represent the global behavior of the structure. An interpolation region is then identified around the critical region as indicated in Fig. 2.1b. An interpolation procedure is used to determine the displacements and rotations used as "boundary conditions" for the local model. The interpolation region is the region within which the generalized displacement solution will be used to define the interpolation matrix. This matrix, discussed in Chapter 3, consists of the coordinates and functions of the coordinates in the interpolation region. The global/local interface boundary, indicated in Fig. 2.1c, coincides with the intersection of the boundary of the local model with the global model. The definition of the interface boundary may affect the accuracy of the interpolation procedure and thus the local stress state. Criteria for defining the interface boundary are discussed in Section 2.4. The local model lies within the interpolation region as shown in Fig. 2.1c and is generally more refined than the global model in order to predict more accurately the detailed state of stress in the critical region. The coordinates or nodes of the local model need not be coincident with any of the coordinates or nodes of the global model.

A schematic which describes the overall solution strategy is shown in Fig. 2.2. The global/local interpolation procedure consists of generating a matrix based on the global solution and a local interpolated field. The local interpolated field is that field which is interpolated from the global analysis and is valid over the domain of the local model. Local stress analysis involves the generation of the local finite element model, use of the interpolated field to impose conditions on the local model, and the detailed stress analysis.

The global/local method described herein may be used to interrogate multiple critical regions of a global structure. The use of multiple regions is depicted in the schematic shown in Fig. 2.3. Once the global analysis is performed, single or multiple critical regions may be identified. Multiple interpolation regions and spline matrices may be defined. Multiple local models are generated and the local interpolated fields are obtained followed by the complete local analyses. Although the definition of the multiple regions and the multiple analyses may be performed sequentially, the approach is readily applicable to concurrent processing.

Multi-level global/local analyses may also be performed. The global and local model definitions change as the levels of the global/local analysis increase. The local region identified at the first level becomes the global model at the next level and another local model is defined. The global/local analysis method, then continues. The multi-level analysis may be used first to obtain a local two-dimensional detailed stress state, and then to obtain an even more detailed stress state by a more refined two-dimensional or three-dimensional local analysis.

2.2 Global Modeling and Analysis

The development of a global finite element model of an aerospace structure for accurate stress predictions near local discontinuities is often too time consuming to impact the design and certification process. Predicting the global structural response of these structures often has many objectives including determining overall structural response, stress analysis, and internal load distributions. Frequently, structural discontinuities such as cutouts are only accounted for in the overall sense. Any local behavior is then obtained by a local analysis, possibly by another analyst. The load distribution for the local region is obtained from the global analysis. The local model is then used to obtain the structural behavior in the specified region. For example, the global response of an aircraft wing is obtained by a coarse finite element

analysis. A typical subcomponent of the wing is a stiffened panel with a cutout. Since cutouts are known to produce high stress gradients, the load distributions from the global analysis of the wing are applied to the stiffened panel to obtain the local detailed stress state. One difficulty in modeling cutouts is the need for the finite element mesh to transition from a circular pattern near the cutout to a rectangular pattern away from the cutout. This transition region is indicated in Fig. 2.4 and will be referred to as a transition square (*i.e.*, a square region around the cutout used to transition from rings of elements to a rectangular mesh). This transition modeling requirement impacts both the region near the cutout and the region away from the cutout. Near the cutout, quadrilateral elements may be skewed, tapered, and perhaps have an undesirable aspect ratio. In addition, as the mesh near the cutout is refined by adding radial "spokes" of nodes and "rings" of elements, the mesh away from the cutout also becomes refined. For example, adding radial spokes of nodes near the cutout also adds nodes and elements in the shaded regions (see Fig. 2.4) away from the cutout. This approach may dramatically increase the computational requirements necessary to obtain the detailed stress state. Alternate mesh generation techniques using transition zones of triangular elements or multipoint constraints may be used; however, the time spent by the structural analyst will increase substantially.

The global modeling herein, although coarse, is sufficient to represent the global structural behavior. The critical regions have been crudely modeled to represent their effect on the global solution. This modeling step is one of the key components of the global/local methodology discussed in this chapter since it provides an "adequate" global analysis. Although the critical regions are known for the numerical studies discussed in a Chapter 5, this a priori knowledge is not required but may be exploited by the analyst.

2.3 Local Modeling and Analysis

The local finite element modeling and analysis is performed to obtain a detailed analysis of the local structural region(s). The local model accurately represents the geometry of the structure necessary to provide the local behavior and stress state. The discretization requirements for the analysis is governed by the accuracy of the solution desired. The discretization of the local model is influenced by its proximity to a high stress gradient.

One approach for obtaining the detailed stress state is to model the local region with an arbitrarily large number of finite elements. Higher–order elements may be used to reduce the number of elements required. Detailed refinement is much more advantageous for use in the local model than in the global model. The local refinement affects only the local model, unlike embedding the same refinement in the global model which would propagate to regions not requiring such a level of detailed refinement. A second approach is to refine the model based on engineering judgement. Mesh grading, in which smaller elements are used near the gradient, may be employed. An error measure based on the change in stress from element to element may be used to determine the accuracy in the stress state obtained by the initial local finite element mesh. If the accuracy of the solution is not satisfactory, additional refinements are required. The additional refinements may be based on the coarse global model or the displacement field in the local model which suggests a third approach. The third approach is a multi–level global/local analysis. At the second local model level, any of the three approaches discussed may be used to obtain the desired local detailed stress state. Detailed refinement is used for local modeling in this study.

2.4 Global/Local Interface Boundary Definition

The definition of the global/local interface boundary is problem dependent. The location of the nodes on the interface boundary need not be coincident with any of the nodes in the coarse global model. Kelley [14] concludes that the distance that the local model must extend away from a discontinuity is highly dependent upon the coarse model used. The more accurate the coarse model displacement field is, the closer the local model boundary may be to the discontinuity. This conclusion is based on the results of a study of a flat, isotropic panel with a central cutout subjected to uniform tension and extends to other structures with high stress gradients.

Stresses are generally obtained from a displacement–based finite element analysis by differentiation of the displacement field. For problems with stress gradients, the element stresses vary from element to element, and in some cases this change, $\Delta\sigma$, may be substantial. The change in stresses, $\Delta\sigma$, may be used as a measure of the adequacy of the finite element discretization. Large $\Delta\sigma$ values indicate structural regions where more modeling refinement is needed. Based on this method, structural regions with small values of $\Delta\sigma$ have uniform stress states away from any gradients. Therefore, the global/local interface boundary should be defined in region(s) with small values of $\Delta\sigma$ (*i.e.*, away from a stress gradient). Exploratory studies to define an automated procedure for selecting the global/local interface boundary have been performed using a measure of the strain energy. The strain energy per unit area is selected since it represents a combination of all the stress components instead of a single stress component. Regions with high stress gradients will also have changes in this measure of strain energy from element to element.

2.5 Global/Local Interpolation Procedure

The global/local analysis method is used to determine local, detailed stress states using independent, refined local models which exploit information from less refined global models. A finite element analysis of the global structure is performed to obtain its overall behavior. Finite element analyses can be performed in which the mesh is successively refined until a converged solution is obtained. However, for some structural analysis problems with high stress gradients, this approach becomes infeasible due to the computational cost for the global finite element model. In these cases, a critical region may be identified from the results of the global analysis. The global solution may be used to obtain an applied displacement field along the boundary (*i.e.*, boundary conditions) of an independent local model of the critical region. This step is one of the key components of the global/local methodology; namely, interpolation of the global solution to obtain boundary conditions for the local model.

Many interpolation methods are used to approximate functions (*e.g.*, refs. [21-23]). The interpolation problem may be stated as follows: given a set of function values $\mathbf{f}_i$ at n coordinates (x_i, y_i), determine a "best-fit" surface for these data. Mathematically, this problem can be stated as

$$[\mathbf{S}(x_i, y_i)] \begin{Bmatrix} \mathbf{a}_1 \\ \mathbf{a}_2 \\ \vdots \\ \mathbf{a}_n \end{Bmatrix} = \begin{Bmatrix} \mathbf{f}_1 \\ \mathbf{f}_2 \\ \vdots \\ \mathbf{f}_n \end{Bmatrix} \tag{2.1}$$

where $\mathbf{S}(x_i, y_i)$ is a matrix of interpolated functions evaluated at n points, the array $\mathbf{a}$ defines the unknown coefficients of the interpolation functions, and the array $\mathbf{f}$ consists of known values of the field being interpolated based on n points in the global model.

Common interpolation methods include linear interpolation, Lagrangian interpolation and least–squares techniques for polynomial interpolation. Elementary linear interpolation is perhaps the simplest method and is an often used interpolation method in trigonometric and logarithmic tables. Another method is Lagrangian interpolation which is an extension of linear interpolation. For this method, data for n points are specified and a unique polynomial of degree $n-1$ passing through the points can be determined. However, a more common method involving a least–squares polynomial fit minimizes the square of the sum of the residuals. The drawbacks of least–squares polynomial fitting include the requirement for repeated solutions to minimize the square of the sum of the residuals, and the development of an extremely ill–conditioned matrix of coefficients when the degree of the approximating polynomial is large. A major limitation of the approximating polynomials which fit a given set of function values is that they may be excessively oscillatory between the given points or nodes.

Chapter 3

Mathematical Formulation

Spline interpolation is a numerical analysis tool used to obtain the "best" local fit through a set of points. Spline functions are piecewise polynomials of degree m that are connected together at points called knots so as to have $m-1$ continuous derivatives. The mathematical spline is analogous to the draftman's spline used to draw a smooth curve through a number of given points. The spline may be considered to be a perfectly elastic thin beam resting on simple supports at given points. A surface spline is used to interpolate a function of two variables and removes the restriction of single variable schemes which require a rectangular array of grid points. The derivation of the surface spline interpolation function used herein is based on the principle of minimum potential energy for linear plate bending theory. This approach incorporates a classical structural mechanics formulation into the spline interpolation procedure in a general sense. Using an interpolation function which also satisfies the linear plate bending equation provides inherent physical significance to a numerical analysis technique. The spline interpolation is used to interpolate the displacements and rotations from a global analysis and thereby provides a functional description of each field over the domain. The displacement and rotation fields are interpolated separately; that is, the out–of–plane deflections and the bending rotations are interpolated independently rather than calculating the bending rotations by differentiating the interpolated out–of–plane displacement field. The separate interpolation of displacements and rotations provides a consistent basis for interpolating solutions based on a plate theory with shear flexibility effects incorporated.

The derivation of the spline interpolation is presented. The implementation of the spline interpolation consisting of the spline coefficients, constraint equations, and the equation solver is discussed. The interpolation procedure which includes the independent interpolation of the fields is discussed.

3.1 Derivation of the Spline Interpolation

The derivation of the spline interpolation used herein follows the approach described by Harder and Desmarais in reference [24] and is included in Appendix A for completeness. A spline surface is generated based on the solution to the linear plate bending equation [24]

$$D\nabla^4 w = q \tag{3.1}$$

The solution of Eq. (3.1) in Cartesian coordinates may be written in the general form

$$f(x,y) = a_0 + a_1 x + a_2 y + \sum_{i=1}^{n} F_i r_i^2 \ln r_i^2 \tag{3.2}$$

where $r_i^2 = (x - x_i)^2 + (y - y_i)^2, n$ is the total number of nodes in the interpolation region, and a_0, a_1, a_2 and F_i are undetermined coefficients representing loads.

The $n + 3$ unknowns (a_0, a_1, a_2, F_i) are found by solving the set of equations:

$$\sum_{i=1}^{n} F_i \quad = 0 \tag{3.3}$$

$$\sum_{i=1}^{n} F_i x_i = 0 \tag{3.4}$$

$$\sum_{i=1}^{n} F_i y_i = 0 \tag{3.5}$$

and

$$f_i(x_i, y_i) = a_0 + a_1 x_i + a_2 y_i + \sum_{j=1}^{n} F_j r_{ij}^2 \ln r_{ij}^2;\ i = 1, n \tag{3.6}$$

where $r_{ij}^2 = (x_i - x_j)^2 + (y_i - y_j)^2$, or in matrix form:

$$\mathbf{f_g} = \mathbf{Sa} \tag{3.7}$$

where $\mathbf{S}$ is the spline coefficient matrix, $\mathbf{a}$ is the vector of unknown coefficients, and $\mathbf{f_g}$ is the vector containing the known values of the global field to be interpolated (*i.e.*, displacements). The constraint equations given in Eqs. (3.3)–(3.5) are used to prevent Eq. (3.1) from becoming unbounded when expressed in Cartesian coordinates.

Specifically, the vector $\mathbf{a}$ is defined to be

$$\mathbf{a} = \begin{Bmatrix} a_0 \\ a_1 \\ a_2 \\ F_1 \\ \vdots \\ F_n \end{Bmatrix} \tag{3.8}$$

The vector $\mathbf{f_g}$ is defined to be

$$\mathbf{f_g} = \begin{Bmatrix} 0 \\ 0 \\ 0 \\ f_1 \\ \vdots \\ f_n \end{Bmatrix} \tag{3.9}$$

The spline coefficient matrix is then given by

$$\mathbf{S} = \begin{bmatrix} 0 & 0 & 0 & 1 & 1 & \dots & 1 \\ 0 & 0 & 0 & x_1 & x_2 & \dots & x_n \\ 0 & 0 & 0 & y_1 & y_2 & \dots & y_n \\ 1 & x_1 & y_1 & r_{11}^2 \ln(r_{11}^2 + \varepsilon) & r_{12}^2 \ln(r_{12}^2 + \varepsilon) & \dots & r_{1n}^2 \ln(r_{1n}^2 + \varepsilon) \\ 1 & x_2 & y_2 & r_{21}^2 \ln(r_{21}^2 + \varepsilon) & r_{22}^2 \ln(r_{22}^2 + \varepsilon) & \dots & r_{2n}^2 \ln(r_{2n}^2 + \varepsilon) \\ \vdots & \vdots & \vdots & \vdots & \vdots & \ddots & \vdots \\ 1 & x_n & y_n & r_{n1}^2 \ln(r_{n1}^2 + \varepsilon) & r_{n2}^2 \ln(r_{n2}^2 + \varepsilon) & \dots & r_{nn}^2 \ln(r_{nn}^2 + \varepsilon) \end{bmatrix} \tag{3.10}$$

where x_i, y_i and x_j, y_j in the expression given for r_{ij} are coordinates of nodes in the interpolation region and ε is a parameter used to insure numerical stability for the case when r_{ij} vanishes.

The matrix **S** is formed, inverted, and multiplied by $\mathbf{f_g}$ to compute the vector, **a**. The vector **a** is then used to interpolate the local values through the following equation:

$$f_i = a_0 + a_1 x_i + a_2 y_i + \sum_{j=1}^{n} F_j r_{ij}^2 \ln r_{ij}^2; \qquad i = 1, 2, \ldots, l \tag{3.11}$$

where for $r_{ij}^2 = (x_i - x_j)^2 + (y_i + y_j)^2$, x_i, y_i are coordinates of the nodes in the local model, x_j, y_j are coordinates of the nodes in the interpolation region, l is the number of nodes of the local model where the interpolated field is required, and the coefficients, a_0, a_1, a_2, and F_j are contained in **a**.

Extensions have been made to the formulation presented above to include higher–order polynomial terms (underlined terms in Eq. (3.12)). The extended Cartesian form analogous to Eq. (3.2) which also satisfies Eq. (3.1) is written as

$$f_g(x,y) = a_0 + a_1 x + a_2 y + \underline{a_3 x^2 + a_4 xy + a_5 y^2 + a_6 x^3 + a_7 x^2 y +}$$

$$\underline{a_8 x y^2 + a_9 y^3} + \sum_{i=1}^{n} F_i r_i^2 \ln(r_i^2) \tag{3.12}$$

where

$$r_i^2 = (x - x_i)^2 + (y - y_i)^2 \tag{3.13}$$

and x_i, y_i are the coordinates of the i-th node in the interpolation region. The higher–order polynomial terms were added to help represent a higher–order bending response than was being approximated by the natural logarithm term in the earlier formulation. The additional terms increase the number of unknown coefficients and

constraint equations to $n+10$. The $n+10$ unknowns $(a_0, a_1, a_2, \ldots, a_9, F_i)$ are found by solving Eq. (3.12) and the set of equations:

$$\begin{aligned}
\sum_{i=1}^{n} F_i &= 0 & \sum_{i=1}^{n} F_i y_i^2 &= 0 \\
\sum_{i=1}^{n} F_i x_i &= 0 & \sum_{i=1}^{n} F_i x_i^3 &= 0 \\
\sum_{i=1}^{n} F_i y_i &= 0 & \sum_{i=1}^{n} F_i x_i^2 y_i &= 0 \\
\sum_{i=1}^{n} F_i x_i^2 &= 0 & \sum_{i=1}^{n} F_i x_i y_i^2 &= 0 \\
\sum_{i=1}^{n} F_i x_i y_i &= 0 & \sum_{i=1}^{n} F_i y_i^3 &= 0
\end{aligned} \tag{3.14}$$

The matrix form of the extended equations, $\mathbf{S_g a = f_g}$, is given by

$$\begin{bmatrix}
0 & 0 & 0 & \ldots & 0 & 1 & 1 & \ldots & 1 \\
0 & 0 & 0 & \ldots & 0 & x_1 & x_2 & \ldots & x_n \\
0 & 0 & 0 & \ldots & 0 & y_1 & y_2 & \ldots & y_n \\
0 & 0 & 0 & \ldots & 0 & x_1^2 & x_2^2 & \ldots & x_n^2 \\
0 & 0 & 0 & \ldots & 0 & x_1 y_1 & x_2 y_2 & \ldots & x_n y_n \\
0 & 0 & 0 & \ldots & 0 & y_1^2 & y_2^2 & \ldots & y_n^2 \\
0 & 0 & 0 & \ldots & 0 & x_1^3 & x_2^3 & \ldots & x_n^3 \\
0 & 0 & 0 & \ldots & 0 & x_1^2 y_1 & x_2^2 y_2 & \ldots & x_n^2 y_n \\
0 & 0 & 0 & \ldots & 0 & x_1 y_1^2 & x_1 y_2^2 & \ldots & x_n y_n^2 \\
0 & 0 & 0 & \ldots & 0 & y_1^3 & y_2^3 & \ldots & y_n^3 \\
1 & x_1 & y_1 & \ldots & y_1^3 & \Omega_{11} & \Omega_{12} & \ldots & \Omega_{1n} \\
1 & x_2 & y_2 & \ldots & y_2^3 & \Omega_{21} & \Omega_{22} & \ldots & \Omega_{2n} \\
\vdots & \vdots & \vdots & \ddots & \vdots & \vdots & \vdots & \vdots & \vdots \\
1 & x_n & y_n & \ldots & y_n^3 & \Omega_{n1} & \Omega_{n2} & \ldots & \Omega_{nn}
\end{bmatrix}
\begin{Bmatrix} a_0 \\ a_1 \\ a_2 \\ a_3 \\ a_4 \\ a_5 \\ a_6 \\ a_7 \\ a_8 \\ a_9 \\ F_1 \\ F_2 \\ \vdots \\ F_n \end{Bmatrix}
=
\begin{Bmatrix} 0 \\ 0 \\ 0 \\ 0 \\ 0 \\ 0 \\ 0 \\ 0 \\ 0 \\ 0 \\ f_1 \\ f_2 \\ \vdots \\ f_n \end{Bmatrix} \tag{3.15}$$

where $\Omega_{ij} = r_{ij}^2 \ln(r_{ij}^2 + \varepsilon)$ for $i, j = 1, 2, \ldots, n$ and r_{ij}, x_i, y_i, and x_j, y_j are as defined in the earlier formulation. The extended local interpolation function is similar to Eq. (3.12) except that it is evaluated at points along the global/local interface boundary. That is,

$$f_{g/l}(x_i, y_i) = a_0 + a_1 x_i + a_2 y_i + a_3 {x_i}^2 + a_4 x_i y_i + a_5 {y_i}^2 + a_6 {x_i}^3 + a_7 {x_i}^2 y_i +$$

$$a_8 x_i {y_i}^2 + a_9 {y_i}^3 + \sum_{j=1}^{n} F_j r_{ij}^2 \ln(r_{ij}^2); \qquad i = 1, 2, \ldots, l \tag{3.16}$$

Upon solving Eq. (3.15) for the coefficients $(a_0, a_1, a_2, \ldots, a_9, F_j)$, Eq. (3.16) is used to compute the interpolated data at the required local model nodes. That is, in matrix form:

$$\mathbf{f_{g/l}} = \mathbf{S_{g/l}} \mathbf{a} \tag{3.17}$$

3.2 Implementation of Spline Interpolation

The polynomial coefficients $(a_0, a_1, a_2, \ldots, a_9)$ of Eq. (3.16) are linear combinations of the constants of integration in the polar coordinate solution given in Eq. (A.1) of Appendix A. The logarithmic coefficients F_i are given as

$$F_i = \frac{p_i}{16\pi D} \tag{3.18}$$

where p_i is a point load applied at the coordinate (x_i, y_i) of the plate.

The first of the constraint equations in Eq. (3.14) states that the sum of the applied point loads p_i is equal to zero. The additional constraint equations state that the sum of the first, second and third moments introduced by the applied point loads p_i about the x and y axes are equal to zero.

The Ω_{ij} terms of the extended spline coefficient matrix given in Eq. (3.15) are zero when $i = j$, since $r_{ii} = (x_i - x_i)^2 + (y_i - y_i)^2 = 0$. The matrix, $\mathbf{S_g}$ is not a positive definite matrix since there exists a vector $\mathbf{x}$ with a single nonzero element (*i.e.*, $\mathbf{x} = \{0, 0, 0, \ldots, 1\}$) for which $\mathbf{x}^T \mathbf{S_g} \mathbf{x} = 0$. The positive definite condition is used to show the stability and convergence of many linear solution techniques. The zero diagonal presents some difficulty in factoring the $\mathbf{S_g}$ matrix. During the

factorization process, zero diagonal elements of the matrix may become nonzero, however, since $\mathbf{S}_{ii}$ is zero, the factorization can not continue without pivoting. Therefore, a method which employs pivoting is required. Gaussian elimination with pivoting has been implemented in the global/local interpolation procedure to invert the spline matrix, $\mathbf{S_g}$.

3.3 Interpolation Procedure

Although Eq. (3.16) is derived from the linear plate bending equation, it may be used to interpolate each displacement component u, v, and w, independently. The interpolation of the inplane displacements, u and v is accurate provided the inplane behavior can be represented by the interpolation function. If the full polynomial and logarithmic expansion of Eq. (3.16) is not required to approximate the displacement field, the associated coefficients vanish. The rotations θ_x, θ_y, and θ_z are interpolated from the rotations in the interpolation region specified in the global model instead of differentiating the out–of–plane displacement field or differentiating the interpolation function for the out–of–plane deflection, w, to obtain the rotations (*e.g.*, $w_{,x}$).

The global interpolation function $\mathbf{f_g}$ given in Eq. (3.12) is evaluated at the nodes in the interpolation region specified within the global model. In the matrix form of Eq. (3.15), the matrix $\mathbf{S_g}$ is based on the coordinates (x_i, y_i) in the interpolation region. The function values $\mathbf{f}_g$ are the displacements and rotations at the nodes in the interpolation region. These displacements and rotations have been obtained from the global analysis. The vector $\mathbf{a} = \{a_i, F_i\}^T$ contains the unknown coefficients of the interpolation function. The unknown coefficients **a** are computed by solving a system of simultaneous equations. The interpolated data along the global/local interface boundary are obtained by solving the system of equations given in Eq. (3.17) for $\mathbf{f_{g/l}}$ using the new spline coefficient matrix $\mathbf{S_{g/l}}$ which is

based on the coordinates along the global/local interface boundary and the vector of coefficients **a**.

In the present study, the interpolation procedure is used to obtain the displacements and rotations on the global/local interface boundary. However, the interpolation procedure may be used in general to interpolate any field at any location in the local model. The interpolation procedure was originally developed for interpolating wing deflections and computing slopes for aeroelastic calculations.

Chapter 4

Computational Strategy

The computational strategy described herein is implemented through the use of the Computational Structural Mechanics (CSM) Testbed (see refs. [25] and [26]). The CSM Testbed is used to model and analyze both the global and local finite element models of a structure. Two new computational modules or processors were developed to perform the global/local interpolation procedure. Various other Testbed processors are used in the stress analysis. The overall computational strategy for the global/local stress analysis methodology is controlled by a high–level procedure written using the command language of the Testbed called CLAMP, an acronym for Command Language for Applied Mechanics Processors (see ref. [26]). The command language provides a flexible tool for performing computational structural mechanics research.

4.1 Overview of the CSM Testbed

The field of computerized structural analysis is dominated by two types of computer programs. One type is the huge, 2000 subroutine general purpose program (see ref. [27]), that is the result of over a hundred man years of effort spanning more than a decade. The other type is the relatively small, special–purpose code resulting from a research environment that represents a one– to two–year effort for a specific research application. This dichotomy has resulted in long delays in making research technology available for critical structural analysis problems that the aerospace

community faces. To accelerate the introduction of successful research technology into large–scale applications programs, a modular, public–domain, machine–independent, architecturally–simple, software development environment has been constructed. This system is denoted the CSM Testbed and its concept is depicted by a pyramid (see Fig. 4.1). The base of the pyramid is the computer and its operating system. The computer operating system is provided by the computer vendor and may be different for each vendor. The Testbed architecture insulates both the engineer and the methods developer from those differences by providing a consistent interface across various computer systems. The Testbed command language CLAMP procedures and application processors may be accessed as part of a methods research activity or as part of an application study. The methods development environment of the CSM Testbed is further described by Gillian and Lotts [26]. One goal of the CSM Testbed is to provide a common structural analysis environment for three types of users — engineers solving complex structures problems, researchers developing advanced structural analysis methods, and developers designing the software architecture to exploit multiprocessor computers.

4.2 Global/Local Analysis Processors

Processor SPLN (see ref. [25]) evaluates the spline coefficient matrix $\mathbf{S_g}(x_i, y_i)$ given in Eq. 3.15. The coordinates of the global model within the interpolation region are read from the Testbed data library. The spline coefficient matrix is formed, inverted, and stored in the database. Other data associated with the interpolation region (*i.e.*, coordinates and node numbers) are also written to the database. The matrix is evaluated once for each interpolation region specified.

Processor INTS (see ref. [25]) reads the spline coefficient matrix and the other associated data from the Testbed data library. In addition, the displacement and rotation components at each node within the interpolation region are read. Each

field is independently used to define the vector $\mathbf{f_g}$ in Eq. 3.15. Processor INTS solves for a set of interpolation coefficients $\mathbf{a} = \{a_i, F_i\}^T$ for each field and performs the local interpolation for each field to obtain the "boundary conditions" for the local model.

4.3 Global/Local Analysis Procedures

Runstreams are the vehicle used to perform structural analyses with the CSM Testbed. The term "runstream" most commonly refers to the file (or files) used to perform a specific analysis. A runstream will typically contain CLAMP directives and procedures. The runstream which performs the complete, linear global analysis of an isotropic panel with a circular cutout discussed in Chapter 5 is given in Appendix B. A driver procedure calls subsequent lower level procedures to perform the analysis.

The runstream used to generate the spline coefficient matrix, interpolate the global solution, and perform the local analysis for the square local model (Model LC1) discussed in Chapter 5 is given in Appendix C. A driver command file is used in the analysis. This driver command file calls subsequent CLAMP procedures for different phases of the analysis. These CLAMP procedures have been included in Appendix C for completeness. The procedure flow and in-line comments have been provided for both the global and local analyses.

Chapter 5

Numerical Results

5.1 Problem Selection

The effectiveness of the computational strategy for the global/local stress analysis outlined in the previous chapters is demonstrated by obtaining the detailed stress states for an isotropic panel with a cutout and a blade–stiffened graphite–epoxy panel with a discontinuous stiffener. The first problem was selected to verify the global/local analysis capabilities while the second problem was selected to demonstrate its use on a representative aircraft subcomponent. The objectives of these numerical studies are:

1. To demonstrate the global/local stress analysis methodology, and
2. To obtain and interrogate the detailed stress states of representative subcomponents of complete aerospace structures.

All numerical studies were performed on the NASA Langley Research Center Convex C220 minisupercomputer. The computational effort of each analysis is quantified by the number of degrees of freedom used in the finite element model, the computational time required to perform a stress analysis, and the amount of auxiliary storage required. The computational time is measured in central processing unit (CPU) time. The amount of auxiliary storage required is measured by the size of the data library used for the input/output of information to a disk during a Testbed execution.

5.2 Isotropic Panel Results

Panels with cutouts are common subcomponents of structures in the aerospace industry. Although, the use of composite materials has become prominent for secondary aircraft components, most primary aircraft components (*i.e.*, wing, fuselage) are currently made from isotropic materials (*e.g.*, aluminum). The isotropic panel with a cutout shown in Fig. 5.1 is an ideal structure to demonstrate the global/local computational strategy, since closed–form elasticity solutions are available. Elasticity solutions for an infinite isotropic panel with a circular cutout (*e.g.*, Timoshenko and Goodier [28]), predict a stress concentration factor of three at the edge of the cutout. The influence of finite–width effects on the stress concentration factors for isotropic panels with cutouts have been reported by Peterson [29]. The stress concentration factor as a function of the cutout diameter to width ratio ($\frac{2r_0}{W}$) is shown in Fig. 5.1. By including finite–width effects, the stress concentration factor is reduced from the value of three for an infinite panel.

When using theoretical stress concentration factors K_t, one of the points that should be borne in mind is that the stress concentration factors should be applied to the nominal stresses. The nominal stresses are based on the same cross sectional area as that used for the original determination of the stress concentration factor [30]. This area is usually the net sectional area A_{net} which remains after any notch has been cut. For the case of a cutout, the net sectional area corresponds to

$$A_{net} = (W - 2r_0)h = Wh(1 - \frac{2r_0}{W}) \tag{5.1}$$

where r_0 is the radius of the cutout, W is the overall width of the panel and h is the panel thickness. The nominal longitudinal stress $(\sigma_x)_{nom}$ for a uniform axial load P can then be expressed as

$$(\sigma_x)_{nom} = \frac{P}{A_{net}} \tag{5.2}$$

where P is the applied load. From this value, the longitudinal stress resultant $(N_x)_{nom}$ for an isotropic panel is readily obtained as

$$(N_x)_{nom} = (\sigma_x)_{nom} h \tag{5.3}$$

The stress concentration factor K_t corresponds to the ratio of the maximum longitudinal stress to the nominal longitudinal stress,

$$K_t = \frac{(\sigma_x)_{max}}{(\sigma_x)_{nom}} \quad \text{or} \quad K_t = \frac{(N_x)_{max}}{(N_x)_{nom}} \tag{5.4}$$

The global/local linear stress analysis of the isotropic panel with a circular cutout shown in Fig. 5.1 has been performed. The overall panel length L is 20 in., the overall width W is 10 in., the thickness h is .1 in., and the cutout radius r_0 is 0.25 in. This geometry gives a cutout diameter to panel width ratio of 0.05 which corresponds to a stress concentration factor of 2.85 from Fig. 5.1. The loading is uniform axial tension with the loaded ends of the panel clamped and the sides free. The material system for the panel is aluminum with a Young's modulus of 10,000 ksi and Poisson's ratio of 0.3.

5.2.1 Global Analysis

Predicting the global structural response of these structures often has many objectives including overall structural response, stress analysis, and determining internal loads distributions. Frequently, structural discontinuities such as cutouts are only accounted for in the overall sense.

The finite element model shown in Fig. 5.2 of the isotropic panel with a circular cutout is a representative finite element model for representing the global behavior of the panel as well as a good approximation to the local behavior. The finite element model shown in Fig. 5.2, will be referred to as the "coarse" global model or Model G1 in Table 5.1. The finite element model has a total of 256 4-node quadrilateral

elements, 296 nodes, and 1644 active degrees of freedom for the linear stress analysis. This quadrilateral element corresponds to a flat C^1 shell element which is based on a displacement formulation and includes rotation about the outward normal axis. Originally developed for the computer code STAGS (see refs. [31, 32]), this element has been installed in the CSM Testbed software system and denoted ES5/E410 (see ref. [25]).

Contour plots of the inplane stress resultants obtained using the "coarse" global model are shown in Figs. 5.3 and 5.4. The longitudinal stress resultant N_x distribution shown in Fig. 5.3 reveals several features of the global structural behavior of this panel. First, away from the cutout, the N_x distribution in the panel is uniform. Secondly, the N_x load near the center of the panel is much greater than the N_x load in other portions of the panel due to the redistribution of the N_x load as a result of the cutout. Thirdly, the N_x load at the edge of the cutout at ninety degrees away from the stress concentration is small relative to the uniform far–field stress state. The transverse inplane stress resultant N_y distribution shown in Fig. 5.4 indicates a smaller stress gradient ninety degrees from the N_x gradient. This gradient may have a secondary influence on the definition of the global/local interface boundary.

The distribution of the longitudinal stress resultant N_x at the panel midlength normalized by the nominal stress resultant is shown in Fig. 5.5 as a function of the distance from the cutout normalized by the cutout radius. The results indicate that high inplane stresses and a high gradient exist near the cutout. However, a stress concentration factor of 2.06 is obtained from a linear stress analysis using the "coarse" finite element model (see Fig. 5.2). This value is 28% lower than the theoretical value of 2.85 reported by Peterson [29]. Therefore, even though the overall global response of the panel is qualitatively correct as indicated by the

stress resultant contours in Figs. 5.3 and 5.4, the detailed stress state near the discontinuity is inaccurate.

Accurate detailed stress distributions require a finite element mesh that is substantially more refined near the cutout. Adding only rings of elements (Model G2 in Table 5.1) does not affect the discretization away from the cutout, however, the stress concentration factor is still 22% lower than the theoretical value. To obtain a converged solution for the stress concentration factor, a sequence of successively refined finite element models were developed by increasing the number of radial spokes of nodes and rings of elements in the region around the cutout. A converged solution is obtained using a total of 3168 4-node quadrilateral shell elements (ES5/E410) in the global model. Using an intermediate refined finite element model with a total of 832 4-node quadrilateral elements, 888 nodes, and 5156 active degrees of freedom, a stress concentration factor of 2.72 is obtained which is within 4.6% of the theoretical solution. This finite element model is referred to as the "refined" global model or Model G3 in Table 5.1. Normalized longitudinal stress resultant N_x distributions are shown in Fig. 5.5 for the "coarse" global model (G1) and the "refined" global model (G3). The stress gradient for this panel becomes nearly zero at a distance from the center of the panel of approximately six times the cutout radius.

The inplane stress resultant distributions obtained using the "refined" global model are qualitatively the same as the distributions obtained for the "coarse" global model (shown in Figs. 5.3 and 5.4, respectively). The value of the longitudinal inplane stress resultant N_x near the center of the panel is larger for the "refined" model than for the "coarse" model indicating that the refined model more accurately predicts the stress gradient near the cutout. The N_x load at the edge of the cutout

ninety degrees away from the stress concentration is closer to zero for the "refined" model than for the "coarse" model.

The distribution of the strain energy for Model G1 is shown in Fig. 5.6. The change in the strain energy per unit area within the transition square indicates that a high stress gradient exists near the cutout and rapidly decays away from the cutout. These results are consistent with the structural analyst's intuition, and the local analyses described subsequently will further interrogate the region near the cutout.

5.2.2 Local Analyses

A global/local analysis capability provides an alternative to global mesh refinement and a complete solution using a more refined mesh. For this example, the "critical" region is well known and easily identified by even a casual examination of the stress resultant distributions given in Fig. 5.3. The global model, the interpolation region and the local models considered are shown in Fig. 5.7. The global model corresponds to the "coarse" global model (G1) and the shaded region corresponds to the interpolation region which is used to generate the spline matrix and to extract boundary conditions for the local models. As indicated in Fig. 5.7, two different local models are considered: one square and one circular. Both local models completely include the critical region with the stress concentration. The boundary of the square local model coincides with the boundary of the transition square in the global model. The circular model is inscribed in the transition square. That is, the outer radius of the circular model is equal to half the length of a side of the transition square. Both local models (Models LS1 and LC1 in Table 5.1) have the same number of 4-node quadrilateral shell elements (512), number of nodes (544) and number of degrees of freedom (3072). Both local models have only 62% of the elements used in the refined global analysis. The global/local interpolation

for both local models is performed from the data obtained from the "coarse" global model analysis. The radius of the interpolation region R_I is $5.7r_0$ which includes the 48 data points within the transition square of the global model.

The distribution of the longitudinal stress resultant N_x at the panel midlength normalized by the nominal stress resultant using the square local model is shown in Fig. 5.8a as a function of distance from the cutout normalized by the cutout radius. These results indicate that the global/local analysis based on the coarse global solution and the square local model accurately predicts the stress concentration factor at the cutout as well as the distribution at the global/local interface boundary. A stress concentration factor of 2.76 is obtained which is within 1.5% of the "refined" global model (G3) solution and 3.2% of the theoretical solution. A contour plot of the longitudinal stress resultant distribution is given in Fig. 5.8b and indicates that the local solution correlates well overall with the global solution shown in Fig. 5.3.

The distribution of the longitudinal stress resultant N_x at the panel midlength normalized by the nominal stress resultant obtained using the circular local model is shown in Fig. 5.9a as a function of distance from the cutout normalized by the cutout radius. These results indicate that the global/local analysis based on the coarse global solution and the circular local model accurately predicts the stress concentration factor at the cutout. A stress concentration factor of 2.75 is obtained which is within 1.5% of the "refined" global model (G3) solution and 3.2% of the theoretical solution. At the global/local interface boundary, the results from the circular local model differ slightly from the results obtained from the refined global model analysis. This difference is attributed to interaction between the "coarse" global model, the interpolation region, and the location of the global/local interface boundary. A contour plot of the longitudinal stress resultant distribution is given

in Fig. 5.9b and indicates the overall correlation with the distributions obtained using the global models.

The interaction between the global model, the interpolation region, and the location of the global/local interface boundary is assessed below. This assessment involves refining the global model in the transition square, varying the radius of the interpolation region R_I and varying the radius of the local model R_L. Using an interpolation region defined as $R_I = 14r_0$ (72 points from the global model), several local models are considered in which R_L is increased from twice the cutout radius to five times the cutout radius. The results in Fig. 5.10a are based on using the coarse global model (G1) for the global solution. These results indicate that the local solution deteriorates as the global/local interface boundary is moved closer to the cutout. The results in Fig. 5.10b are based on a slightly more refined global model(G2) for the global solution. This global model has two additional rings of elements in the transition square. Comparing the results in Figs. 5.10a and 5.10b reveals the interaction between the global model and the location of the interface boundary. To obtain an accurate local solution for the case when the global/local interface boundary is located within a region with a high stress gradient requires that sufficient data from the global model be available in the area to provide accurate "boundary conditions" for the local model. These results indicate that by adding just two rings of elements near the cutout (Model G2), the extraction of the local model boundary conditions from the spline interpolation is improved such that the global/local interface boundary may be located very near the cutout.

The influence of the radius of the interpolation region on the local solution is determined to be minimal provided the global model discretization is adequate. For the cases considered, identical local solutions are obtained using an interpolation

region larger than the local model or an interpolation region which coincides with the local model.

For the isotropic panel with a central cutout, the critical region is known. It may be desirable to model only a portion (*e.g.*, part of annular plate or sector) of the structural region around the cutout. Three sector models were considered including a $\pm 45°$ sector, a $\pm 67.5°$ sector, and a $\pm 90°$ sector, each with its center at 90° from the loading direction. The interpolation is performed from the "coarse" global model solution. The sector local analyses introduce several additional factors not evident in the previous local analyses. The longitudinal stress resultant N_x distributions at the panel midlength for the sector local models differ slightly at the cutout edge from the distribution obtained for the circular local model. The N_x distribution around the circumference of the cutout reveals an inaccurate distribution at the straight edges of the sectors. The error in the N_x distribution along the sector straight edges may be attributed to their proximity to the gradient of the longitudinal stress resultant. The straight edges of the smaller $\pm 45°$ sector are near the N_x stress resultant gradient, while the straight edges of the $\pm 90°$ sector are in a region in which a secondary gradient associated with the transverse inplane stress resultant, N_y (see Figs. 5.3 and 5.4), may affect the accuracy of the interpolated boundary conditions. Applying boundary conditions at the cutout edge may also be, in effect, over constraining the local structural model. These sector analyses reinforce the importance of the local model boundary location.

The influence of the global model discretization on the accuracy of the solution obtained by the $\pm 90°$ sector local model was assessed. The interpolation was performed from successively more refined global models. As the global model refinement was increased, a more accurate N_x distribution was obtained. The results from the sector analyses reduce the feasibility of modeling a portion of the cutout

in this manner. The global modeling requirements must be increased substantially to maintain the same level of accuracy for the sector local model analyses as for the circular local model analysis.

5.2.3 Computational Requirements

A summary of the computational requirements for the global and local analyses of the isotropic panel with the circular cutout is given in Table 5.2. The computational cost in central processing unit (CPU) seconds of the local analyses is approximately 74% of the CPU time of the refined global analysis. The CSM Testbed data libraries for the local analyses are 41% smaller than the data library for the refined global analysis. The local models have 60% and 16% of the total number of degrees of freedom required for the refined model (G3) and converged global model, respectively.

5.2.4 Usage Guidelines

Usage guidelines derived from the global/local analysis of the isotropic panel with a circular cutout are as follows. An "adequate" global analysis is required to ensure a sufficient number of accurate data points to provide accurate "boundary conditions" for the local model. When the global/local interface boundary, R_L is within the high stress gradient (*i.e.*, within a distance of two times the cutout radius from the cutout edge), the importance of an "adequate" global analysis in the high gradient region is increased. The interpolation region should coincide with or be larger than the local model. To satisfy the compatibility requirements at the global/local interface boundary, the local model boundary R_L should be defined sufficiently far from the cutout (*i.e.*, a distance of approximately six times the radius from the cutout).

5.3 Blade–Stiffened Panel Results

Discontinuities and eccentricities are common in aircraft structures. For example, the lower surface of the Bell–Boeing V-22 tilt–rotor wing structure has numerous cutouts and discontinuous stiffeners (see Fig. 5.11). Predicting the structural response of such structures in the presence of discontinuities, eccentricities, and damage is particularly difficult when the component is built from graphite–epoxy materials or is loaded into the nonlinear range. In addition, potential damage of otherwise perfect structures is often an important design consideration. Recent interest in applying graphite–epoxy materials to aircraft primary structures has led to several studies of postbuckling behavior and failure characteristics of graphite–epoxy components (see ref. [33]). One goal of these studies has been the accurate prediction of the global response of the composite structural component in the postbuckling range. In one study of composite stiffened panels, a blade–stiffened panel was tested (see ref. [34]). A composite blade–stiffened panel was proof–tested and used as a "control specimen". The panel was subsequently used in a study on discontinuities in composite blade–stiffened panels. The global structural response of these composite blade–stiffened panels presented in reference [35] correlate well with the earlier experiment data. The composite blade–stiffened panel with a discontinuous stiffener shown in Fig. 5.12 is representative of a typical aircraft structural component and will be used to demonstrate and assess the global/local methodology. This problem was selected because it has characteristics which often require a global/local analysis. These characteristics include a discontinuity, eccentric loading, large displacements, large stress gradients, high inplane loading, and a brittle material system. This problem represents a generic class of laminated composite structures with discontinuities for which the interlaminar stress state becomes important. The local and global finite element modeling and analysis needed to

predict accurately the detailed stress state of flat blade–stiffened graphite–epoxy panels loaded in axial compression is described in this section.

The overall panel length L is 30 in., the overall width W is 11.5 in., the stiffener spacing b is 4.5 in., the stiffener height h_s is 1.4 in., and the cutout radius r_0 is 1.0 in. The three blade–shaped stiffeners are identical. The loading is uniform axial compression. The loaded ends of the panel are clamped and the sides are free. The material system for the panel is T300/5208 graphite–epoxy unidirectional tapes with a nominal ply thickness of 0.0055 in. Typical lamina properties for this graphite–epoxy system are 19,000 ksi for the longitudinal Young's modulus, 1,890 ksi for the transverse Young's modulus, 930 ksi for the shear modulus, and 0.38 for the major Poisson's ratio. The blade–stiffeners are 24-ply laminates $\left([\pm 45/0_{20}/\mp 45]\right)$ and the panel skin is a 25-ply laminate $\left([\pm 45/0_2/\mp 45/0_3/\pm 45/0_3/\mp 45/0_3/\pm 45/0_2/\mp 45]\right)$.

End–shortening results are shown in Fig. 5.13 for the "control specimen" and for the configuration with a discontinuous stiffener. These results indicate that the presence of the discontinuity markedly changes the structural response of the panel. The structural response of the "control specimen" is typical of stiffened panels. Two equilibrium configurations are exhibited; namely, the prebuckling configuration and the postbuckling configuration. The structural response of the configuration with a discontinuous stiffener is nonlinear from the onset of loading due to the eccentric loading condition and the cutout. The blade–stiffened panel with a discontinuous stiffener was tested to failure. Local failures occurred prior to overall panel failure as is evident from the end–shortening results shown in Fig. 5.13.

5.3.1 Global Analysis

A global linear stress analysis of the composite blade–stiffened panel with a discontinuous stiffener was performed for an applied load corresponding to P/EA of 0.0008 (*i.e.*, an applied compressive load P of 19,280 pounds normalized by the

extensional stiffness EA). At this load level, the structural response of the panel is essentially linear. Four–node quadrilateral elements (ES5/E410) were used in the linear analysis. Out–of–plane deflections are present, however, due to the eccentric loading condition caused by the discontinuous stiffener. Several global finite element models are considered as indicated in Table 5.3 to obtain a converged solution for comparison purposes since the theoretical solution is not available. The value of the longitudinal stress resultant at the edge of the cutout changed by less than 2% between Models G2 and G4. Therefore, Model G1 will be referred to as the "coarse" global model (see Fig. 5.14), Model G2 will be referred to as the "refined" global model, and Model G4 will be referred to as the "converged" global model.

The distribution of the longitudinal stress resultant N_x normalized by the applied running load $(N_x)_{avg}$ (*i.e.*, applied load divided by the panel width) as a function of the lateral distance from the center of the panel normalized by the radius of the cutout is shown in Fig. 5.15 for both the "coarse" (G1) and the "refined" (G2) global models. These results are similar to those obtained for the isotropic panel with a cutout. The maximum longitudinal stress resultants $(N_x)_{max}$ normalized by the average running load $(N_x)_{avg}$ are given in Table 5.3. The results obtained using the coarse global model adequately predicts the distribution away from the discontinuity but underestimates (by 24%) the stress concentration at the edge of the discontinuity.

Oblique views of the deformed shape with exaggerated deflections are shown in Figs. 5.16 and 5.17 for the coarse global model with contour plots of the inplane stress resultants N_x and N_y, respectively. The distribution indicates that the model provides good overall structural response characteristics. The N_x distributions reveal several features of the global structural behavior of this panel. First, away from the discontinuity, the N_x distribution in the panel skin is nearly uniform and

less than the value of the N_x load in the outer two blade–stiffeners. Second, load is diffused from the center discontinuous stiffener into the panel skin rapidly such that the center stiffener has essentially no N_x load at the edge of the cutout. Third, the N_x load in the outer stiffeners increases towards the center of the panel and is concentrated in the blade free edges (*i.e.*, away from the stiffener attachment line at the panel skin). Fourth, the N_x load in the panel skin near the center of the panel is much greater than the N_x load in other portions of the panel skin.

The distribution of the strain energy for Model G1 is shown in Fig. 5.18. The change in the strain energy per unit area within the transition square again indicates that a high stress gradient exists near the discontinuity and rapidly decays away from the discontinuity. These results are consistent with the structural analyst's intuition, and the local models described subsequently will further interrogate the region near the discontinuity. For this load level, the skin–stiffener interface region has not yet become heavily loaded. However, this region will also be studied further to demonstrate the flexibility of the global/local stress analysis procedure presented herein.

5.3.2 Local Analyses

A global/local analysis capability provides an alternative approach to global mesh refinement and a complete solution using a more refined mesh. For this example, one "critical" region is easily identified by even a casual examination of the stress resultant distributions given in Fig. 5.16. A second critical region that may require further study is indicated by the slight gradient near the intersection of the blade–stiffener and the panel skin as shown in Fig. 5.15. Skin–stiffener separation has been identified as a dominant failure mode for stiffened composite panels (*e.g.*, see refs. [33-37]). The global model, the interpolation regions and the local models considered are shown in Fig. 5.19. The global model corresponds to the "coarse"

global model (G1) and the shaded regions correspond to the interpolation regions which are used to generate the spline matrix and to extract boundary conditions for the local models. As indicated in Fig. 5.19, two different critical regions are considered. One region is near the discontinuity and again square and circular local models are used in the local analysis. The boundary of the square local model coincides with the boundary of the transition square in the global model. The circular model is inscribed in the transition square. That is, the outer radius of the circular model is equal to half the length of a side of the transition square. The other region is near the skin–stiffener interface region at the panel midlength for one of the outer stiffeners. The global/local interpolation for all local analyses is performed from the data obtained from the "coarse" global model analysis. Two interpolation regions were used for each of the local analyses. The first interpolation region, specified in the plane of the panel skin, is used to obtain the boundary conditions on the global/local interface boundary of the panel skin. The second interpolation region, specified in the plane of the stiffener, is used to obtain the boundary conditions on the global/local interface boundary of the stiffener. The boundary conditions for the panel skin and the stiffener were interpolated separately. Compatibility of the displacements and rotations at the skin–stiffener intersection on the global/local boundaries was enforced by imposing the boundary conditions obtained for the panel skin.

The local models (Models LS1 and LC1 in Table 5.3) of the first critical region near the discontinuity have the same number of 4-node quadrilateral shell elements (576), number of nodes (612) and number of degrees of freedom (3456). Both local models have only 56% of the elements used in the refined global analysis. The results for the two local models are nearly the same, and therefore only the results of the circular local model (LC1) are shown in Table 5.3. The distribution of the longitudinal stress resultant N_x at the panel midlength normalized by the average

running load $(N_x)_{avg}$ for Model LC1 is shown in Fig. 5.20a as a function of lateral distance from the cutout normalized by the cutout radius. These results indicate that the global/local analysis based on the coarse global solution and using either the square or circular local model accurately predicts the stress concentration factor at the cutout as well as the distribution at the global/local interface boundary. A contour plot of the longitudinal stress resultant distribution is given in Fig. 5.20b. These results indicate that the local solution correlates well with the global solution shown in Fig. 5.16.

The second critical region near the intersection of the outer blade–stiffener and the panel skin at the midlength is studied further. Three different local finite element models of this critical region are considered as indicated in Table 5.3. The first, Model LR1, has the same number of nodes (25) and number of elements (16) within the critical region as the coarse global model (G1). The second, Model LR2, has the same number of nodes (45) and number of elements (32) within the critical region as the refined global model (G2). The third and most refined model, Model LR3, has 117 nodes, 96 elements and 462 degrees of freedom. The longitudinal stress resultant N_x distributions obtained for the local models (LR1 and LR2) correlate well with the N_x distributions for the coarse and refined global models (Models G1 and G2). However, these models are not sufficiently refined in the skin–stiffener interface region to accurately predict the gradient at the skin–stiffener intersection. The distribution of the longitudinal stress resultant N_x normalized by the applied running load as a function of the lateral distance from the center of the panel normalized by the radius of the cutout is shown in Fig. 5.21. These results indicate that the global/local analysis using the local model Model LR3 predicts a higher gradient at $\frac{y}{r_0} = -4.5$ in the skin–stiffener interface region than the other global and local analyses. A third global model Model G3 is used to investigate the local structural behavior predicted by Model LR3. The global analysis performed with

Model G3 predicts the same local behavior as the analysis performed with Model LR3 as indicated in Fig. 5.21. Several factors should be borne in mind. First, the local analysis revealed local behavior at the skin–stiffener interface region that was not predicted by either of the global models. Second, the global modeling requirement for examining the skin–stiffener interface region is substantial. Because the global models were generated to predict the stress distribution around the discontinuity, additional radial "spokes" in the transition square are required to refine the panel skin in the skin–stiffener interface region in the longitudinal direction. Third, the global/local analysis capability provides the analyst with the added modeling flexibility to obtain an accurate detailed response at multiple critical regions (*i.e.*, at the discontinuity and at the skin–stiffener interface region) with minimal modeling and computational effort.

5.3.3 Computational Requirements

A summary of the computational requirements for the global and local analyses of the graphite–epoxy blade–stiffened panel with the discontinuous stiffener is given in Table 5.4. The computational cost in CPU seconds of the local analyses around the discontinuity is approximately 57% of the CPU time of the refined global analysis. The CSM Testbed data libraries for the local analyses are approximately half of the size of the data library for the refined global analysis. The local models have 55% and 16% of the total number of degrees of freedom required for the refined model (G2) and converged global model (G4), respectively. The CPU time for the refined local analysis (LR3) of the skin–stiffener interface region is 24% of the CPU time required for the global analysis with Model G3. The size of the data library for the local analysis is 5% of the size of the data library required for the analysis with Model G3.

5.3.4 Usage Guidelines

Usage guidelines derived from the global/local analysis of the blade–stiffened panel with a discontinuous stiffener are as follows. An "adequate" global analysis is required to ensure a sufficient number of accurate data points to provide accurate "boundary conditions" for the local model. When the global/local interface boundary, R_L is within the high stress gradient (*i.e.*, within a distance of two times the cutout radius from the cutout edge), the importance of an "adequate" global analysis in the high gradient region is increased. The interpolation region should coincide with or be larger than the local model. To satisfy the compatibility requirements at the global/local interface boundary, the local model boundary R_L should be defined sufficiently far from the cutout (*i.e.*, a distance of approximately six times the radius from the cutout). For the blade–stiffened panel, two interpolation regions should be specified, one for the interpolation of the boundary conditions on the boundary of the panel skin and a second for the interpolation of the boundary conditions on the outer edges of the stiffeners.

Chapter 6

Conclusions and Recommendations

6.1 Conclusions

A global/local analysis methodology for obtaining the detailed stress state of structural components is presented. The methodology presented is not restricted to having a priori knowledge of the location of the regions requiring a detailed stress analysis. The effectiveness of the global/local analysis capability is demonstrated by obtaining the detailed stress states of an isotropic panel with a cutout and a blade–stiffened graphite–epoxy panel with a discontinuous stiffener.

Although the representative global finite element models represent the global behavior of the structures, substantially more refined finite element meshes near the cutouts are required to obtain accurate detailed stress distributions. Embedding a local refined model in the complete structural model increases the computational requirements. The computational effort for the independent local analyses is less than the computational effort for the global analyses with the embedded local refinement.

The global/local analysis capability provides the modeling flexibility required to address detailed local models as their need arises. This modeling flexibility was demonstrated by the local analysis of the skin–stiffener interface regions of the blade–stiffened panel with a discontinuous stiffener. This local analysis revealed local behavior that was not predicted by the global analysis.

The definition of the global/local interface boundary affects the accuracy of the local detailed stress state. The strain energy per unit area has been selected as a

means for identifying a critical region and the location of the associated global/local interface boundary. The change in strain energy from element to element indicates regions with high stress gradients (*i.e.*, critical regions). A global/local interface boundary is defined outside of a region with large changes in strain energy.

The global/local analysis capability presented provides a general–purpose analysis tool for use by the aerospace structural analysis community by providing an efficient strategy for accurately predicting local detailed stress states that occur in structures discretized with relatively coarse finite element models. The coarse model represents the global structural behavior and approximates the local stress state. Independent, locally refined finite element models are used to accurately predict the detailed stress state in the regions of interest based on the solution predicted by the coarse global analysis.

6.2 Recommendations

Future studies related to the present work are recommended. The present work provides initial capabilities for the global/local linear stress analysis of structural components and subcomponents. Additional recommended studies include:

1. Extending the global/local interpolation procedure to a three–dimensional domain;
2. Automating the procedure for selecting the global/local interface boundary;
3. Developing a multiple local region analysis strategy which exploits concurrent processing;
4. Extending the global/local analysis strategy to geometrically nonlinear problems; and,
5. Assessing the use of hierarchical plate theories for the local stress analyses.

References

1. Pagano, N. J.; and Soni, S. R.: Global-Local Laminate Variational Model. International Journal for Solids and Structures, Vol. 19, No. 3, 1983, pp. 207-228.

2. Soni, S. R.; and Pagano, N. J.: Elastic Response of Composite Laminates. Proceedings of the International Union of Theoretical and Applied Mechanics Symposium on Mechanics of Composite Materials, Hashin, Z.; and Herakovich, C. T. (editors), Blacksburg, VA, August 16-19, 1982, pp. 227-242.

3. Hopkins, Dale A.; and Chamis, Christos C.: Nonlinear Analysis for High–Temperature Composites – Turbine Blades/Vanes. Proceedings of NASA Workshop on Nonlinear Structural Analysis, NASA CP 2297, 1984, pp. 131-147.

4. Knight, N. F., Jr.; Greene, W. H.; and Stroud, W. J.: Nonlinear Response of a Blade–Stiffened Graphite–Epoxy Panel with a Discontinuous Stiffener. Proceedings of NASA Workshop on Computational Methods in Structural Mechanics and Dynamics, W. J. Stroud; J. M. Housner; J. A. Tanner; and R. J. Hayduk (editors), June 19-21, 1985, NASA CP–3034 - PART 1, 1989, pp. 51-66.

5. Noor, A. K.: Global–Local Methodologies and Their Application to Nonlinear Analysis. Finite Elements in Analysis and Design, Vol. 2, No. 4, December 1986, pp. 333-346.

6. Wilkins, D. J.: A Preliminary Damage Tolerance Methodology for Composite Structures. Proceedings of NASA Workshop on Failure Analysis and Mechanisms of Failure of Fibrous Composite Structures, A. K. Noor, M. J. Shuart, J. H. Starnes, Jr., and J. G. Williams (compilers), NASA CP–2278, 1983, pp. 61-93.

7. Han, T.; and Abel, J. F.: Computational Strategies for Nonlinear and Fracture Mechanics, Adaptive Substructuring Techniques in Elasto–Plastic Finite Element Analysis. Computers and Structures, Vol. 20, No. 1-3, 1985, pp. 181-192.

8. Clough, R. W.; and Wilson, E. L.: Dynamic Analysis of Large Structural Systems with Local Nonlinearities. Computer Methods in Applied Mechanics and Engineering, Vol. 17/18, Part 1, January 1979, pp. 107-129.

9. Anon.: ANSYS User's Manual, Swanson Analysis Systems, Inc., Houston, PA, 1979.

10. Zimmerle, D.: Generation of Variable Order Elements by Superelement Generation. Computers and Structures, Vol. 22, No. 3, 1986, pp. 291-297.

11. Bathe, K. J.: Finite Element Procedures in Engineering Analysis. Prentice-Hall, Inc., New Jersey, 1982, pp. 199-207.

12. Griffin, O. H., Jr.; and Vidussoni, M. A.: Global/Local Finite Element Analysis of Composite Materials. Computer–Aided Design in Composite Material Technology, C. A. Brebbia, W. P. de Wikle, and W. R. Blain (editors), Proceedings of the International Conference for Computer–Aided Design in Composite Material Technology, Southampton, UK, April 13-15, 1988, pp. 513-524.

13. Schwartz, D. J.: Practical Analysis of Stress Raisers in Solid Structures. Proceedings of the 4th International Conference on Vehicle Structural Mechanics, Warrandale, PA, Nov. 1981, pp. 227-231.

14. Kelley, F. S.: Mesh Requirements of a Stress Concentration by the Specified Boundary Displacement Method. Proceedings of the Second International Computers in Engineering Conference, ASME, Vol. 3, San Diego, CA, Aug. 1982, pp. 39-42.

15. Schaeffer, H. G.: MSC/NASTRAN Primer, Static and Normal Modes Analysis. Schaeffer Analysis, Inc., Mont Vernon, New Hampshire, 1979, pp. 262-265.

16. Jara-Almonte, C. C.; and Knight, C. E.: The Specified Boundary Stiffness/Force SBSF Method for Finite Element Subregion Analysis. International Journal for Numerical Methods in Engineering, Vol. 26, 1988, pp. 1567-1578.

17. Hirai, I.; Wang, B. P.; and Pilkey, W. D.: An Efficient Zooming Method for Finite Element Analysis. International Journal for Numerical Methods in Engineering, Vol. 20, 1984, pp. 1671-1683.

18. Hirai, I.; Wang, B. P.; and Pilkey, W. D.: An Exact Zooming Method. Finite Element Analysis and Design, Vol. 1, No. 1, April 1985, pp. 61-68.

19. Dong, S. B.: Global–Local Finite Element Methods. State-Of-The-Art Surveys on Finite Element Technology, A. K. Noor and W. D. Pilkey (editors),ASME, New York, 1983, pp. 451-474.

20. Stehlin, P.; and Rankin, C. C.: Analysis of Structural Collapse by the Reduced Basis Technique Using a Mixed Local–Global Formulation. AIAA Paper No. 86-0851-CP, The 27^{th} Structures Dynamics and Materials Conference, San Antonio, TX, May 1986.

21. Ahlberg, J. H.; Nilson, E. N.; and Walsh, J. L.: The Theory of Splines and Their Applications. Academic Press, New York, 1967.

22. Rice, John R.: The Approximation of Functions. Vol. 2, Nonlinear and Multivariate Theory, Addison–Wesley Publishing Co., Reading, Massachusetts, 1969.

23. Gladwell, G. M. L.: Practical Approximation Theory, University of Waterloo Press, 1974.

24. Harder, R. L.; and Desmarais, R. N.: Interpolation Using Surface Splines. Journal of Aircraft, Vol. 9, No. 2, February 1972, pp. 189-191.

25. Stewart, C. B., (compiler): The Computational Structural Mechanics Testbed User's Manual. NASA TM-100644, 1989.

26. Gillian, R. E.; and Lotts, C. G.: The CSM Testbed Software System – A Development Environment for Structural Analysis Methods on the NAS CRAY-2. NASA TM-100642, 1988.

27. McLean, D. M. (editor): MSC/NASTRAN Programmers Manual-MSC NASTRAN Version 63. MSR-50, MacNeal-Schwendler Corp., Oct. 1983.

28. Timoshenko, S. P.; and Goodier, J. N.: Theory of Elasticity. Third Edition, McGraw-Hill Book Company, New York, 1934, pp. 90-97.

29. Peterson, R. E.: Stress Concentration Design Factors. Wiley-International, New York, 1953, pp. 77-88.

30. Juvinall, R. C.: Engineering Considerations of Stress, Strain, and Strength. McGraw-Hill, New York, 1967, pp. 244-249.

31. Almroth, B. O.; Brogan, F. A.; and Stanley, G. M.: Structural Analysis of General Shells - Volume II: User Instructions for STAGSC-1. NASA CR-165671, 1981.

32. Almroth, B. O.; Brogan, F. A.; and Stanley, G. M.: Structural Analysis of General Shells - Volume II: User Instructions for STAGSC-1. Report No. LMSC-D633873, Lockheed Palo Alto Research Laboratory, Palo Alto, CA, December 1982.

33. Starnes, J. H., Jr.; Dickson, J. N.; and Rouse, M.: Postbuckling Behavior of Graphite–Epoxy Panels. ACEE Composite Structures Technology: Review of Selected NASA Research on Composite Materials and Structures, NASA CP–2321, 1984, pp. 137-159.

34. Williams, J. G.; Anderson, M. S.; Rhodes, M. D.; Starnes, J. H., Jr.; and Stroud, W. J.: Recent Developments in the Design, Testing, and Impact–Damage Tolerance of Stiffened Composite Panels. NASA TM–80077, 1979.

35. Knight, N. F., Jr.; McCleary, S. L.; Macy, S. C.; and Aminpour, M. A.: Large–Scale Structural Analysis: The Structural Analyst, The CSM Testbed, and The NAS System. NASA TM-100643, 1989.

36. Starnes, J. H., Jr.; Knight, N. F., Jr.; and Rouse, M.: Postbuckling Behavior of Selected Flat Stiffened Graphite–Epoxy Panels Loaded in Compression. AIAA Journal, Vol. 23, No. 8, pp. 1236-1246.

37. Knight, N. F., Jr.; and Starnes, J. H., Jr.: Postbuckling Behavior of Selected Curved Stiffened Graphite–Epoxy Panels Loaded in Axial Compression. AIAA Journal, Vol. 26, No. 3, pp. 344-352.

APPENDIX A

Derivation of Harder–Desmarais Spline Interpolation Function

The derivation of the spline interpolation function used in this study is given in this appendix and also in reference [24]. The solution to Eq. (3.1) in polar coordinates is given in reference [28] as

$$w(r) = A + Br^2 + C\ln r + \bar{D}r^2\ln r^2 \tag{A.1}$$

The constant, C, in the term $C\ln r$, must be equal to zero to maintain a bounded solution at $r = 0$.

The first step is to determine the deflection due to a point load at the origin. From equilibrium, the point load at the origin may be expressed as

$$p = 2\pi r Q_r \tag{A.2}$$

where $Q_r = D\frac{d}{dr}(\nabla^2 w)$. Differentiating Eq. (A.1) and substituting into Eq. (A.2) yields $\bar{D} = \frac{p}{16\pi D}$. Therefore, the deflection due to a point load at the origin is

$$w(r) = A + Br^2 + (\frac{p}{16\pi D})r^2\ln r^2 \tag{A.3}$$

The deflection of the entire spline will be taken as the sum of the solutions of Eq. (A.3)

$$w(x,y) = \sum_{i=1}^{n}(A_i + B_i r_i^2 + \frac{p_i}{16\pi D}r_i^2\ln r_i^2) \tag{A.4}$$

where $r_i^2 = (x - x_i)^2 + (y - y_i)^2$, n is the total number of nodes in the interpolation region which contains the local model.

The surface spline should be flat a long distance from the applied loads. Let $x = r\cos\theta, y = r\sin\theta$, and expand Eq. (A.4) for large r.

$$w(r,\theta) = r^2 \ln r^2 \sum_{i=1}^{n} \frac{p_i}{16\pi D} + r^2 \sum_{i=1}^{n} B_i - 2r \ln r^2 \sum_{i=1}^{n} (x_i \cos\theta + y_i \sin\theta) \frac{p_i}{16\pi D}$$

$$+2r \sum_{i=1}^{n} (x_i \cos\theta + y_i \sin\theta)(\frac{p_i}{16\pi D} - B_i) + \ln r^2 \sum_{i=1}^{n} (x_i^2 + y_i^2) \frac{p_i}{16\pi D} + \ldots \quad \text{(A.5)}$$

The unbounded terms of the order $r^2 \ln r^2, r^2$, and $r \ln r^2$ can be eliminated from Eq. (A.5) by setting

$$\sum P_i = 0 \quad \text{(A.6)}$$

$$\sum x_i P_i = 0 \quad \text{(A.7)}$$

$$\sum y_i P_i = 0 \quad \text{(A.8)}$$

and

$$\sum B_i = 0 \quad \text{(A.9)}$$

Expanding r_i^2 and substituting into Eq. (A.4) yields

$$w(x,y) = \sum_{i=1}^{n} A_i + (x^2 + y^2) \sum_{i=1}^{n} B_i + \sum_{i=1}^{n} B_i (x_i^2 + y_i^2) - 2x \sum_{i=1}^{n} B_i x_i$$

$$-2y \sum_{i=1}^{n} B_i y_i + \sum_{i=1}^{n} \frac{p_i}{16\pi D} r_i \ln r_i^2 \quad \text{(A.10)}$$

Recall that

$$\sum_{i=1}^{n} B_i = 0 \quad \text{(A.11)}$$

and letting

$$a_0 = \sum_{i=1}^{n} [A_i + B_i (x_i^2 + y_i^2)] \quad \text{(A.12)}$$

$$a_1 = -2 \sum_{i=1}^{n} B_i x_i \quad \text{(A.13)}$$

$$a_2 = -2 \sum_{i=1}^{n} B_i y_i \quad \text{(A.14)}$$

and

$$F_i = \frac{p_i}{16\pi D} \tag{A.15}$$

Eq. (A.4) reduces to

$$w(x,y) = a_0 + a_1 x + a_2 y + \sum_{i=1}^{n} F_i r_i^2 \ln r_i^2 \tag{A.16}$$

where a_0, a_1, a_2 and F_i are undetermined coefficients.

APPENDIX B

Runstream for the Global Analysis of the Isotropic Panel

The CSM Testbed is used for the global analysis of an isotropic panel with a circular cutout. The Testbed command language (see ref. [25]) is used in the analysis. A driver procedure is used to perform the global analysis. The additional lower level procedures are also listed for completeness. The procedure flow is given before the call to the driver procedure and limited in–line documentation is given.

```
cd /scr/jbr
rm ISO_FOC.L01
rm PANEL.PRC
time $CSM_EXE/testbed << *EOI*
*set echo=off
*set plib = 28
*OPEN 1 ISO_FOC.L01
*OPEN/NEW 28 PROCLIB.L28
*add '$GEN_UTIL/utilities.prc'
*add '/usr/u1/knight/csm/prc/utilities/stress.clp'

. Procedure Flow
.  GLOBAL -- Perform analysis
.    MESH_GLOBAL -- Create data for processor CSM1
.    MATDAT      -- Create data for processor LAU
.
*CALL GLOBAL ( es_proc = ES5; es_name = E410; location = 'ALL'; --
               precision = 1;  NNPE = 410; IOPT = 1; NRINGS = 16; --
               NSPOKES = 32; NELS = 0; NELX = 8; NELE = 2; --
               NELBS = 2; RAT = 0.; A = 2.; direction=1 )

*PROCEDURE GLOBAL ( es_proc      = ES1 ; es_name  = EX47 ; --
                    es_pars      = 0.0 ; direction = 1;--
                    location = 'NODES'; precision = 2;  --
                    NNPE = 4; IOPT = 7; NRINGS = 4; --
                    NSPOKES = 16; NELS = 2; NELX = 6; --
                    NELE = 2; NELBS = 2; RAT = 0; A = 4 )
.
*call ES ( function = 'DEFINE ELEMENTS' ; es_proc = [es_proc]; --
          es_name = [es_name]        ; es_pars = [es_pars] )
.
*CALL MESH_GLOBAL ( NNPE = [nnpe]; IOPT = [iopt]; --
                    NRINGS = [nrings]; NSPOKES = [nspokes]; --
```

```
                    NELS = [nels]; NELX = [nelx]; --
                    NELBS = [nelbs]; NELE = [nele]; --
                    RAT = [rat]; A = [A] )
[XQT CSM1
RESET LOAD=TENS
[xqt tab
 online=0
*ADD '/scr/jbr/PANEL.PRC
*CALL PANEL_START
 JLOC
*CALL PANEL_JLOC
 MATC
 1 1.0 0.3
 CON 1
*CALL PANEL_BC
*CALL MATDAT
[xqt lau
[xqt ELD
 online=0
*CALL PANEL_CONN
STOP
*CALL ES ( function = 'DEFINE FREEDOMS')
[xqt aus
 sysvec : APPL MOTI
*CALL PANEL_AD
 STOP
   [xqt E
   [xqt RSEQ
     reset maxcon=41,method=1
   [xqt TOPO
    RESET MAXSUB = 40000,lram = 8196
.
.  ------------------------------------
.  Initialize Element Computational Data
.  ------------------------------------
   *call ES ( function = 'INITIALIZE' )
.
.  ----------------------------------------
.  Form Element Material Stiffness Matrices
.  ----------------------------------------
   *call ES ( function = 'FORM STIFFNESS/MATL' )
.
.  --------------------------------
.  Assemble Material Stiffness Matrix
.  --------------------------------
   [xqt K
.
.  ----------------------
.  Factor Stiffness Matrix
.  ----------------------
   [xqt INV
    online = 2
    reset lra = 7168
```

```
    reset dzero=1.E-10
    reset spdp = [precision]
   [xqt AUS
.
.  ----------------------
.  Solve for Displacements
.  ----------------------
   [XQT SSOL
    RESET SET=1, CON=1
.
.     ---------------------
.     Form Element Stresses
.     ---------------------
     *call STRESS ( STRESS = <true> ; LOCATION = [location]; --
                    DIRECTION = [direction]; SMOOTH = <true> )
     *call STRESS ( STRESS = <true> ; LOCATION = 'NODES'; --
                    DIRECTION = 0  )
*end

*procedure MESH_GLOBAL ( NNPE = 9; IOPT = 7; NRINGS = 4; --
                         NSPOKES = 16; NELS = 0; NELX = 3; --
                         NELBS = 2; NELE = 1; RAT = 0; A = 4. )
[xqt aus
.
. build table of integer user data
.
TABLE(NI=33,NJ=1,itype=0): CSMP FOCS 1 1
J=1: [nnpe] [iopt] [nrings] [nspokes] >
     001 111>    .  Edge x=0.0                (Edge 1)
     000 000>    .  Edge y=A+2*(nele+nelbs)   (Edge 2)
     101 111>    .  Edge x=Al                 (Edge 3)
     000 000>    .  Edge y=0.0                (Edge 4)
     001 111>    .  Corner at (0.,0.)
     011 111>    .  Corner at (0.,[A+2*(nele+nelbs)])
     111 111>    .  Corner at (Al,[A+2*(nele+nelbs)])
     101 111>    .  Corner at (Al,0.)
     011 111>    .  Stiffeners at x=0.0
     111 111>    .  Stiffeners at x=Al
.
. iwall jwall iref jref   nelx     nele       nelbs     nels  ifill
.
    1     1    1     1    [nelx]    [nele]     [nelbs]   [nels]  0
.
. build table of floating point user data
.
TABLE(NI=10,NJ=1): CSMP FOCS 1 2
.
.     a   dhole xc       yc   zc  rat    al    be    bs   hs
.
 J=1: [A]  .5  <[A]/2.>  0.0  0.0 [rat]  20.0    1.    4.  1.4
*END

*procedure MATDAT
```

```
[xqt aus
.
.
. E11 NU12 E22 G12 G13 G23 ALPHA1 ALPHA2 WTDEN
.
     TABLE(NI=16,NJ=1): OMB DATA 1 1
.
     I=1,2,3,4,5,6,7,8,9
*def g = 3.84615e+6
     J=1: 10.0E+6 .30 10.0E+6 <g> <g> <g> 0.0 0.0 .1
.
     TABLE (NI=3,NJ=1,itype=0):  LAM OMB  1  1
           J=1 : 1 .1 0.00
.
*end
[xqt exit
*EOI*
```

APPENDIX C

Runstream for the Global Analysis of the Isotropic Panel

A driver command file is used to perform the local analysis. The command file calls several CLAMP procedures during the analysis. Additional lower level procedures are listed for completeness. The procedure flow is given before the call to each procedure in the driver command file and limited in-line documentation is given.

```
cd /scr/jbr
rm LOC_CSM1.L01 PANEL.PRC
time $CSM_EXE/testbed << *EOI_MAIN*
*set echo=off
*set plib = 28
*OPEN/new 1 LOC_CSM1.L01
*OPEN/NEW 28 PROCLIB.L28
*open/old 2 glob216.l01
*add '$GEN_UTIL/utilities.prc'
*add '/usr/u1/knight/csm/prc/utilities/utilities.prc'
*add '$ISO_PANEL/local/local.prc'
.
*def/a es_proc = 'ES5'
*def/a es_name = 'E410'
*def/i nnpe = 410
*def/i iopt = 1
*def/i nrings = 16        . number of rings of elements
*def/i nspokes = 32      . number of spokes of nodes
.
. Procedure Flow
.  FORM_SPLN_MATR -- Forms and inverts spline coefficient matrix and
.                      reads interpolation region data
.
*CALL FORM_SPLN_MATR ( nels = 0 )
.
.
. Procedure Flow
.  FORM_MOD_CSM1 -- Defines global/local interface boundary and
.                     uses processor CSM1 to generate the model
.    MESH_LOCAL
.    BOUN_COND
.    FORM_PANEL_BOUN
.    FORM_STIFF_BOUN
.
*CALL FORM_MOD_CSM1 ( es_proc = <es_proc>; es_name = <es_name>; --
```

```
                        nrings = <nrings>; nspokes = <nspokes>; --
                        nels  = 0; --
                        NELX = 0; NELE = 0; NELBS = 0; --
                        ndof = 6 )
.
. Procedure Flow
.  INTERP_FIELD -- Generates interpolated local field for each degree
.                  of freedom
.
*CALL INTERP_FIELD ( nels = 0 )
.
. Procedure Flow
.  SOLVE -- Applies ''boundary conditions'' and performs local
.           analysis
.   FORM_APPL_MOTI
.
*CALL SOLVE ( direction = 1; location = 'ALL'; num_strs = 3; --
              nels = 0; --
              ndof = 6; nrings = <nrings>; nspokes  = <nspokes> )
[XQT EXIT
*EOI_MAIN*



.
. procedure FORM_SPLN_MATR - forms the spline interpolation matrices
.                            for the skin and the stiffeners if
.                            applicable
*PROCEDURE FORM_SPLN_MATR ( corner1 = 9.,4.,0.; --
                            corner2 = 11.,6.,0.; --
                            nels = 0; ldi = 2; hs = 1.4; --
                            pdeg = 3; be = 1.25 )
.
*def/i nels == [nels]
*def/e c1[1:3] = [corner1]
*def/e c2[1:3] = [corner2]
.
. *OPEN 2 '/scr/jbr/glob216.101'
 *COPY 1 = [ldi],2:15
 *COPY 1,PROP.*.* = [ldi],PROP.*.*
 *COPY 1,MATC.*.* = [ldi],MATC.*.*
 *COPY 1,STAT.DISP.* = [ldi],STAT.DISP.*
 *CLOSE [ldi]
.
   [xqt SPLN
     RESET DEGREE=[pdeg]
     SURF 1 XLOC=1, YLOC=2, SYM=0
     INPUT
          BOUN 1
          <c1[1]>,<c1[2]>,<c1[3]> <c2[1]>,<c2[2]>,<c2[3]>
STOP
.
. make a separate run through spln for stiffeners
*remark Generate coefficient matrices
```

```
*if <[nels] /ne 0> /then
. *open/new 27 PROCLIB.L27
. *set plib=27
*add '$HOME/focus/STIFF.PRC'
. get global model parameters
[xqt aus
 macro 1 CSMP FOCS 1 1 local 3 3 1 'ngr
 macro 1 CSMP FOCS 1 1 local 4 4 1 'ngs
 macro 1 CSMP FOCS 1 1 local 32 32 1 'ngst
stop
 *OPEN/new 3 bsp_stiff.l03
[XQT SPLN
  RESET SLIB = 3
  RESET DEGREE=2
  RESET ZDATA=1
     SURF 1 XLOC=1, YLOC=2, SYM=0
     INPUT
  BOUN 1
          <c1[1]>,5.,0.  <c2[1]>,5.,[hs]
          DS 1 STIF INPU 1 1
STOP
. *set plib=28
*endif
*end

*procedure MESH_LOCAL ( NNPE = 4; IOPT = 7; NRINGS = 4; --
                        NELS = 2; NELX = 6; NELE = 2; NELBS = 2; --
                        PNSECT=1; SNSECT=1; NSPOKES = 16; --
                        A = 2.; LENGTH=20.; DHOLE=0.5; BE=1.; --
                        BS=4. )
*show arg
.
[xqt aus
.
. build table of integer user data
.
TABLE(NI=33,NJ=1,itype=0): CSMP FOCS 1 1
 J=1: [nnpe]  [iopt] [nrings]  [nspokes] >
      001 111>   .  Edge x=0.0                (Edge 1)
      000 000>   .  Edge y=A+2*(nele+nelbs)   (Edge 2)
      101 111>   .  Edge x=Al                 (Edge 3)
      000 000>   .  Edge y=0.0                (Edge 4)
      001 111>   .  Corner at (0.,0.)
      011 111>   .  Corner at (0.,[A+2*(nele+nelbs)])
      111 111>   .  Corner at (Al,[A+2*(nele+nelbs)])
      101 111>   .  Corner at (Al,0.)
      011 111>   .  Stiffeners at x=0.0
      111 111>   .  Stiffeners at x=Al
.
. iwall   jwall   iref jref  nelx   nele   nelbs     nels  ifill
.
 [pnsect] [snsect]  1   1  [nelx]  [nele]  [nelbs]  [nels]   0
.
```

```
. build table of floating point user data
.
TABLE(NI=10,NJ=1): CSMP FOCS 1 2
.
.     a    dhole       xc   yc   zc   rat   al        be    bs   hs
.
 J=1: [A]  [dhole]  <[A]/2>  0.0  0.0  0.  [length]  [BE]  [BS]  1.4
*END
.
*procedure STIFF_NODE ( nels = 0; nirngs = 4; nspokes = 16; --
                        ds_name = 'STIF' )
*sho arg
*def/i icnt = 0
*def/i nelsx == <2*[nirngs]>
*def/i nnodsx == < <nelsx> + 2 >
*def/i nhole == < <[nirngs]+1>*[nspokes] >
*do $is = 1,2
 *do $js = 1,[nels]
  *def/i icnt = < <icnt> + 1 >
  *def/i nstiff1[<icnt>]==< <nhole>+<<$is>-1>*<<nnodsx>+[nirngs]> --
                           + <<$js>-1>*<[nirngs]+1> + 1 >
 *enddo
*enddo
.
*def/i nnstif1 == <icnt>
.
 [xqt AUS
   TABLE (ni=1,nj=<nnstif1>,ITYPE=0): [ds_name] NODE 1 1
   *do $is = 1,<nnstif1>
    J=<$is>: <nstiff1[<$is>]>
   *enddo
 stop
*end

. procedure BOUN_COND added to facilitate boundary condition
. definition with procedure GEN_SHELL the procedure may
. still be used with original model definition procedures.
.
.
*procedure BOUN_COND ( axial_nodes = 0; --
                       circum_nodes = 0; --
                       es_nodes = 0;     --
                       drilling_dof = ' '; --
                       ndof = 6 )
*if <[es_nodes] /ne 0> /then
 *def/i nnod = < [axial_nodes]*<[circum_nodes]-1> >
 *def/i nnint = <[circum_nodes]-1>
 [xqt AUS
  TABLE (NI=1,NJ=<[circum_nodes]-1>,ITYPE=0): BOUN NODE 1 1
   *do $i=1,<[circum_nodes]-1>
    J = <$i>: < <$i>*[axial_nodes] >
   *enddo
*else
```

```
 *gal2mac /name=nnod /maxn=1 1,JDF1.BTAB.1.8,DATA.1
 *find record_key 1,BOUN.NODE.1.1,DATA.1 /dim=nbn
 *def/i nnint = <nbn>
*endif
[XQT AUS
     MACRO 1 BOUN NODE 1 1 'bnod
[XQT TAB
     online=0
     CON 1
      *if < [ndof] /eq 5 > /then
       NONZERO 1,2,3,4,5
      *else
       NONZERO 1,2,3,4,5,6
      *endif
         *do $i = 1, <nnint>
             <bnod[<$i>]>
         *enddo
         *if <<nels> /ne 0> /then
         *do $i = 1, <nnstif1>
             <nstiff1[<$i>]>
         *enddo
         *endif
*end
.

.
*PROCEDURE FORM_MOD_CSM1 ( es_proc  = ES1 ; es_name  = EX47 ; --
                           nrings = 10; nspokes = 64; nels = 0; --
                           nelx  = 6; nele = 2;  nelbs =2; --
                           pnsect=1; snsect=1; a = 2.; --
                           length=20.; dhole=0.5; be=1.; bs=4.; --
                           ndof = 6 )
.
*call ES ( function = 'DEFINE ELEMENTS' ; es_proc = [es_proc]; --
           es_name = [es_name]          ; es_pars = 0.0 )
.
 *if <ifeqs(<Es_name>;E410)> /then
     *def/i csmnen == 410
     *def/i csmopt == 1
 *elseif <ifeqs(<Es_name>;E43)> /then
     *def/i csmnen == 4
     *def/i csmopt == 0
 *else
     *def/i csmnen == <Es_nen>
     *def/i csmopt == <Es_opt>
 *endif
.
.
*def/i ndf == [ndof]
.
[XQT AUS
     TABLE(NI=1,NJ=<nnint>,ITYPE=0): BOUN NODE 1 1
.
```

```
         *do $i = 1, <nspok>
             J = <$i>: <<<nrings>-1>*<nspok>+<$i>>
         *enddo
stop
*if <[nels] /ne 0> /then
 *call STIFF_NODE ( nels = <nsnody>; nirngs = <nrng>; --
                    nspokes = <nspok>; ds_name = 'STIF' )
*endif
.
.
*CALL MESH_LOCAL ( NNPE = <csmnen>; IOPT = <csmopt>; --
                   NRINGS = <nrng>; NSPOKES = <nspok>; --
                   NELS = [nels]; NELX = [nelx]; --
                   pnsect=[pnsect]; snsect=[snsect]; a = [a]; --
                   dhole=[dhole]; length=[length]; --
                   be=[be]; bs=[bs]; --
                   NELE = [nele]; NELBS = [nelbs] )
.
. *if <[nels] /eq 0> /then
 [XQT CSMX
. *endif
.
[XQT TAB
 *ADD PANEL.PRC
.
*if <<ndf> /eq -6> /then
 START <<nnod>+<nsnod>>
*else
 *CALL PANEL_START
*endif
     online=0
     *def dtheta = < 360./<nspok> >
     *def tend = < 360. - <dtheta> >
     ALTREF
       4 1 0. 2 0. 3 0. 15.0 5.75
     JLOC
       *CALL PANEL_JLOC
.
*call BOUN_COND
.
[XQT ELD
     online=0
      *CALL PANEL_CONN
stop
.
 *call FORM_PANEL_BOUN ( nspok = <nspok>; nrng = <nnrng> )
.
*undefine/global ri,ro,tend,j1,j2,in,dtheta,n2,n3,nrm1
.
. *OPEN 27 PROCLIB.L27
*set plib = 28
*if <[nels] /ne 0> /then
 *CALL FORM_STIFF_BOUN
```

```
*endif
*end

*procedure INTERP_FIELD ( ndof = 6 ; nels = 0 )
*do $dof = 1,[ndof]
[XQT INTS
     SURF=1
     SYM =0
     XY  = 1 BOUN XY 1 1
     DATA= SYSVEC 1 STAT DISP 1 1 COL <$dof>
     INTER=1 REFI DISP 1 <$dof>
  STOP
*enddo
.
. execute ints a second time to interpolate up stiffeners
.
*if <[nels] /ne 0> /then
*remark Interpolating stiffener displacements
*OPEN 3 bsp_stiff.103
*do $dof = 1,[ndof]
[XQT INTS
     RESET SLIB = 3
     RESET DEGREE = 2
     SURF=1
     SYM =0
     XY  = 1 STIF XY 1 1
     DATA= SYSVEC 1 STAT DISP 1 1 COL <$dof>
     INTER=1 STIF DISP 1 <$dof>
  STOP
*enddo
*endif
*end

*procedure FORM_PANEL_BOUN ( nspok = 16; nrng = 5; snbase = 0; --
                             dnbase = 0; snskip = 0; --
                             append = <false> )
*if <[append]> /then
 *def/a table = 'TABLE,U'
*else
 *def/a table = 'TABLE'
*endif
*find record_key 1,BOUN.NODE.1.1,DATA.1 /dim=nbn
[XQT AUS
 *if <[snbase] /eq 0> /then
  *def/i sbase = < 3*<[nrng]-1>*[nspok]> >
  *def/i sskip = 1
 *else
  *def/i sbase = < 3*[snbase] >
  *def/i sskip = < 3*[snskip] + 1>
 *endif
     DEFINE JLOC = JLOC BTAB 2 5
     <table> (ni=2, nj=<nbn>): BOUN XY 1 1
       TRANSFER(source=JLOC, sbase=<sbase>, sskip=<sskip>, --
```

```
                ilim=2, dbase = <2*[dnbase]>,jlim=[nspok])
stop
*end

*procedure FORM_STIFF_BOUN
.
*remark ================================================
*remark       PROCESSING STIFFENER BOUNDARY LOCATIONS
*remark ================================================
.
*FIND RECORD_KEY 1 STIF.NODE.1.1,DATA.1 /DIM=NNSTF
[XQT AUS
 MACRO 1 STIF NODE 1 1 'nstff
 TABLE (NI=2,NJ=<nnstf>): STIF XY 1 1
*do $ij = 1,<nnstf>
  TRANSFER(source=JLOC,sbase=<3*<<nstff[<$ij>]>-1>>,--
           dbase=<2*<<$ij>-1>>, sskip=1,ilim=1,jlim=2)
*enddo
stop
*end

*procedure FORM_APPL_MOTI ( nspok = 16; nrng = 5; nels = 0; --
                            ndf = 6; ambase = 0; --
                            amskip = 0; snbase = 0; --
                            append = <false>; stiff_only=<false> )
.
*show arg ambase
*if <[ambase] /lt 0> /then
 *return
*endif
*if <[append]> /then
 *def/a table = 'TABLE,U'
*else
 *def/a table = 'TABLE'
*endif
[XQT AUS
 *if <[nels] /ne 0> /then
  MACRO 1 STIF NODE 1 1 'nstff
  *def/i sdskip = < <[ndf]-1> + [ndf]*<<nstff[2]>-<nstff[1]>-1> >
 *endif
 *do $dof = 1,[ndf]
  DEFINE R<$dof> = REFI DISP 1 <$dof>
  *if <[nels]> /ne 0> /then
   DEFINE S<$dof> = STIF DISP 1 <$dof>
  *endif
 *enddo
.
.
*gal2mac /name=nnodes /maxn=1 1,JDF1.BTAB.1.8,DATA.1
  <table> (ni=[ndf],nj=<nnodes>): APPL MOTI 1 1
 *do $dof = 1,[ndf]
  *if <[ambase] /eq 0> /then
   *def/i dbase=<[ndf]*<<[nrng]-1>*[nspok]>+<$dof>-1>
```

```
   *def/i dskip = 5
  *else
   *def/i dbase=<[ndf]*[ambase]+<$dof>-1>
   *def/i dskip = < [ndf]*[amskip]+5 >
  *endif
.
 *if < [stiff_only] /eq <false> /then
   TRANSFER (source=R<$dof>,dbase=<dbase>,dskip=<dskip>, --
             jlim=[nspok], ilim=1, sbase = [snbase] )
 *endif
.
. transfer the interpolated displacements for stiffeners into
. the APPL MOTI dataset
.
 *if <[nels] /ne 0> /then
   *def/i sdbase1 = < [ndf]*<<nstff[1]>-1> + <$dof>-1 >
   *def/i sdbase2 = < [ndf]*<<nstff[<1+[nels]>]>-1> + <$dof>-1 >
.
  *find record_key 1,STIF.NODE.1.1,DATA.1 /dim=nnstf
  *do $ij = 1,<nnstf>
    *def/i sdbase = < [ndf]*<<nstff[<$ij>]>-1> + <$dof>-1 >
     TRANSFER(source=S<$dof>,sbase=<<$ij>-1>,dbase=<sdbase>, --
              sskip=1,ilim=1,jlim=1)
  *enddo
  *endif
 *enddo
.
stop
*end

*procedure SOLVE ( direction = 1; location = 'CENTROIDS'; --
                   num_strs=8; stiffeners = <false>; --
                   nels = 0; ndof = 6; nrings = 10; --
                   nspokes = 64; ambase = 0; amskip = 0 )
*sho arg
.
*def/i ES_PROJ = 2
*def/i ndf = [ndof]
*def/i nspok = [nspokes]
.
*if < <es_nen> /eq 4 > /then
 *def/i nrng  = <[nrings]+1>
 *def/i ngels == [nels]
 *def/i ngrngs == 2
*else
 *def/i nrng  = <2*[nrings]+1>
 *def/i ngels ==  <2*[nels]>
 *def/i ngrngs == 4
*endif
.
.
*if <[stiffeners]> /then
 *def/i ne = <nrng>
```

```
*else
 *def/i ne = 0
*endif
*def/i nnint = < <nspok> + 2*<ne> >
.
[XQT DCU
.    TOC 1
     *do $i = 1,<ndf>
         PRIN 1 REFI DISP 1 <$i>
         *if < [nels] /ne 0 > /then
          PRIN 1 STIF DISP 1 <$i>
         *endif
     *enddo
.
*call FORM_APPL_MOTI ( nspok = <nspok>; nrng = <nrng>; --
                       nels=[nels]; ndf = <ndf>; --
                       ambase = [ambase]; amskip = [amskip] )
.
[XQT RSEQ
     RESET MAXCON=41,METHOD=1
stop
.  ---------------------------
.  Initialize Element Datasets
.  ---------------------------
[XQT TOPO
     RESET MAXSUB=40000, LRAM=8196
[XQT E
.
.  ------------------------------------
.  Initialize Element Computational Data
.  ------------------------------------
   *call ES ( function = 'INITIALIZE' )
.
.  ----------------------------------------
.  Form Element Material Stiffness Matrices
.  ----------------------------------------
   *call ES ( function = 'FORM STIFFNESS/MATL' )
.
.  ---------------------------------
.  Assemble Material Stiffness Matrix
.  ---------------------------------
   [xqt K
.
.  ----------------------
.  Factor Stiffness Matrix
.  ----------------------
   [xqt INV
    online = 2
    reset lra = 7168
    reset dzero=1.E-10
    reset spdp = <csm_precision>
   [xqt AUS
.
```

```
.  ----------------------
.  Solve for Displacements
.  ----------------------
   [XQT SSOL
    RESET SET=1, CON=1
.
.     --------------------
.     Form Element Stresses
.     --------------------
     *call STRESS ( STRESS = <true> ; LOCATION = [location]; --
                    DIRECTION = [direction]; SMOOTH = <true> )
     *call STRESS ( STRESS = <true> ; LOCATION = 'NODES'; --
                    DIRECTION = 0  )
*end
```

Table 5.1 Finite Element Models of Isotropic Panel with Circular Cutout.

Model Designation	Number of Rings of Nodes	Number of Radial Spokes of Elements	Total Number of Elements	Total Number of Nodes	K_t
G1	2	16	256	296	2.06
G2	4	16	288	328	2.23
G3	16	32	832	888	2.72
G4[a]	32	80	3168	3272	2.81
LS1	16	32	512	544	2.76
LC1	16	32	512	544	2.75

[a] G4 is the converged model

Table 5.2 Summary of Computational Requirements.

Model Designation	Measures of Computational Effort		
	Total Number of Degrees of Freedom	CPU, seconds	Size of Data Library, Mbytes
G1	1644	64.0	5.2
G2	1836	69.7	6.0
G3	5156	183.4	22.2
G4[a]	19340	1167.2	160.0
LS1	3072	135.4	13.0
LC1	3072	121.6	12.6

[a] G4 is the converged model

Table 5.3 Finite Element Models of Blade–Stiffened Panel with Discontinuous Stiffener.

Model Designation	Number of Rings of Nodes	Number of Radial Spokes of Elements	Total Number of Elements	Total Number of Nodes	$\frac{(N_x)_{max}}{(N_x)_{avg}}$
G1	2	16	376	424	2.22
G2	16	32	1024	1088	2.88
G3	16	32	1408	1488	2.88
G4[a]	32	80	3472	3584	2.94
LS1	16	32	576	612	2.88
LC1	16	32	576	612	2.92
LR1	-	-	16	25	-
LR2	-	-	32	45	-
LR3	-	-	96	117	-

[a] G4 is the converged model

Table 5.4 Summary of Computational Requirements.

Model Designation	Measures of Computational Effort		
	Total Number of Degrees of Freedom	CPU, seconds	Size of Data Library, Mbytes
G1	2316	99.7	8.7
G2	6252	255.3	28.9
G3	8460	329.6	38.5
G4[a]	21084	1006.0	140.6
LS1	3456	187.7	13.6
LC1	3456	188.7	13.1
LR1	54	58.0	0.5
LR2	126	62.0	0.8
LR3	462	78.7	1.8

[a] G4 is the converged model

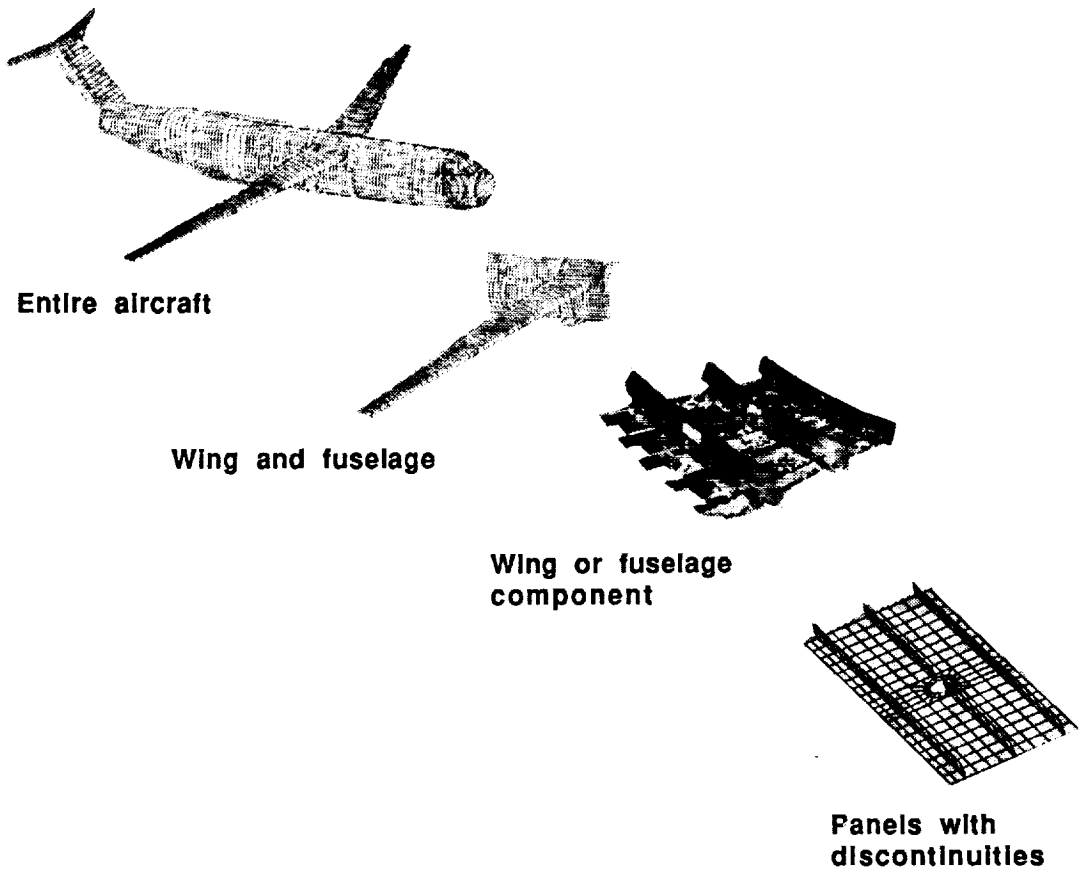

Fig. 1.1 Global/Local Analysis Levels.

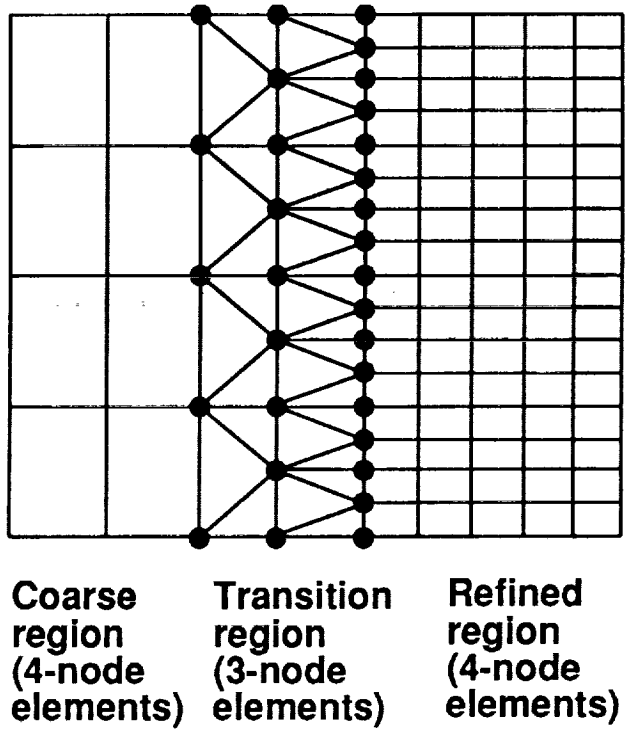

Fig. 1.2 Mesh transitioning using triangular elements.

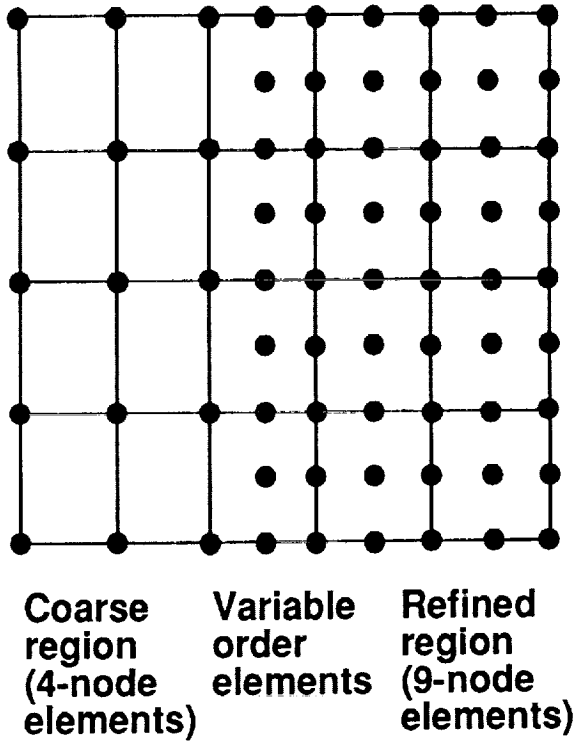

Fig. 1.3 Mesh transitioning using variable–order elements.

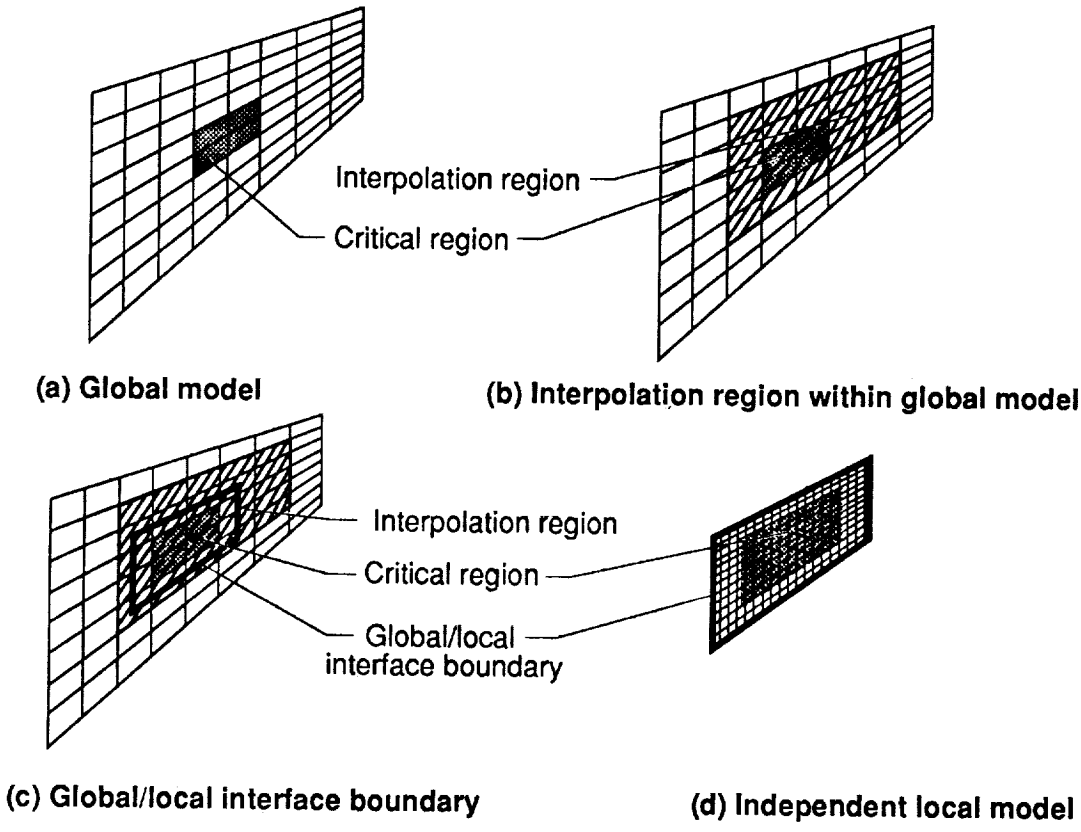

Fig. 2.1 Terminology of the global/local methodology.

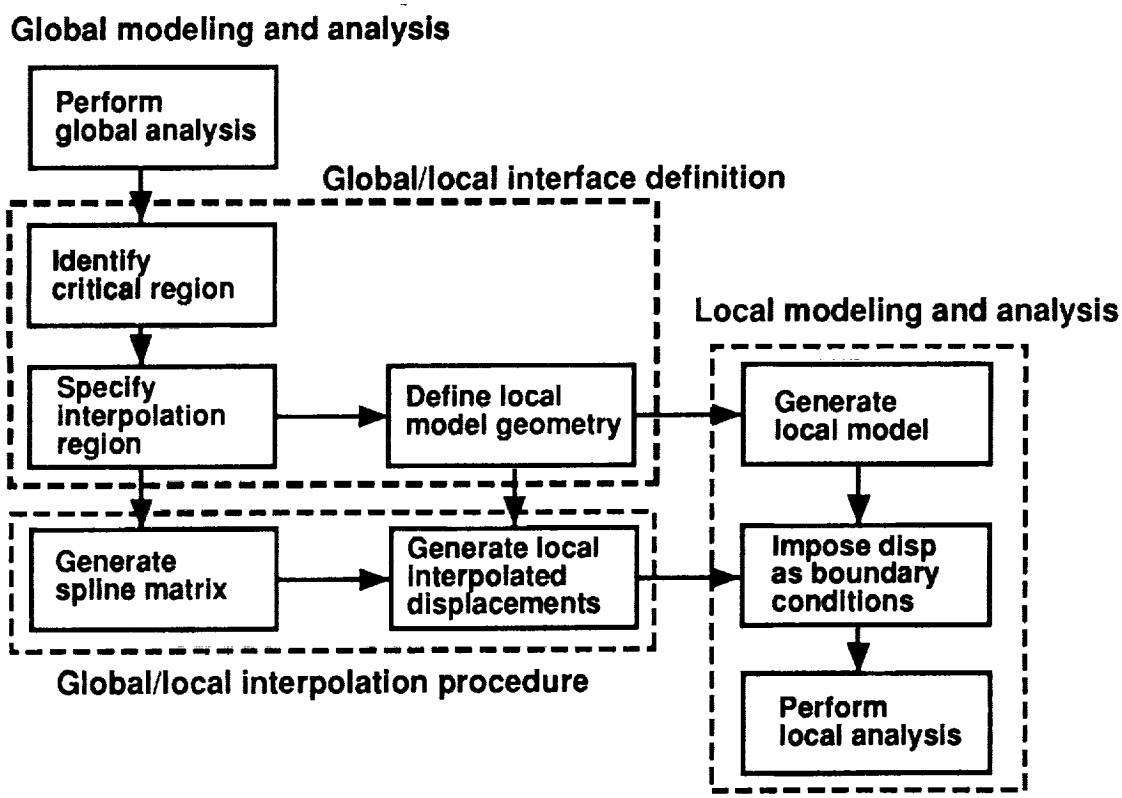

Fig. 2.2 Schematic of overall global/local solution strategy.

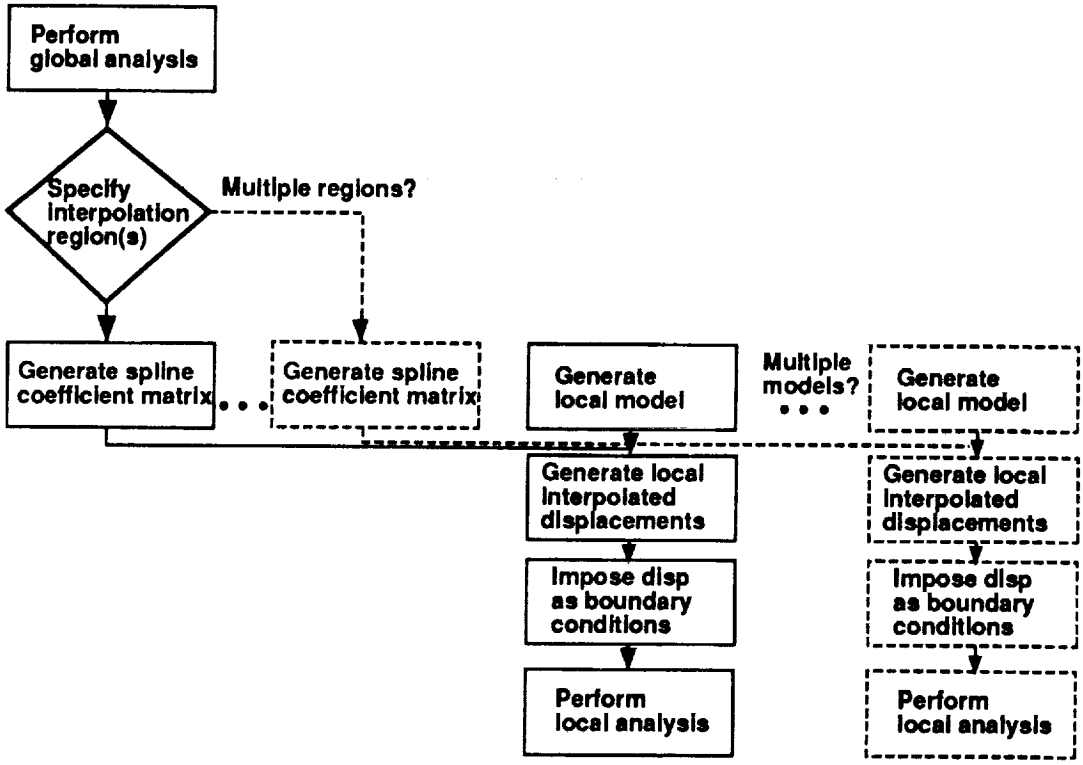

Fig. 2.3 Schematic of global/local solution strategy for multiple regions.

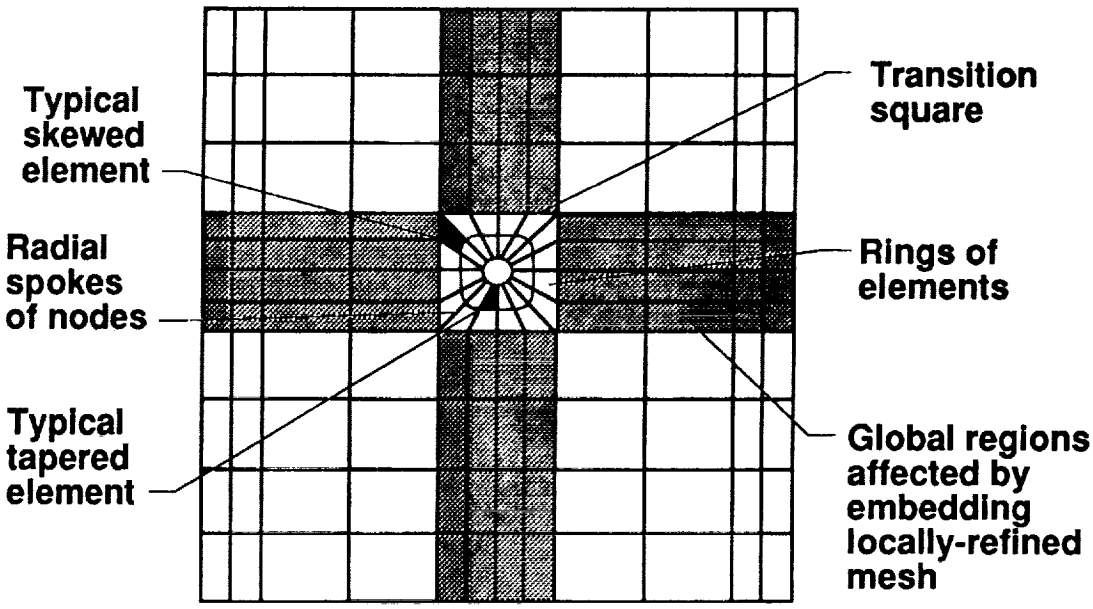

Fig. 2.4 Terminology associated with modeling cutouts.

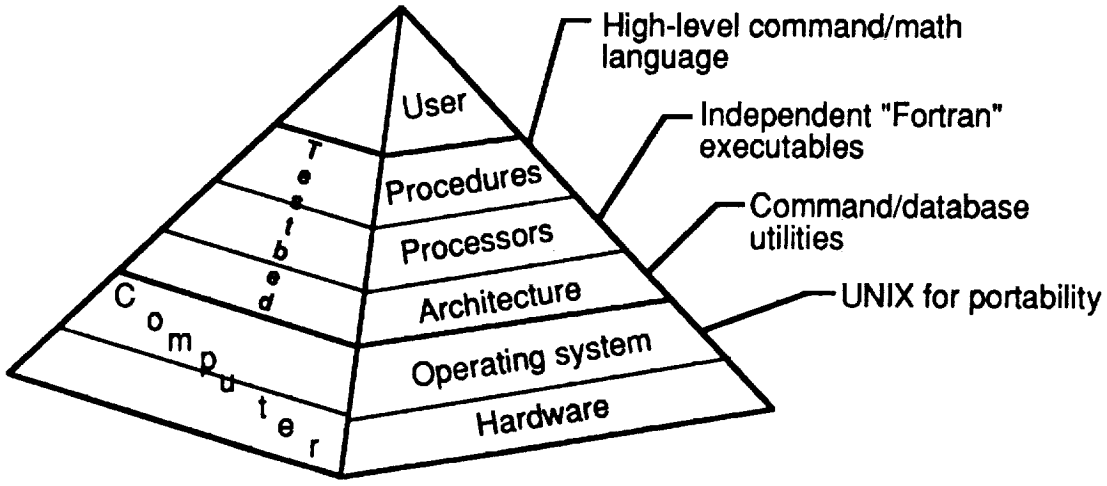

Fig. 4.1 Concept of the CSM Testbed software system.

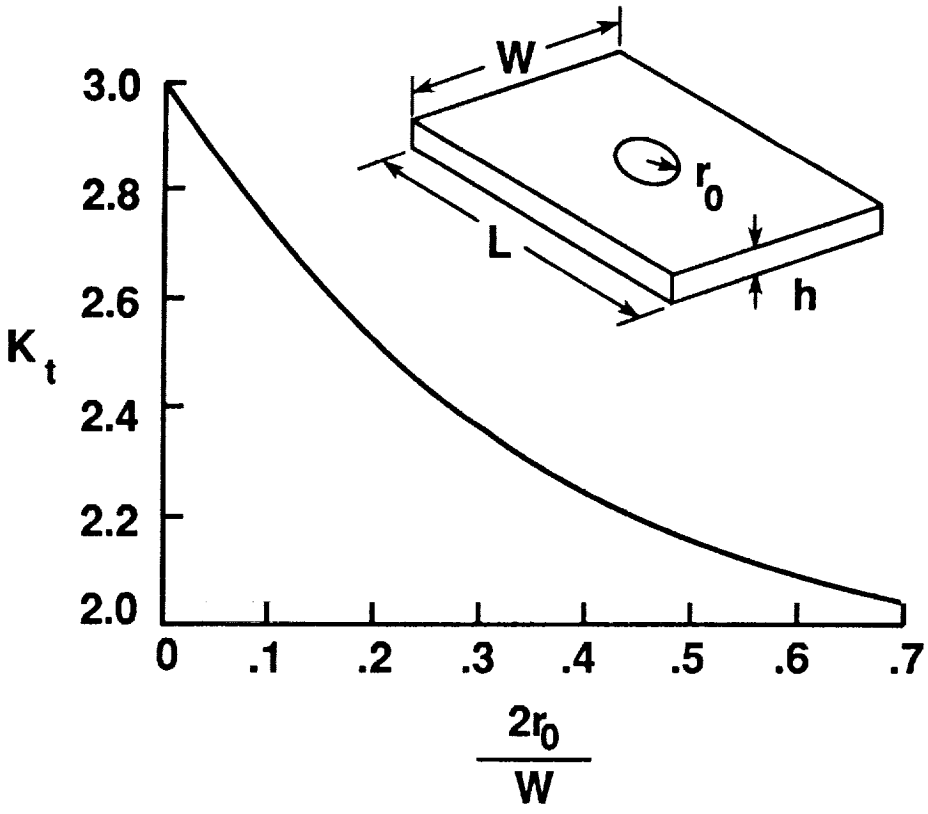

Fig. 5.1 Stress concentration factor K_t for axial loading of a finite-width plate with a transverse hole.

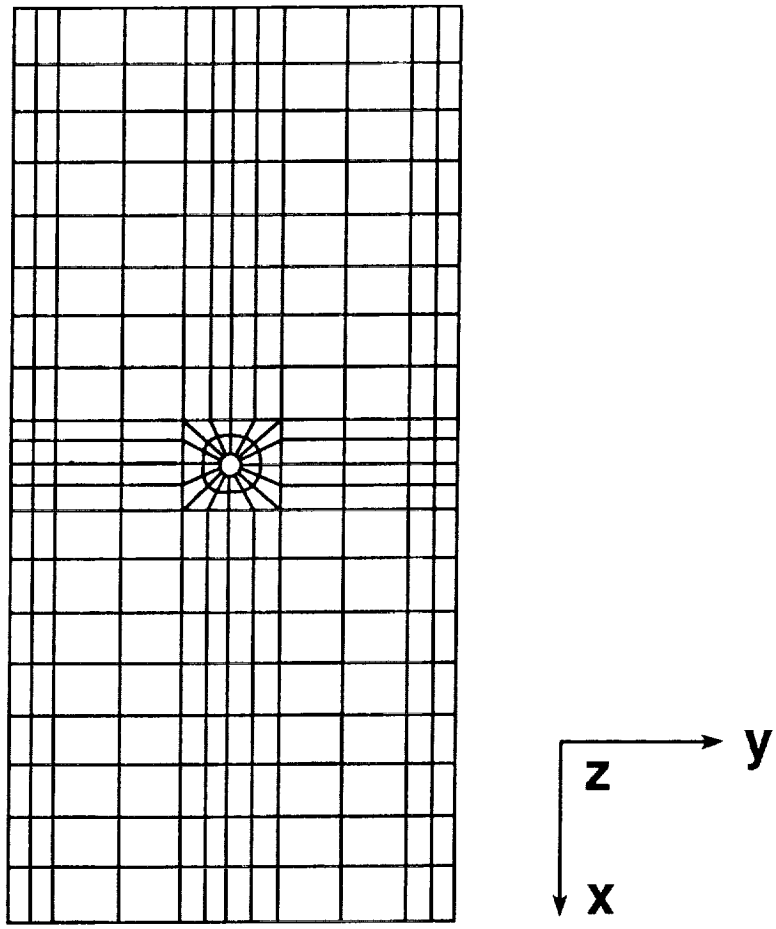

Fig. 5.2 Coarse global finite element model of isotropic panel with a circular cutout.

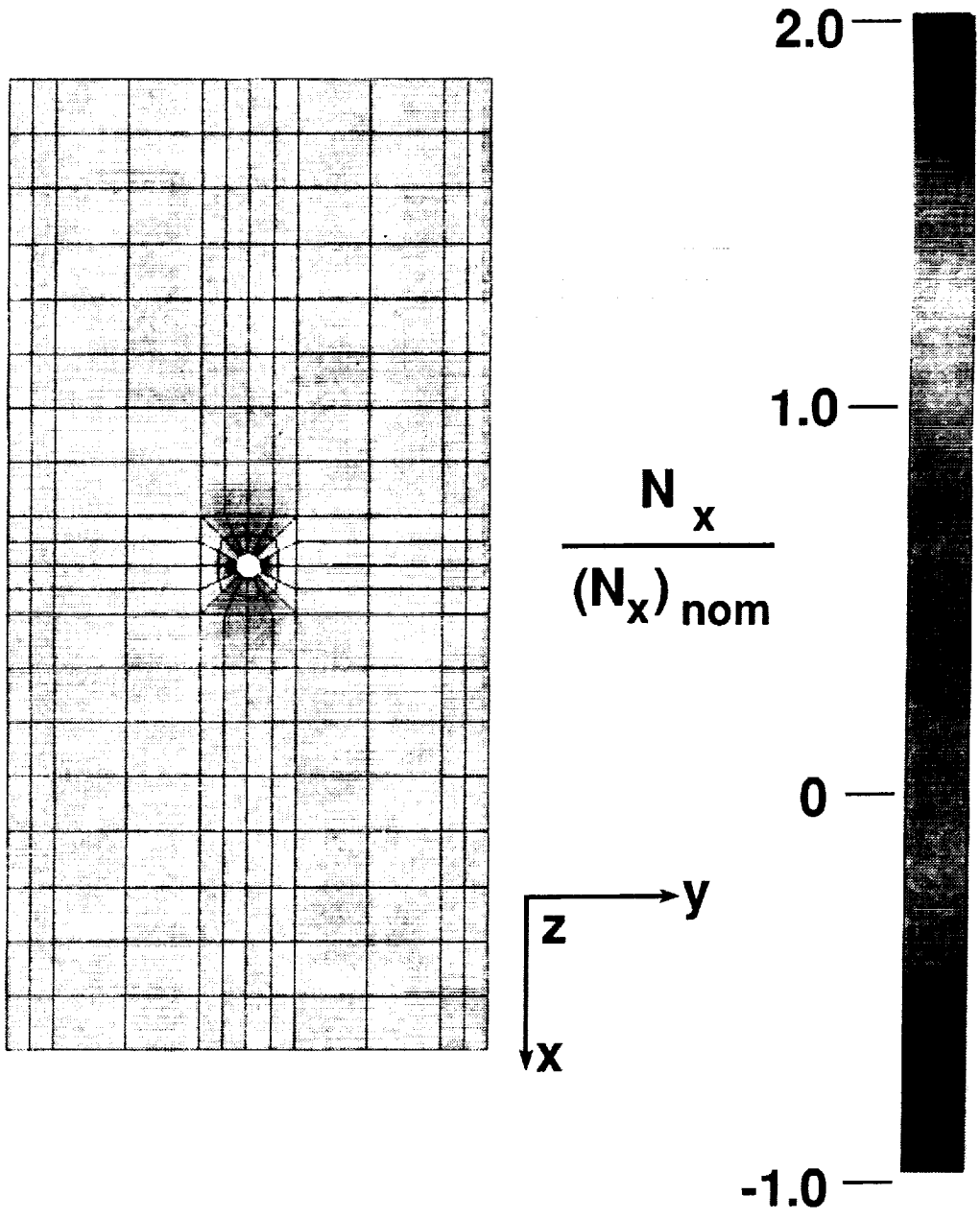

Fig. 5.3 Longitudinal stress resultant N_x distribution for coarse global finite element model of isotropic panel with a circular cutout.

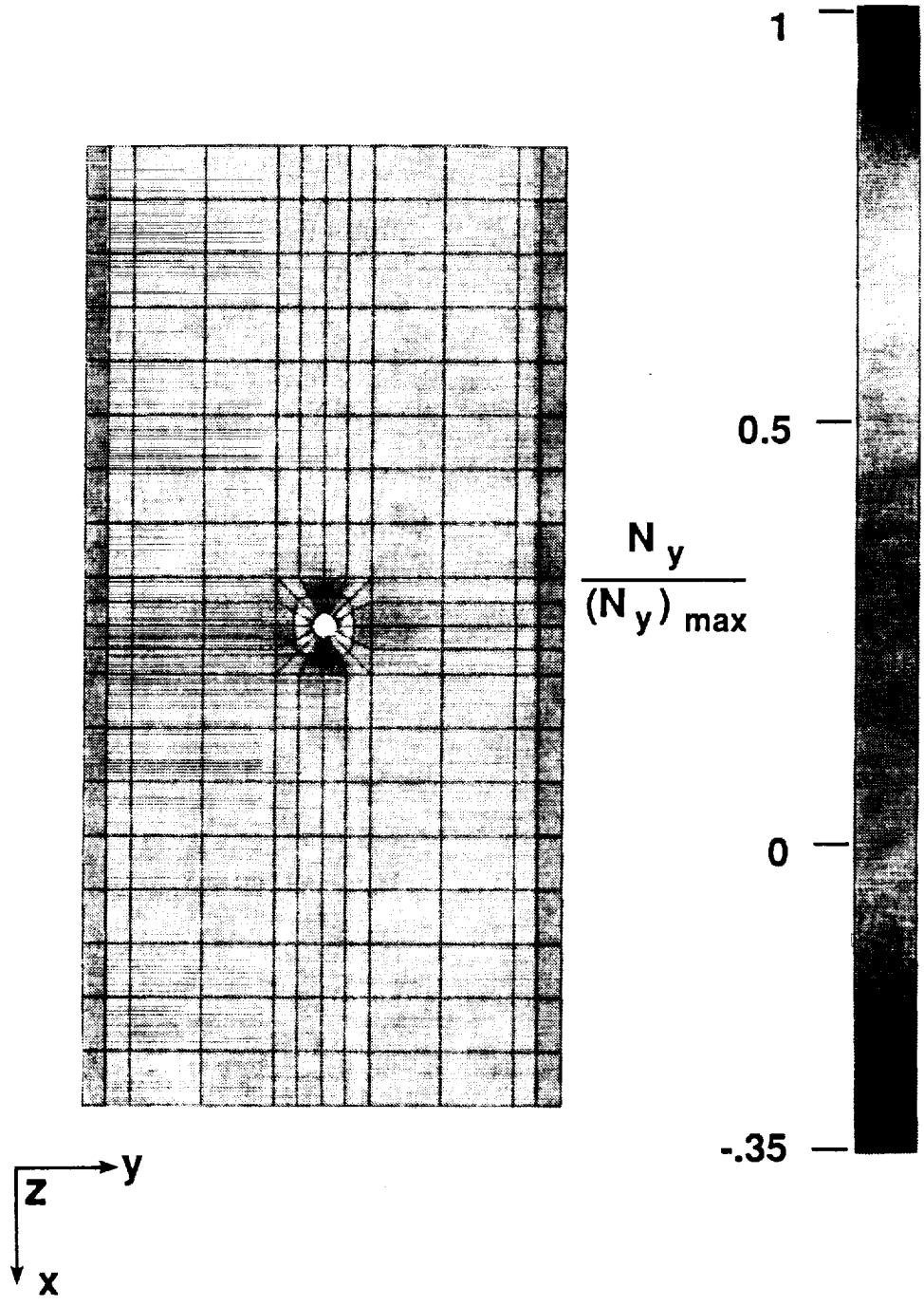

Fig. 5.4 Transverse stress resultant N_y distribution for coarse global finite element model of isotropic panel with a circular cutout.

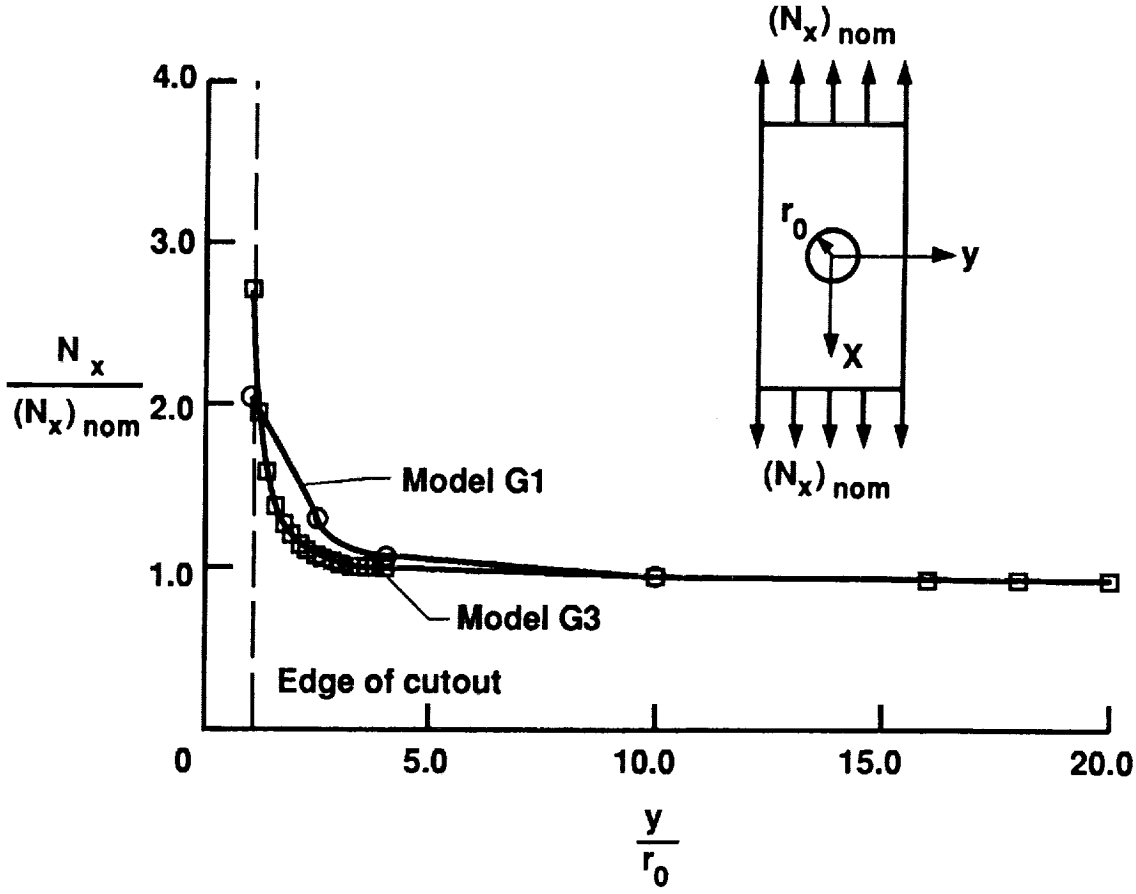

Fig. 5.5 Longitudinal inplane stress resultant N_x distributions at panel midlength for coarse and refined global finite element models.

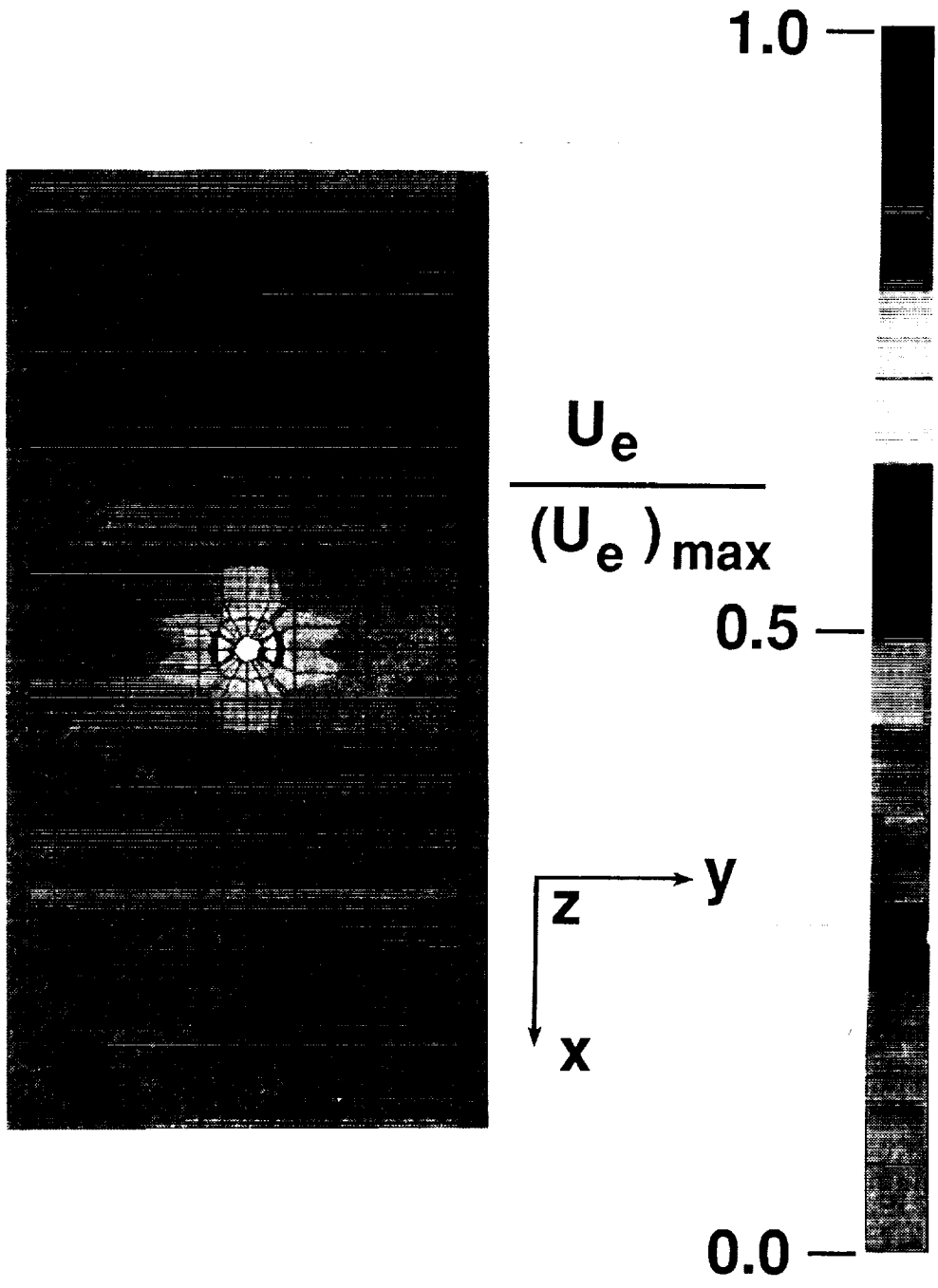

Fig. 5.6 Distribution of the strain energy measure for coarse global model of the panel with a circular cutout.

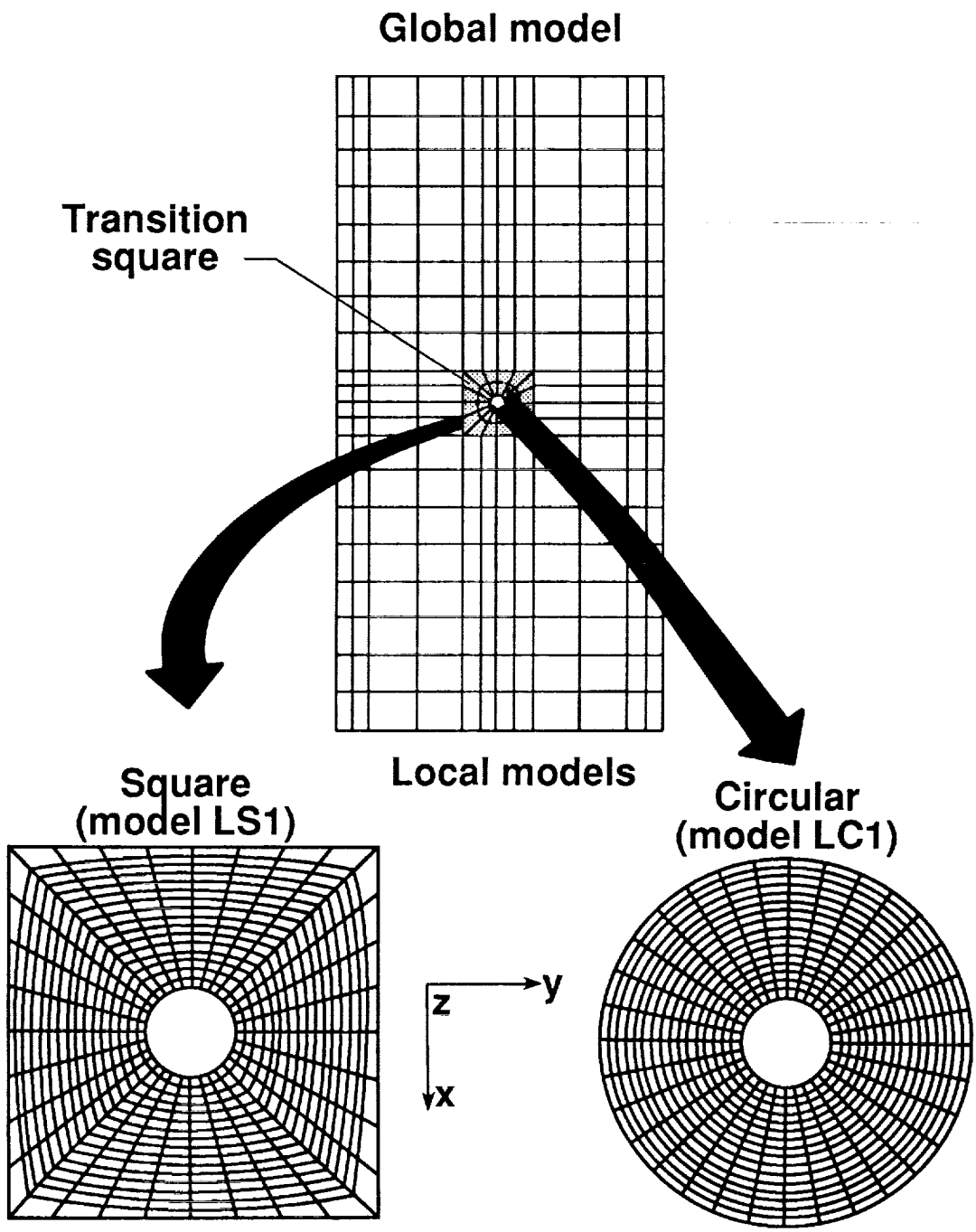

Fig. 5.7 Global/local analysis models for isotropic panel with circular cutout.

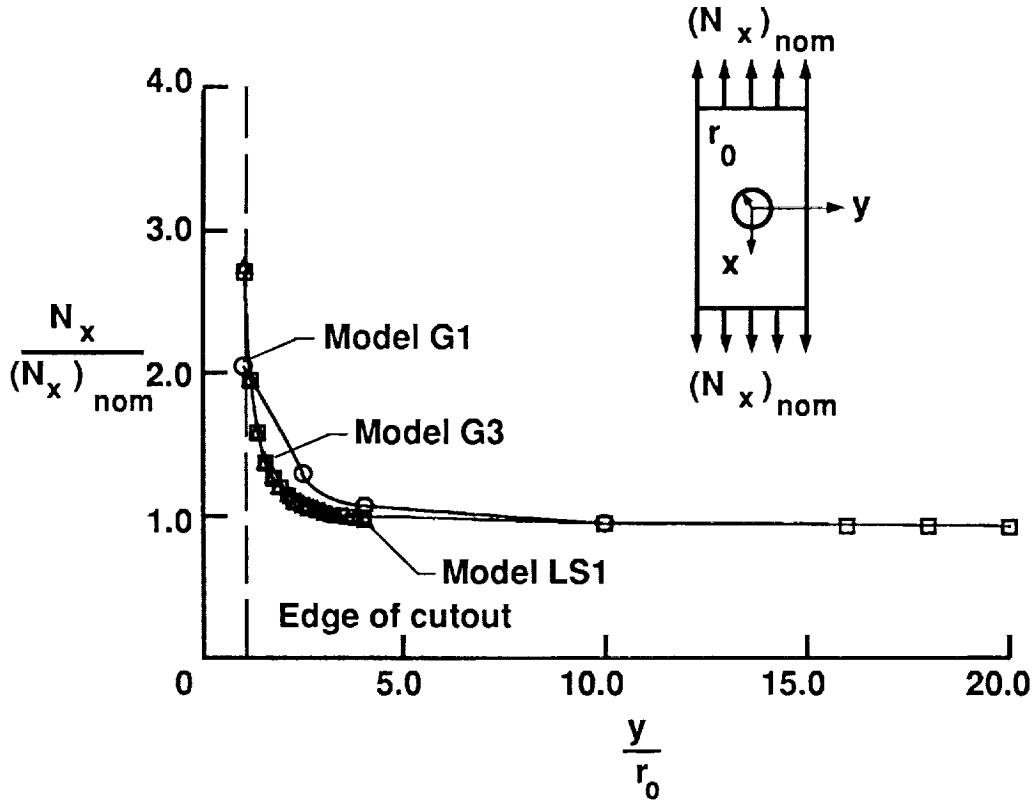

(a) Distribution at panel midlength.

Fig. 5.8 Longitudinal stress resultant N_x distributions for square local finite element model of isotropic panel with a circular cutout.

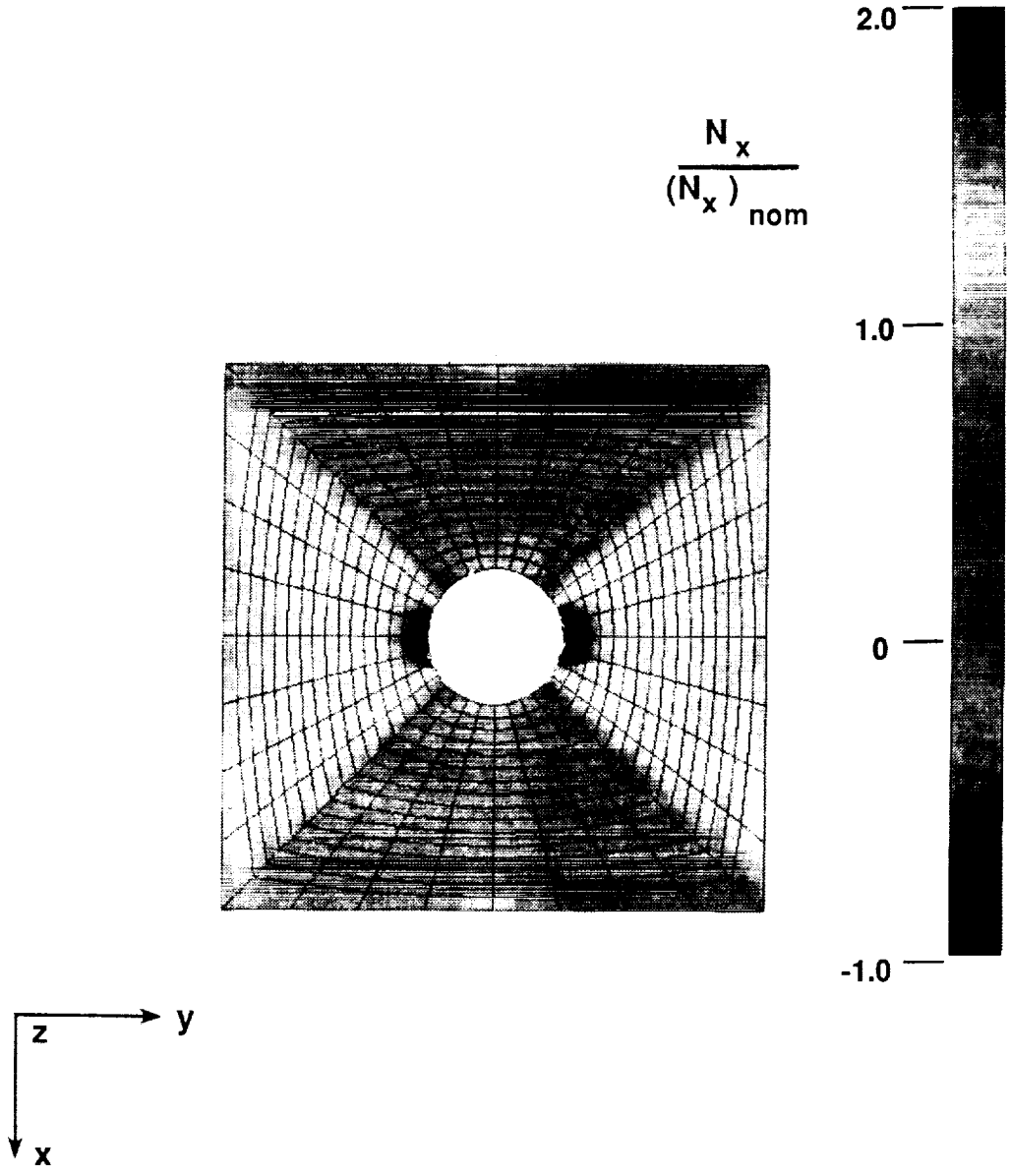

(b) Contour plot.

Fig. 5.8 Concluded.

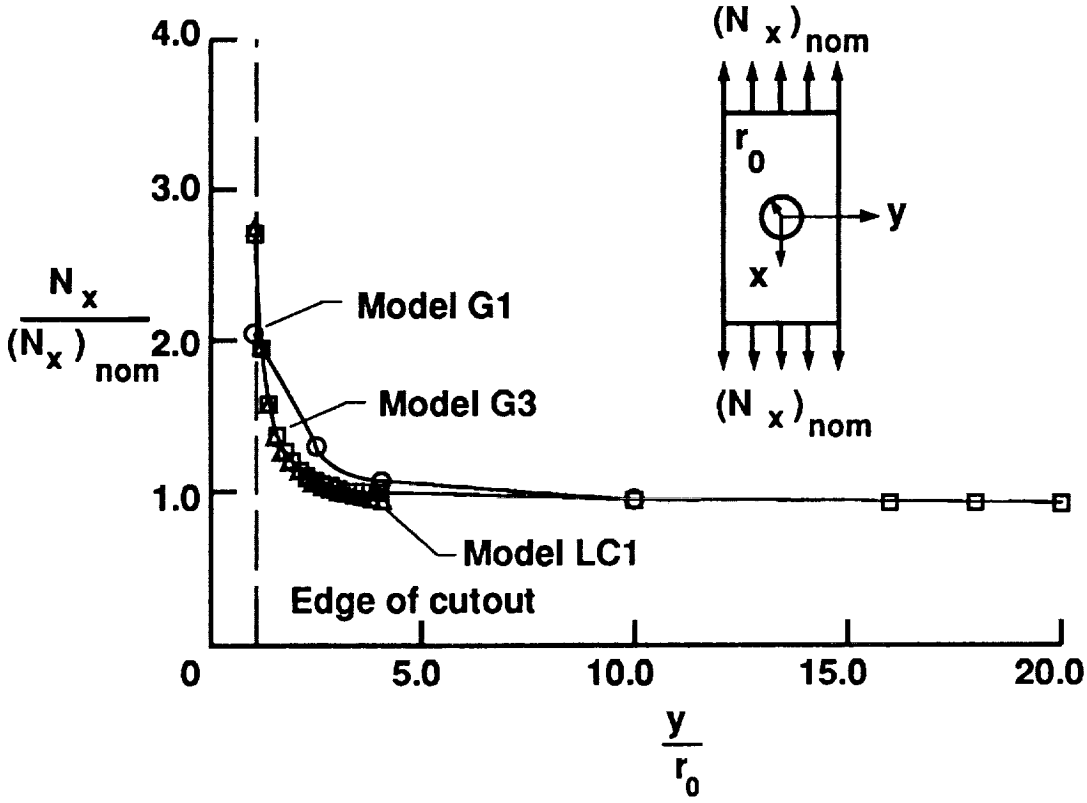

(a) Distribution at panel midlength.

Fig. 5.9 Longitudinal stress resultant N_x distributions for circular local finite element model of isotropic panel with a circular cutout.

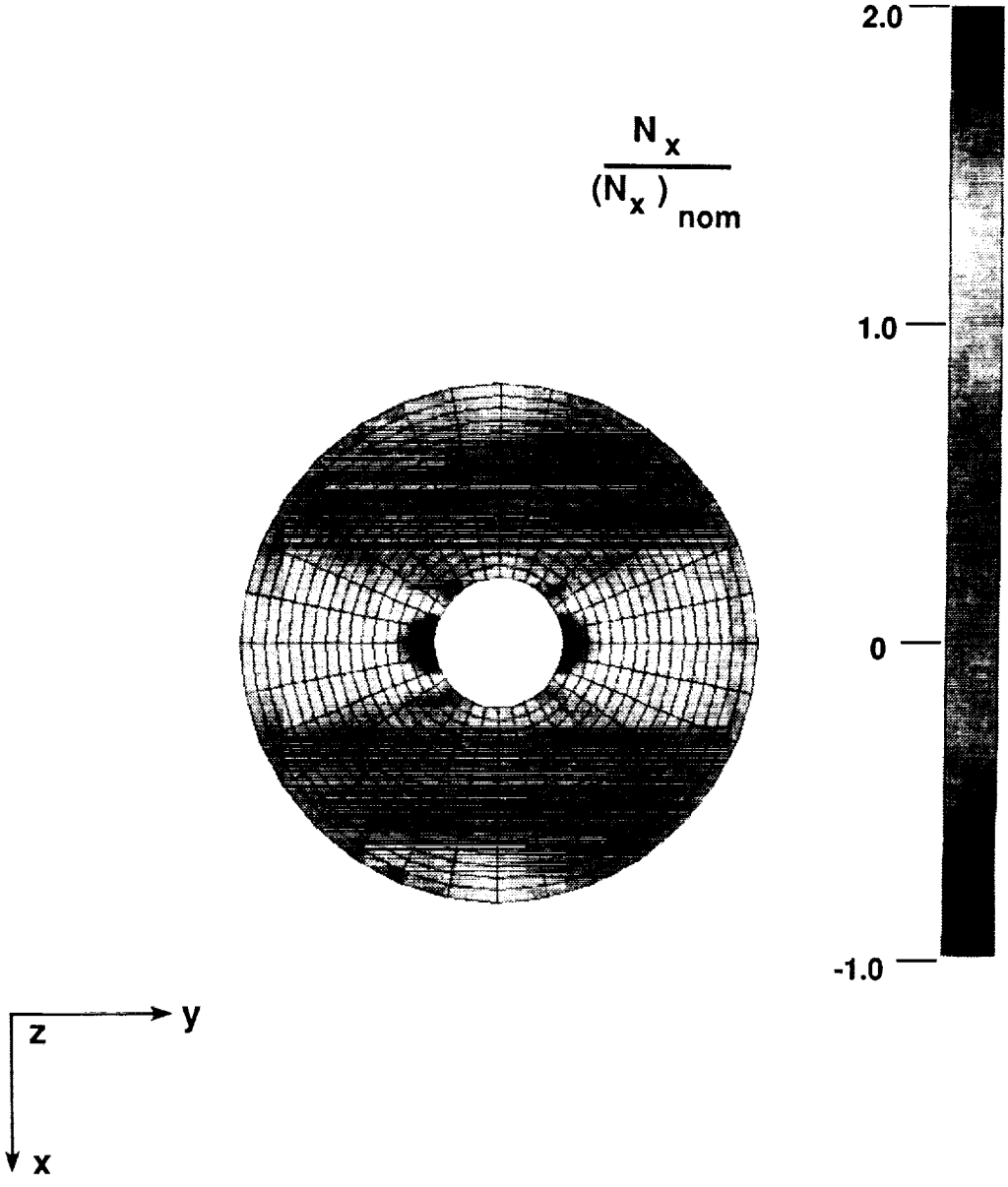

(b) Contour plot.

Fig. 5.9 Concluded.

C-2

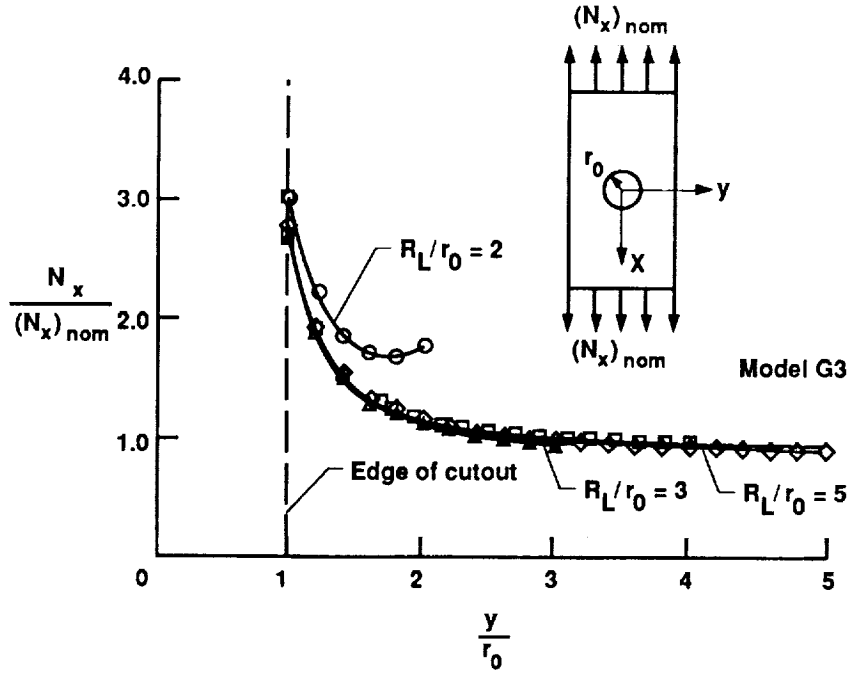

(a) Interpolation from global Model G1.

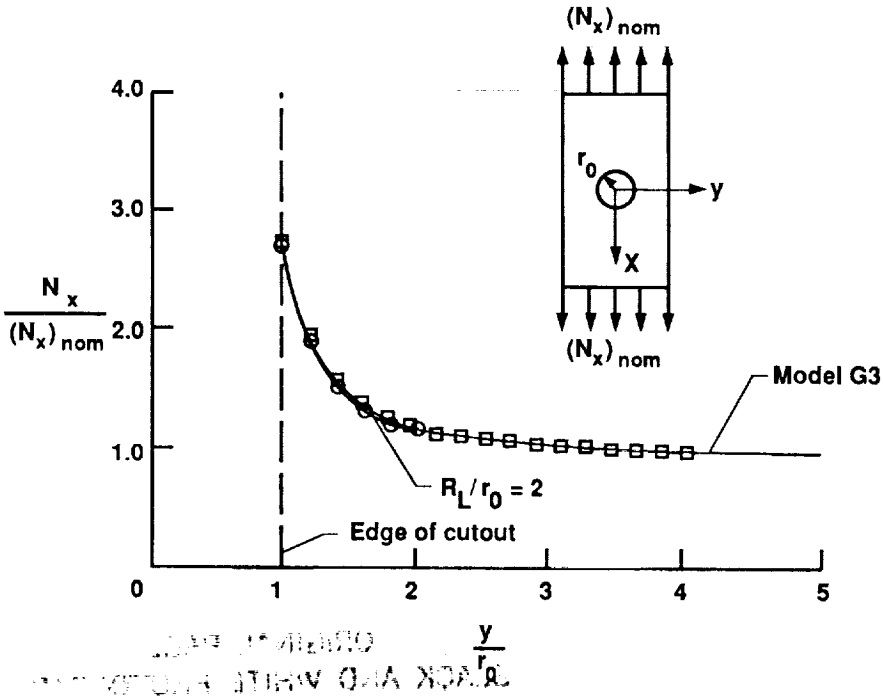

(b) Interpolation from global Model G2.

Fig. 5.10 Longitudinal inplane stress resultant N_x distributions at panel midlength for varied local model boundaries.

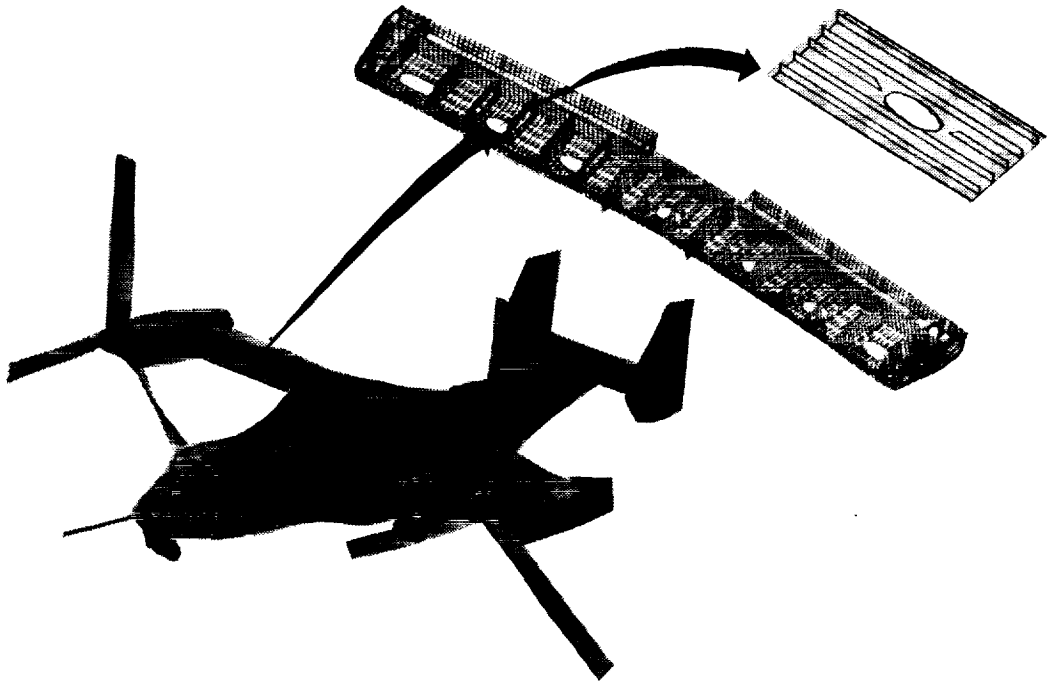

Fig. 5.11 Bell–Boeing V–22 wing panel.

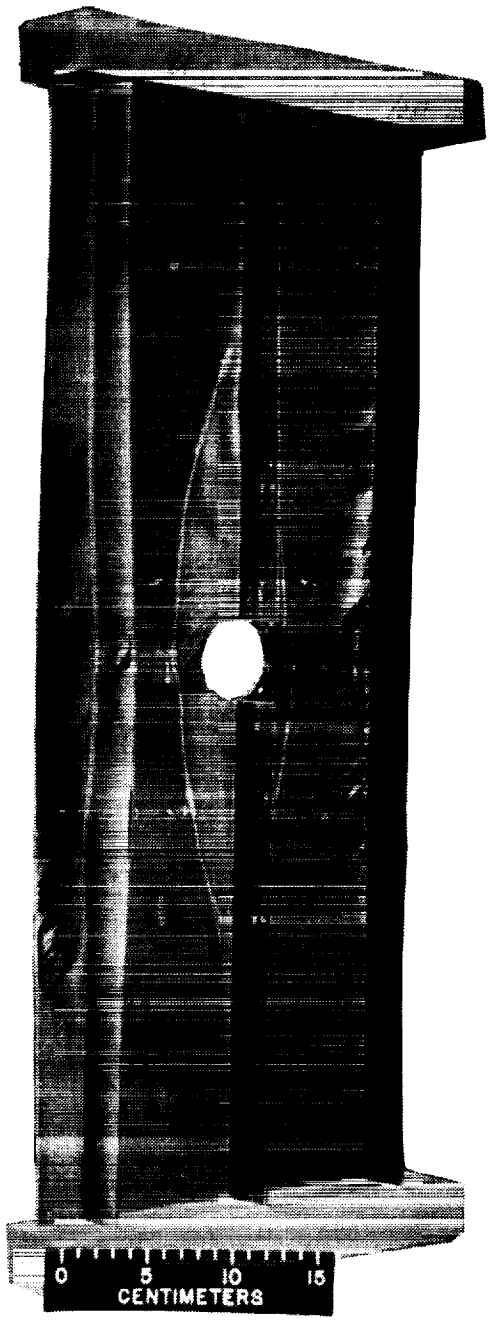

Fig. 5.12 Composite blade–stiffened panel with a discontinuous stiffener.

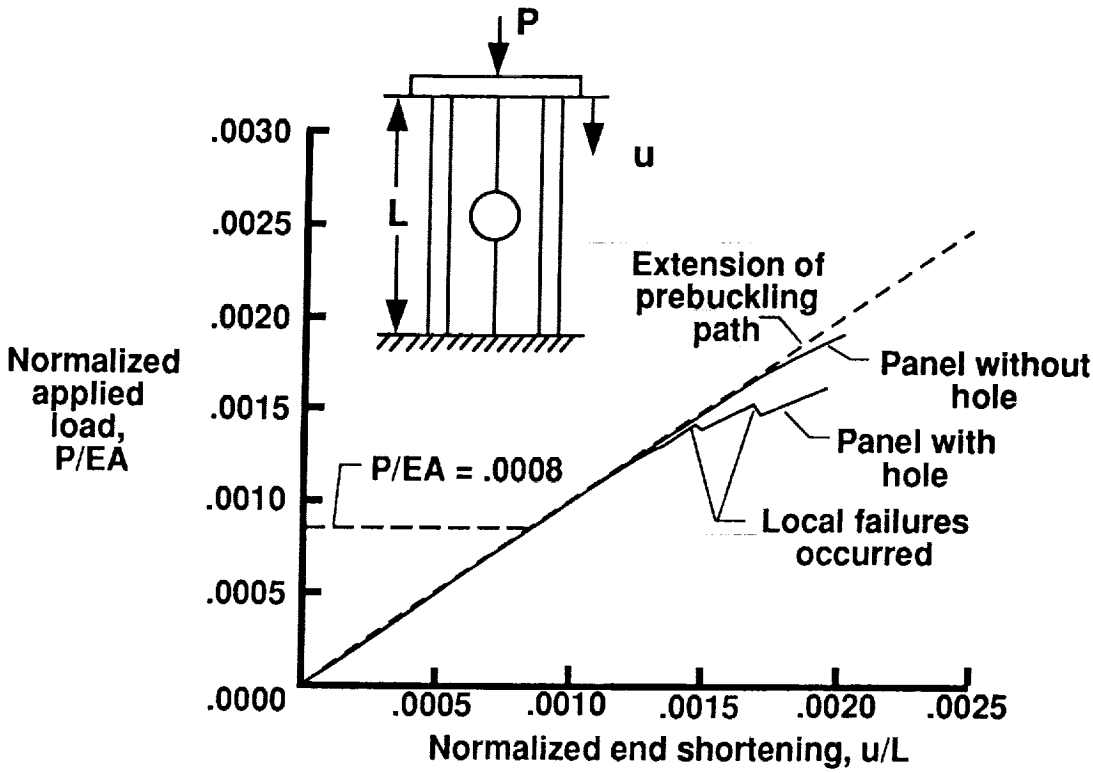

Fig. 5.13 End–shortening results for composite blade–stiffened panel.

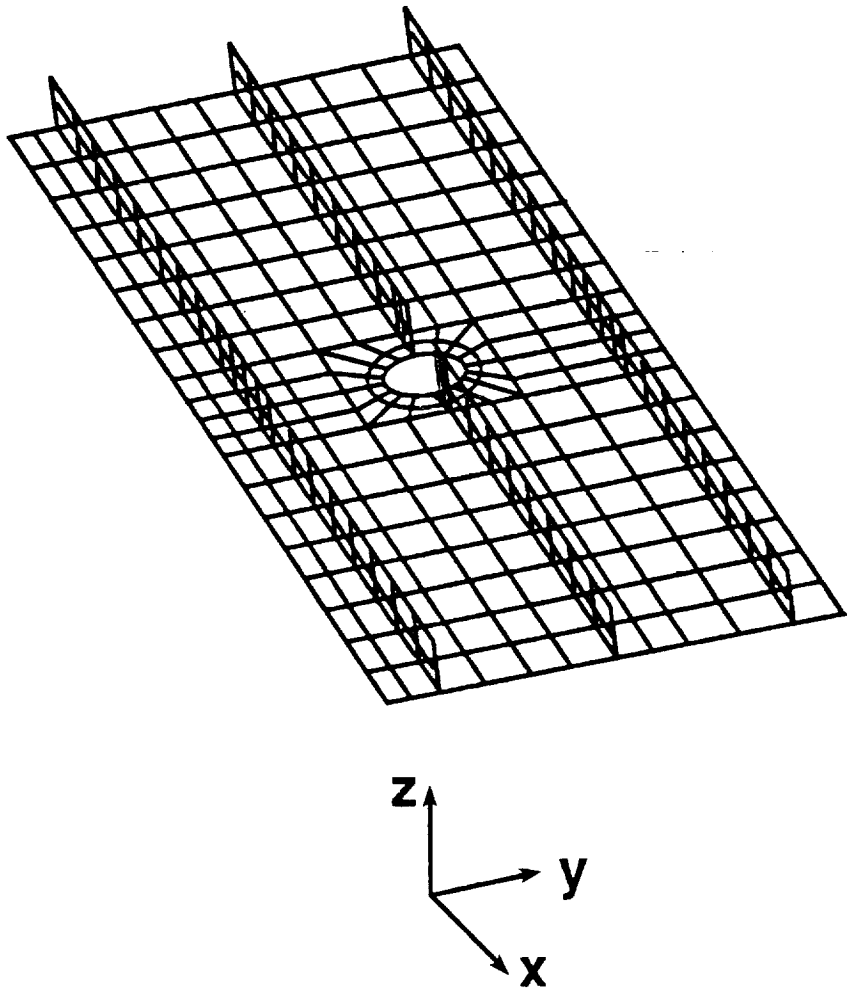

Fig. 5.14 Global finite element model of blade–stiffened panel with discontinuous stiffener.

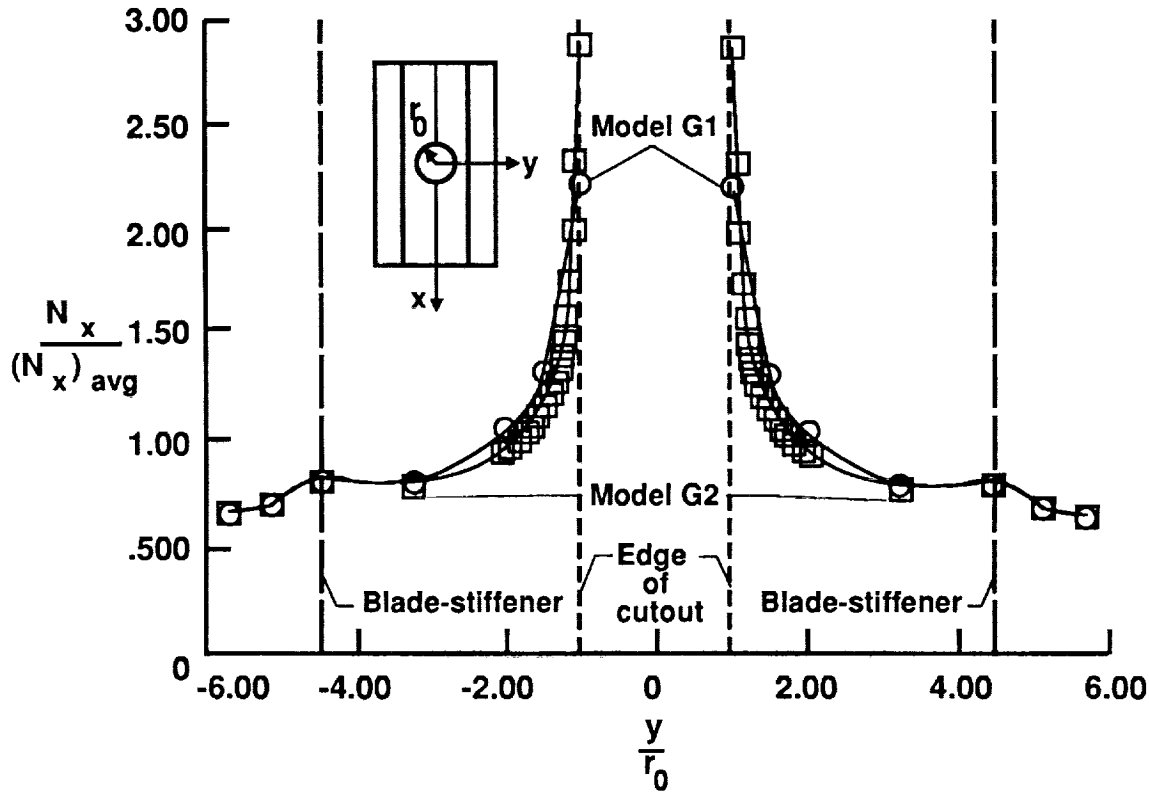

Fig. 5.15 Longitudinal inplane stress resultant N_x distributions at panel midlength for coarse and refined global models.

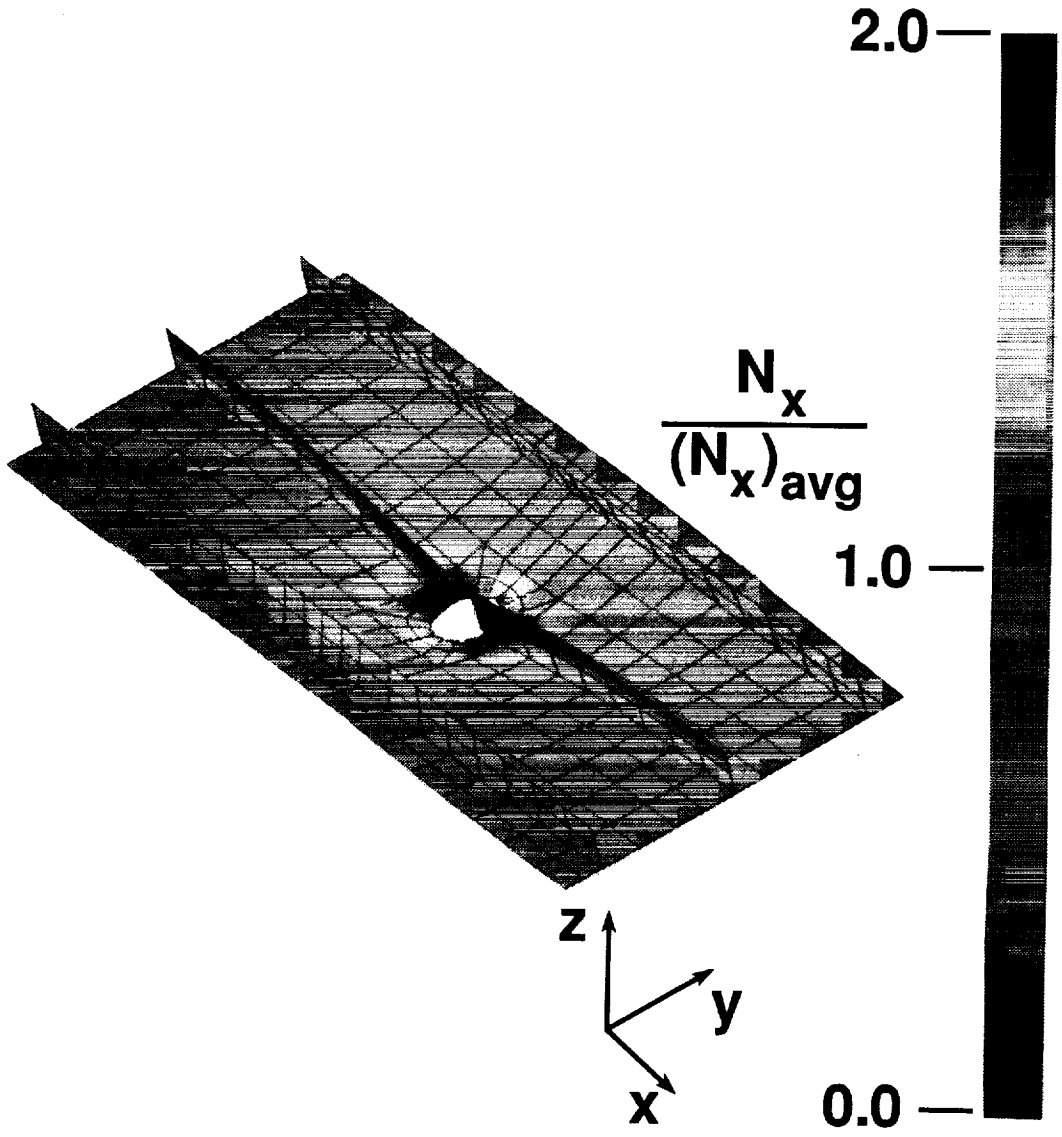

Fig. 5.16 Deformed geometry shape with N_x distributions for coarse global model of blade–stiffened panel with discontinuous stiffener.

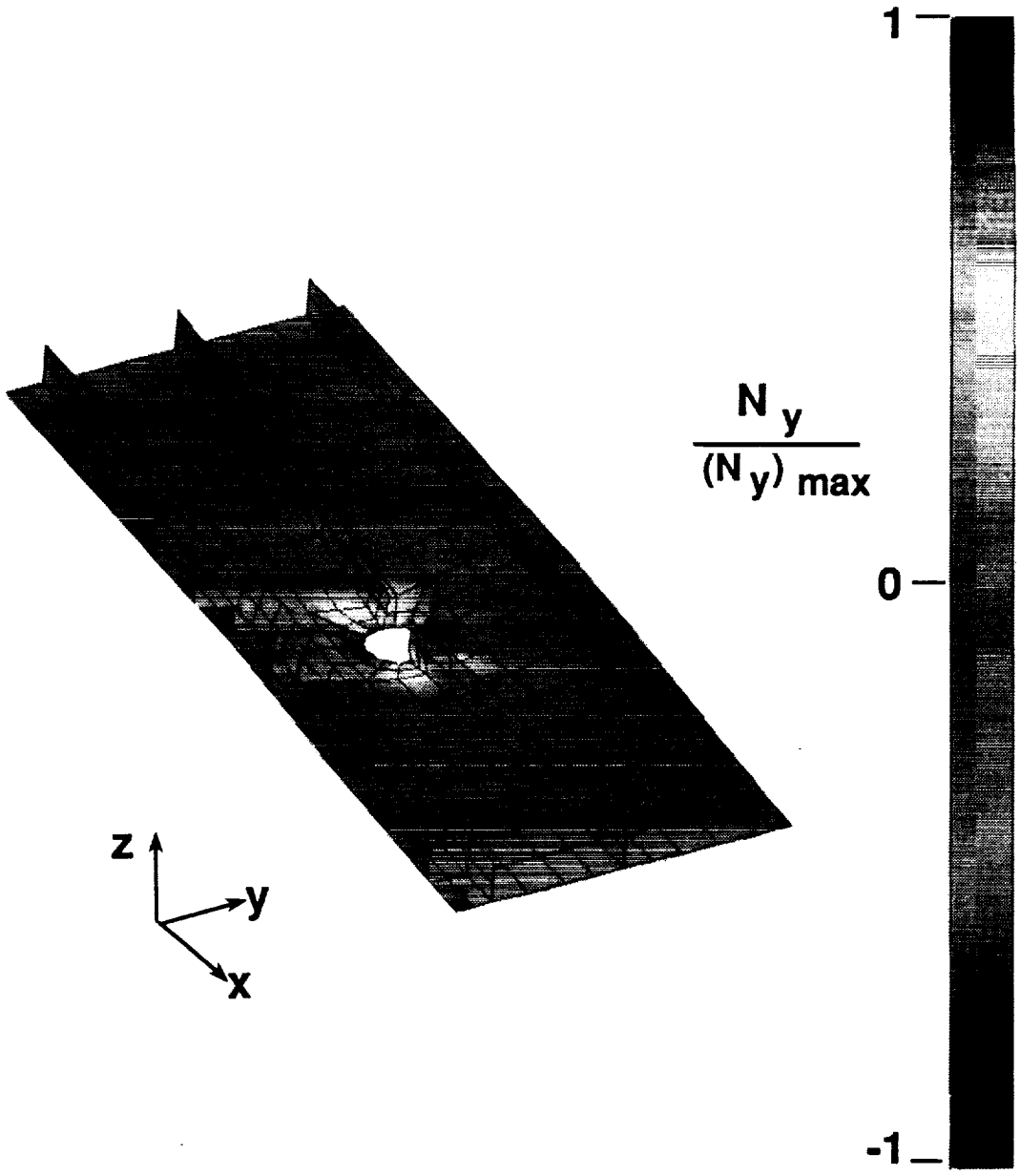

Fig. 5.17 Deformed geometry shape with N_y distributions for coarse global model of blade–stiffened panel with discontinuous stiffener.

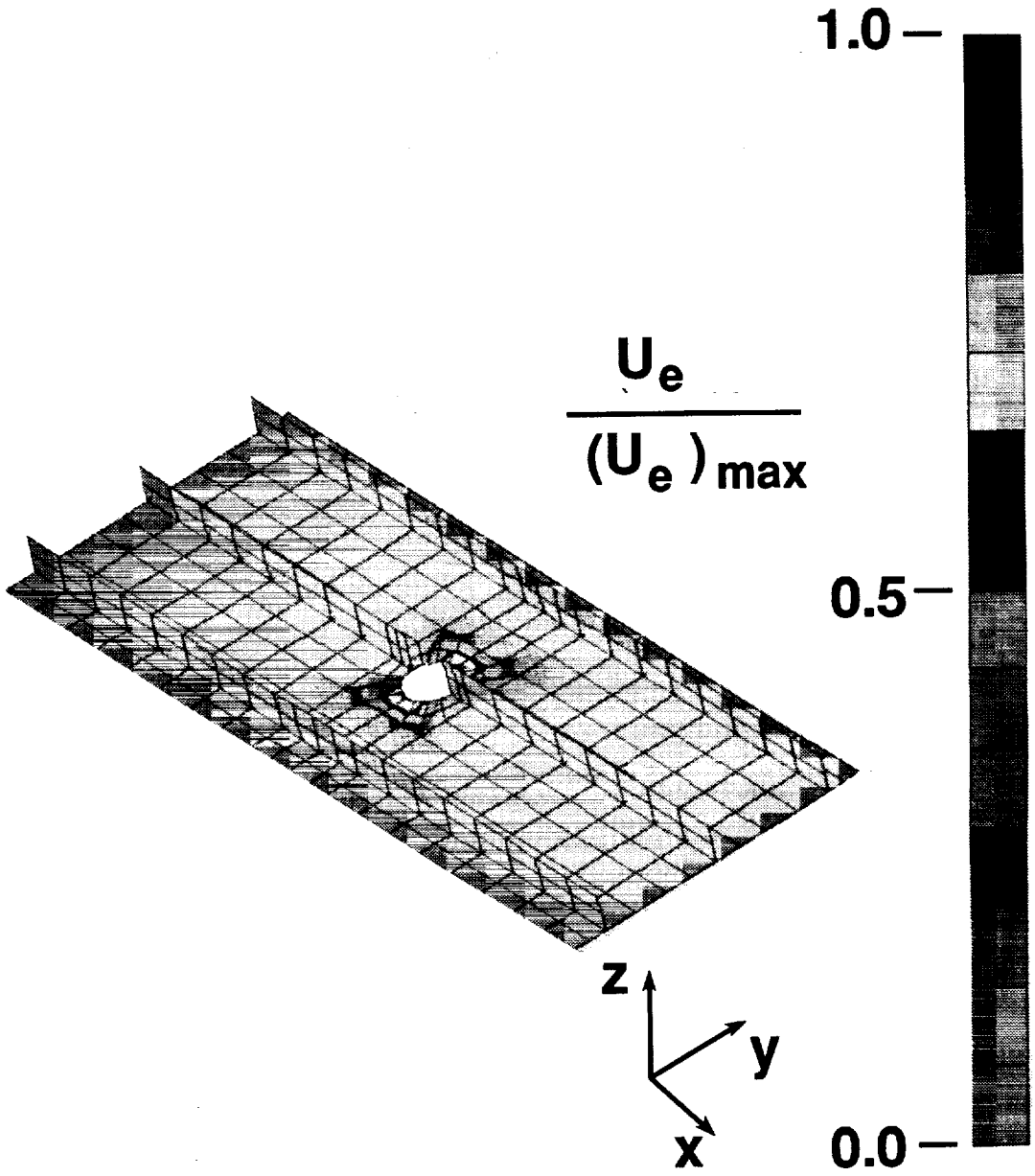

Fig. 5.18 Distribution of the strain energy measure for the coarse model of the blade-stiffened panel with discontinuous stiffener.

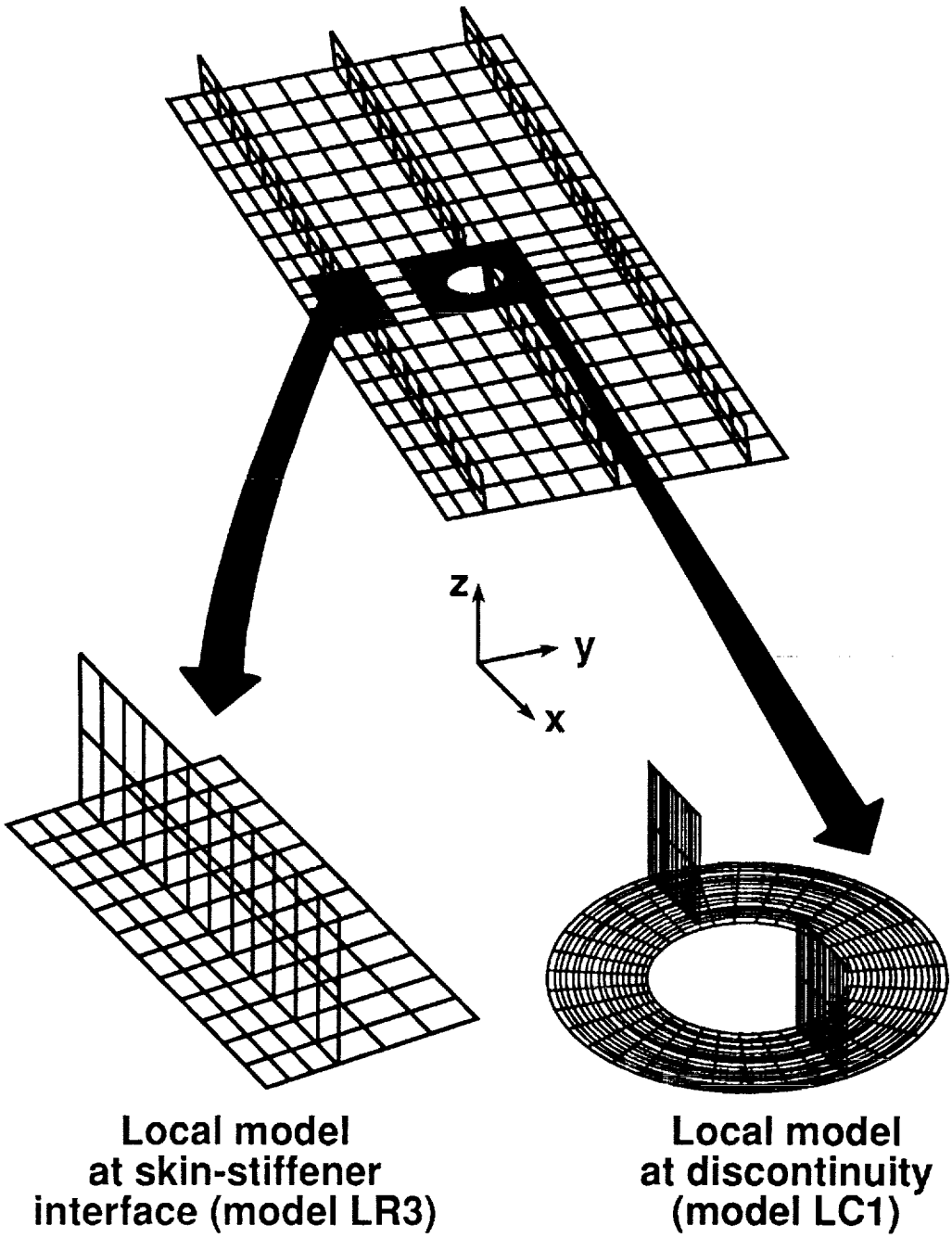

Fig. 5.19 Global/local analysis models for blade–stiffened panel with discontinuous stiffener.

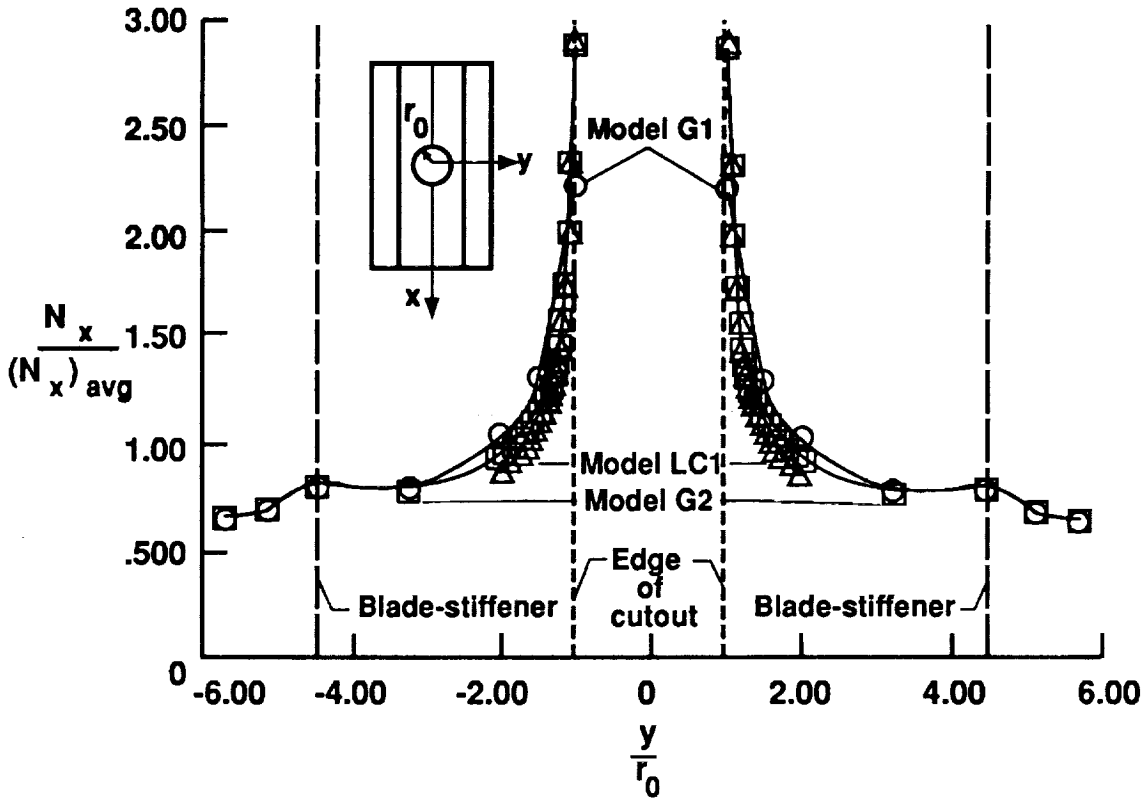

(a) Distribution at panel midlength.

Fig. 5.20 Longitudinal stress resultant N_x distributions for circular local finite element model of blade–stiffened panel with discontinuous stiffener.

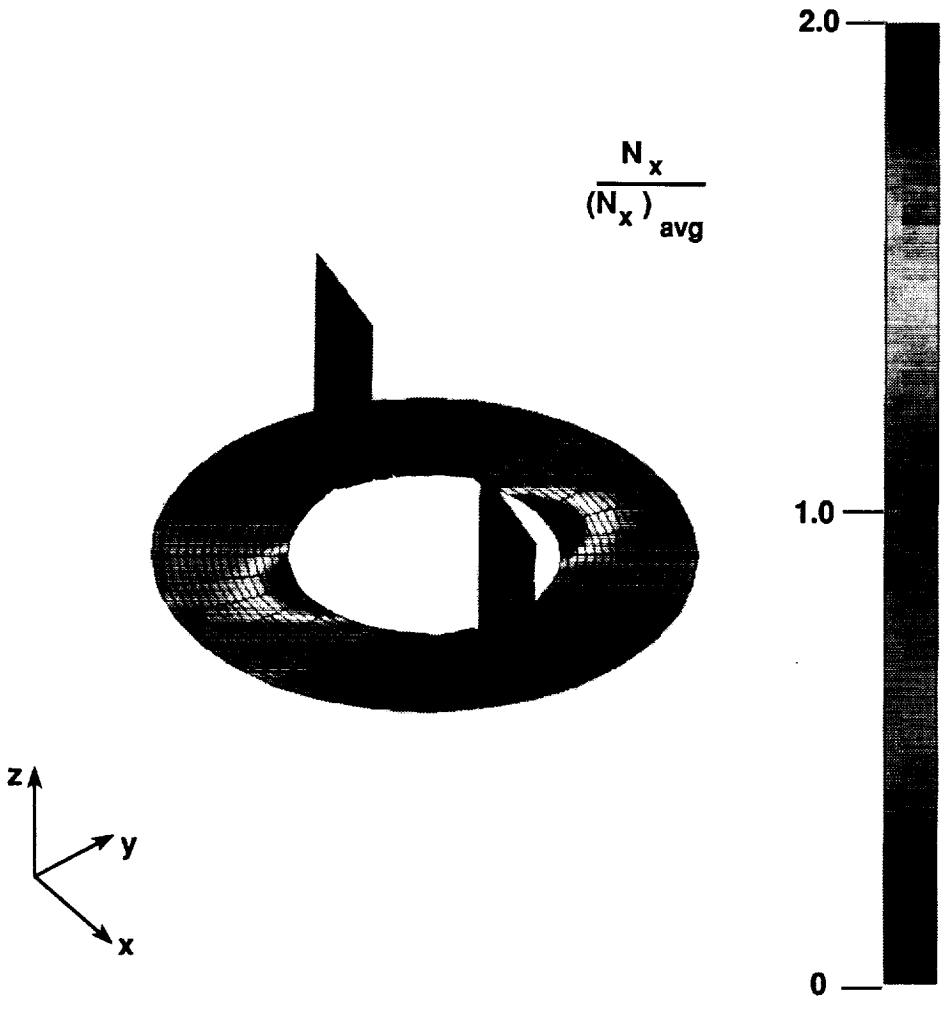

(b) Contour plot.

Fig. 5.20 Concluded.

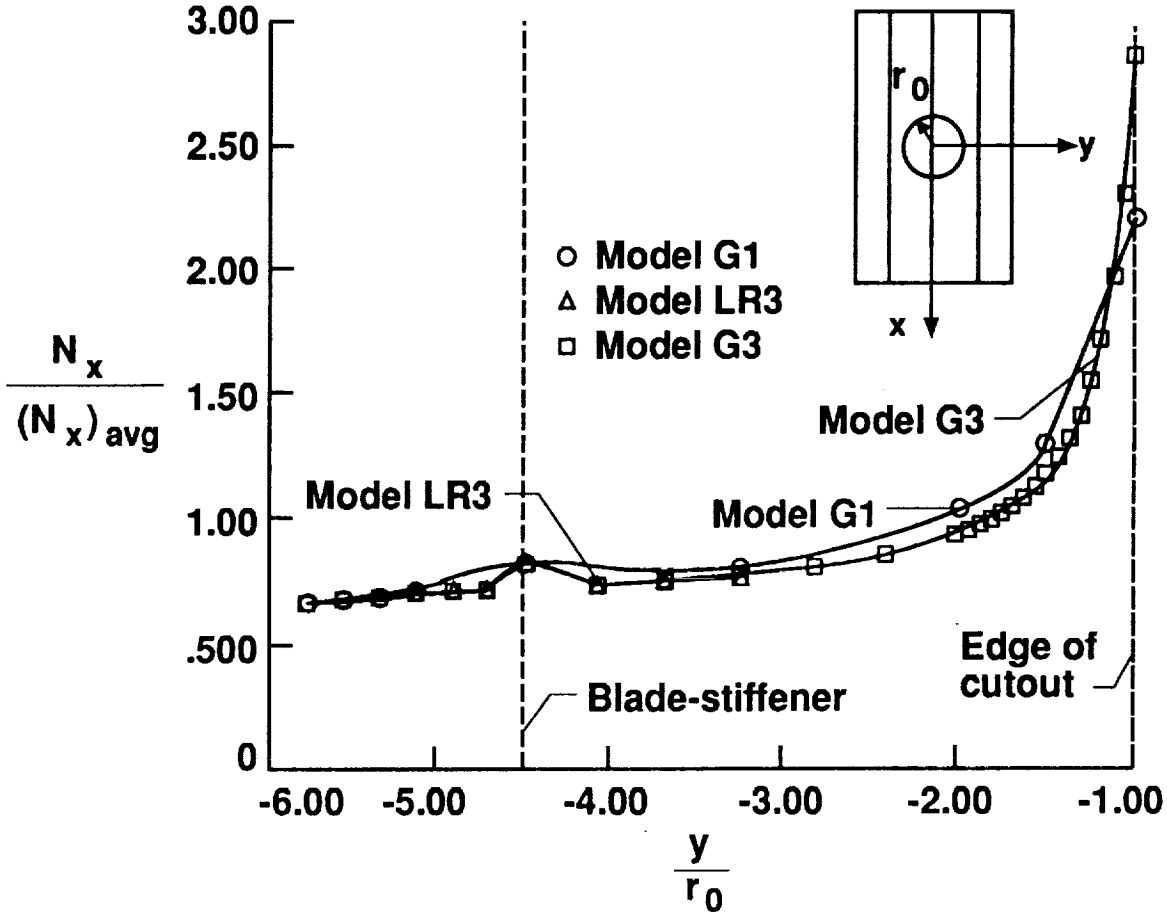

Fig. 5.21 Longitudinal inplane stress resultant N_x distributions at panel midlength for skin-stiffener interface region.

NASA
National Aeronautics and Space Administration

Report Documentation Page

1. Report No.	2. Government Accession No.	3. Recipient's Catalog No.
NASA TM-101640		

4. Title and Subtitle	5. Report Date
Global/Local Stress Analysis of Composite Structures	August 1989
	6. Performing Organization Code

7. Author(s)	8. Performing Organization Report No.
Jonathan B. Ransom	

9. Performing Organization Name and Address	10. Work Unit No.
NASA Langley Research Center Hampton, VA 23665-5225	505-63-01-10
	11. Contract or Grant No.

12. Sponsoring Agency Name and Address	13. Type of Report and Period Covered
National Aeronautics and Space Administration Washington, DC 20546-0001	Technical Memorandum
	14. Sponsoring Agency Code

15. Supplementary Notes

Thesis submitted in partial fulfillment of the requirements for the degree of Master of Science in Engineering Mechanics at Old Dominion University, Norfolk, VA.

16. Abstract

A method for performing a global/local stress analysis is described and its capabilities are demonstrated. The method employs spline interpolation functions which satisfy the linear plate bending equation to determine displacements and rotations from a global model which are used as "boundary conditions" for the local model. Then, the local model is analyzed independent of the global model of the structure. This approach can be used to determine local, detailed stress states for specific structural regions using independent, refined local models which exploit information from less-refined global models. The method presented is not restricted to having a priori knowledge of the location of the regions requiring local detailed stress analysis. This approach also reduces the computational effort necessary to obtain the detailed stress state. Criteria for applying the method are developed. The effectiveness of the method is demonstrated using a classical stress concentration problem and a graphite-epoxy blade-stiffened panel with a discontinuous stiffener.

17. Key Words (Suggested by Authors(s))	18. Distribution Statement
Global/Local Analysis Detailed Stress Analysis Computational Structural Mechanics Surface Splines	Unclassified—Unlimited Subject Category 39

19. Security Classif.(of this report)	20. Security Classif.(of this page)	21. No. of Pages	22. Price
Unclassified	Unclassified	113	A06

For sale by the National Technical Information Service, Springfield, Virginia 22161-2171